CHAPTER IV

RESONANCES AND THE STATISTICAL THEORY OF NUCLEAR REACTIONS

1. INTRODUCTION[‡]

This is the first in a series of chapters in which the formalism of Chapter III will be applied to various types of reaction phenomena that are observed experimentally. Extensions of the formal theory will suggest themselves and be developed.

We begin the chapter with the isolated resonance, the dependence of its width upon projectile energy, and the interference of the resonance amplitude with that for the prompt reactions not only for elastic scattering but for other reactions as well. Threshold phenomena, the existence of cusps in the cross section, are naturally considered at this point. These are followed by a discussion of the case of many overlapping resonances. The very important impact of the details of the empirical analysis of the data upon theoretical considerations is stressed. It is now a quick step to the statistical theory of nuclear reactions since analysis of the resonance data provides us with distribution functions for the widths, spacing of resonance energies, and fluctuations in the cross section. Correlations among these various quantities, either self-correlations or cross-correlations of fluctuations in different channels, are important statistical measures that can indicate the existence of significant phenomena. The simple statistical theory for the average reaction cross section can be formulated and compared with experiment, suggesting the need, in some cases, for a more detailed statistical description of a reaction.

[‡]Hodgson (87); Mahaux and Weidermüller (79).

Channels; Angular Distributions. The description of the angular distribution of reaction products differs according to the scheme adopted for labeling the open channels. One common method is to couple the projectile spin **i** and the target spin **I** to form a channel spin **s**, as indicated by the equation

$$\mathbf{I} + \mathbf{i} = \mathbf{s} \tag{1.1}$$

The vector notation is shorthand for $|I - i| < s < I + i$. The spin is then coupled to the orbital angular momentum **l** to obtain the total angular momentum of the system, **J**:

$$\mathbf{J} = \mathbf{s} + \mathbf{l} = \mathbf{I} + \mathbf{i} + \mathbf{l} \tag{1.2}$$

This procedure is referred to as the *channel coupling scheme*. It is also possible to couple the projectile spin and the orbital angular momentum as would be appropriate if spin-orbit effects were overriding:

$$\mathbf{i} + \mathbf{l} = \mathbf{j} \tag{1.3}$$

To form J, **j** would be coupled to **I**:

$$\mathbf{j} + \mathbf{I} = \mathbf{J} \tag{1.4}$$

This coupling scheme is referred to as the *spin-orbit coupling scheme*. Finally, the *helicity coupling scheme* of Jacob and Wick (59) has often been used [see Chapter VIII of deShalit and Feshbach (74)], particularly for relativistic phenomena. In this scheme the projections of the projectile and target spin along the direction of motion, λ_a and λ_X, respectively, similar quantities for the reaction products, λ_b and λ_Y, together with the total angular momentum J (and its projection M) are used.

Of course, in addition to the angular momenta, one must also include the parity of the channel, the energies of the system in the center-of-mass frame, and the excitation energies of any of the complex particles in the initial or final states of the system. For the sake of definiteness we shall use the channel coupling scheme in this chapter. Then the angular distribution of the reaction products for a two-body final state in which both products are in well-defined quantum states of a given energy is

$$\begin{aligned}\frac{d\sigma(\alpha,\alpha')}{d\Omega} = \frac{1}{k^2}\sum \frac{1}{(2I+1)(2i+1)} &(l_1, s, J_1 \| \sqrt{4\pi}\, Y_L \| l_2, s, J_2) \\ &\times (l_1', s', J_1 \| \sqrt{4\pi}\, Y_L \| l_2', s', J_2)\, \mathrm{Re}\, \pi^2 \mathscr{T}_{\alpha'\alpha}(l_1' s'; l_1 s; J, \Pi_1) \\ &\times \mathscr{T}^*_{\alpha'\alpha}(l_2' s'; l_2 s; J_2 \Pi_2)] P_L(\cos\vartheta)\end{aligned} \tag{1.5}$$

The sum is taken over all angular momentum and parity quantum numbers

with the exception of I, i, and of course α and α'. The final states are normalized per unit energy that is $\langle \chi_c(E)|\chi_c(E')\rangle = 4\pi\delta(E-E')$.

As a consequence, $\mathscr{T}_{\alpha'\alpha}$, the transition matrix, is dimensionless‡. The integrated cross section is

$$\sigma(\alpha',\alpha) = \frac{4\pi}{k^2}\sum \frac{2J+1}{(2I+1)(2i+1)} |\pi\mathscr{T}_{\alpha'\alpha}(l's'; ls; J\Pi)|^2 \tag{1.6}$$

The reduced matrix elements $(l_1 s J_1 \| \sqrt{4\pi}\, Y_L \| l_2 s J_2)$ in (1.5) are kinematical in the sense that they do not depend on the nuclear interaction. The angular momenta l_1, l_2 are two possible values in the decomposition of the incident wave into partial waves; s is a possible value of the channel spin. The primed quantities describe the situation for the final state. In addition to (1.2), the reduced matrix elements yield

$$\mathbf{J}_1 + \mathbf{J}_2 = \mathbf{L} \tag{1.7}$$

which together with (1.2) yields

$$\mathbf{l}_1 + \mathbf{l}_2 = \mathbf{L} \qquad \text{and} \qquad \mathbf{l}'_1 + \mathbf{l}'_2 = \mathbf{L} \tag{1.8}$$

These results can also be obtained from the explicit expression

$$(l_1 s J_1 \| \sqrt{4\pi}\, Y_L \| l_2 s J_2) = (-)^{s+L+J_2}[(2l_1+1)(2l_2+1)(2J_2+1)(2J_1+1)(2L+1)]^{1/2} \times \begin{pmatrix} l_1 & L & l_2 \\ 0 & 0 & 0 \end{pmatrix} \begin{Bmatrix} l_1 & J_1 & s \\ J_2 & l_2 & L \end{Bmatrix} \tag{1.9}$$

Note the requirements that both $l_1 + l_2 + L$ and $l'_1 + l'_2 + L$ must be even, thus guaranteeing parity conservation. We immediately see from (1.7) and (1.8) that

$$L_{\max} = \min(2l, 2l', 2J) \tag{1.10}$$

where l is the maximum incident angular momentum, l' the maximum emergent, and J the maximum value of the total angular momentum. Equation (1.10) is a precise statement of the complexity theorem [Yang (48)] described in Chapter I.

The $\mathscr{T}$ matrix in (1.5) depends on the nuclear interaction. We see that in the channel spin coupling scheme it describes a transition between two channels c and c' defined by the quantum numbers

$$\begin{aligned} c &\equiv \{\alpha l s; J\Pi\} \\ c' &\equiv \{\alpha' l' s'; J\Pi\} \end{aligned} \tag{1.11}$$

‡For spinless particles, $\mathscr{T}_l = -(1/\pi)\sin\delta_l e^{i\delta_l}$, where δ_l is the phase shift.

We shall often, for notational compactness, replace

$$\mathscr{T}_{\alpha'\alpha}(l's'; ls; J\Pi)$$

by

$$\mathscr{T}_{cc'}(J\Pi) \tag{1.12}$$

$\mathscr{T}$ is a symmetric function of c' and c:

$$\mathscr{T}_{c'c} = \mathscr{T}_{cc'}$$

Therefore, from (1.6) it follows that

$$\sigma(\alpha', \alpha) = \frac{k'^2(2I'+1)(2i'+1)}{k^2(2I+1)(2i+1)}\sigma(\alpha, \alpha') \tag{1.13}$$

This reciprocity relation interchanging initial and final states. $I \to I'$, $i \to i'$, and so on, has been used to determine a spin when three of the four I, i, I', i' are known. For example, the spin of the π meson can be obtained by comparing $p + p \to \pi^+ + D$ and $\pi^+ + D \to p + p$ [Marshak (51); Cheston (51)].

2. ISOLATED RESONANCES; INTERFERENCE WITH THE PROMPT AMPLITUDE

The transition $\mathscr{T}_{c'c}(J\Pi)$ can, according to (III.2.25), be written as a sum of two terms, the prompt and the resonant amplitude:

$$\mathscr{T}_{c'c} = \mathscr{T}^{(P)}_{c'c} + \mathscr{T}^{(R)}_{c'c} \tag{2.1}$$

Therefore, the differential cross section (1.5) can be broken up into three parts:

$$\frac{d\sigma(\alpha', \alpha)}{d\Omega} = \frac{d\sigma^{(P)}(\alpha', \alpha)}{d\Omega} + \frac{d\sigma^{(R)}(\alpha', \alpha)}{d\Omega} + \frac{d\sigma^{(I)}(\alpha', \alpha)}{d\Omega} \tag{2.2}$$

The first term on the right side of this equation gives the angular distribution of the reaction products as generated by the prompt processes as indicated by the superscript P. The second, with superscript R, the angular distribution originating in the resonance, while the third, with superscript I, is the angular distribution developed by the interference between the two, the prompt and the resonance process. A similar decomposition is possible for the integrated cross section. From (1.6)

$$\sigma(\alpha', \alpha) = \sigma^{(P)}(\alpha', \alpha) + \sigma^{(R)}(\alpha', \alpha) + \sigma^{(I)}(\alpha', \alpha) \tag{2.3}$$

For example, inserting (2.1) into (1.6) yields

$$\sigma^{(P)}(\alpha',\alpha)=\frac{4\pi}{k^2}\sum\frac{2J+1}{(2I+1)(2i+1)}|\pi\mathscr{T}^{(P)}_{c'c}|^2=\Sigma\sigma^{(P)}_{c'c} \tag{2.4}$$

$$\sigma^{(R)}(\alpha',\alpha)=\frac{4\pi}{k^2}\sum\frac{2J+1}{(2I+1)(2i+1)}|\pi\mathscr{T}^{(R)}_{c'c}|^2=\sum\sigma^{(R)}_{c'c} \tag{2.5}$$

$$\sigma^{(I)}(\alpha',\alpha)=\frac{4\pi}{k^2}\sum\frac{2J+1}{(2I+1)(2i+1)}[\pi^2\mathscr{T}^{(R)}_{c'c}\mathscr{T}^{(P)*}_{c'c}+\pi^2\mathscr{T}^{(R)*}_{c'c}\mathscr{T}^{(P)}_{c'c}] \tag{2.6}$$

We consider the case of a single isolated resonance which is designated (just as in the case of bound states) by a specific J and Π. Thus

$$\frac{d\sigma^{(R)}(\alpha',\alpha)}{d\Omega}=\frac{\pi^2}{k^2}\sum\frac{1}{(2I+1)(2i+1)}(l_1sJ\|\sqrt{4\pi}\,Y_L\|l_2sJ)(l'_1s'J\|\sqrt{4\pi}\,Y_L\|l'_2s'J)$$
$$\times\,\mathrm{Re}(\mathscr{T}^{(R)}_{c'c}\mathscr{T}^{(R)*}_{c'c})P_L \tag{2.7}$$

To excite a resonant state of a given parity, l_1+l_2 and $l'_1+l'_2$ must be even; that is, l_1 and l_2 must have the same parity and similarly for l'_1 and l'_2. Since [see (1.9)]

$$(l_1sJ\|Y_L\|l_2sJ)\sim\begin{pmatrix}l_1 & L & l_2\\ 0 & 0 & 0\end{pmatrix}$$

it follows that L is even. Hence the resonant angular distribution (2.7) is symmetric about 90°.

Problem. Prove directly from (1.9) that if both the projectile and target have zero spin, and if the reaction products have zero spin, then

$$\frac{d\sigma^{(R)}}{d\Omega}\sim[P_J(\cos\vartheta)]^2$$

This result is applicable to resonance reactions such as $^{12}C+{}^{12}C\to{}^{20}Ne+\alpha$, $^{12}C+{}^{16}O\to{}^{24}Mg+\alpha$, and so on, when the residual nucleus and emergent particles are in spin-zero states.

Before the effect of interference can be discussed, it is necessary to provide explicit expressions for $\mathscr{T}^{(R)}_{c'c}$ and $\mathscr{T}^{(P)}_{c'c}$. The former is given by (III.2.25) as follows:

$$\pi\mathscr{T}^{(R)}_{c'c}=\tfrac{1}{2}e^{i(\delta_{c'}+\delta_c)}\frac{g_{c'\lambda}(J\Pi)g_{c\lambda}(J\Pi)}{E-E_\lambda+(i/2)\Gamma_\lambda} \tag{2.8}$$

In this last expression the g's are real numbers and the δ's give the phases of the distorted waves generated by the potential scattering [Eq. (III.2.24)]:

$$\chi_c = e^{i\delta_c}|\chi_c| \tag{III.2.24}$$

and from (III.2.23),

$$\Gamma_{\lambda c} = g_{\lambda c}^2 \tag{III.2.23}$$

and from (III.2.22),

$$\Gamma_\lambda = \sum_c \Gamma_{\lambda c} \tag{III.2.22}$$

Each channel c with an l and s that can combine to give the $J\Pi$ of the resonant state will contribute to (1.5).

The prompt transition amplitude is constructed out of the solutions of

$$(E - H_{PP})\chi^{(\pm)} = 0 \tag{2.9}$$

where generally this is a set of coupled equations connecting the different channels. The DWA (distorted wave amplitude) is constructed by treating the coupling pertubatively. More explicitly, the relevant equations are of the form

$$\begin{aligned}(E - H_{cc})\chi_c &= H_{cc'}\chi_{c'} \\ (E - H_{c'c'})\chi_{c'} &= H_{c'c}\chi_c\end{aligned} \tag{2.10}$$

so that‡

$$\mathscr{T}_{c'c} = \langle \chi_{c'0}^{(-)} | H_{c'c}\chi_{c0}^{(+)} \rangle \tag{2.11}$$

where $\chi_{c0}^{(+)}$ and $\chi_{c0}^{(-)}$ are solutions of the uncoupled equation (2.10) that is with $H_{cc'} = H_{c'c} = 0$.

In the discussion that follows we shall employ the DWA approximation for the χ_c and $\chi_{c'}$ appearing in the definition of $\Gamma_{\lambda c}$:

$$\Gamma_{\lambda c} = 2\pi |\langle \Phi_\lambda | H_{QP}\chi_c^{(+)} \rangle|^2 \tag{2.13}$$

‡One can improve upon (2.11) by obtaining a better χ_c by eliminating $\chi_{c'}$, so that

$$\left[E - H_{cc} - H_{cc'} \frac{1}{E - H_{c'c'}} H_{c'c} \right] \chi_c = 0 \tag{2.12}$$

Then the exact $\mathscr{T}_{cc'}^{(P)}$ is given by $\langle \chi_{c0}^{(-)} | H_{c'c} | \chi_c^{(+)} \rangle$, where $\chi_c^{(+)}$ is a solution of (2.12) [Lamarsh and Feshbach (65)]. Since the wave functions are usually obtained using an empirically determined $H_{cc'}$ it is possible that the DWA is a more accurate approximation than would at first appear.

and the amplitude given by (2.11) for the prompt amplitude. This is a reasonably accurate procedure when the prompt process is a single step and in any event will serve to illustrate the effects of interference between the direct and the resonant amplitude.

From (2.11) it then follows that

$$\pi\mathscr{T}_{c'c}^{(P)} = -e^{i(\delta_{c'}+\delta_c)}A_{c'c}(J\Pi) \tag{2.14}$$

where A is a real amplitude.

To illustrate the effect of interference we consider a simplified situation. Let us first restrict the discussion to elastic scattering. Second, let us assume that the *target nucleus has zero spin*, so that $s' = s$, and in addition assume that the energy is so low that only one angular momentum, the lowest possible value of l, contributes significantly to the formation of the compound nucleus. Suppose that the resonance occurs therefore for a particular combination of $(l, s, J, \Pi) = C$. Then from (1.6) and (2.4),

$$\sigma(\alpha,\alpha) = \sum{}'\sigma_{c'c}^{(P)} + \sigma_C \tag{2.15}$$

where the prime indicates the omission of the terms $c' = c = C$. The cross section σ_C is

$$\sigma_C = \frac{4\pi}{k^2}\frac{2J+1}{2i+1}|\pi\mathscr{T}(l_i; l_i; J\Pi)|^2 \tag{2.16}$$

For this term the potential scattering amplitude is

$$\pi\mathscr{T}_C^{(\mathrm{pot})} = -e^{-i\delta_C}\sin\delta_C \tag{2.17}$$

Combining (2.17) and (2.8), σ_C is

$$\sigma_C = \frac{4\pi}{k^2}\frac{2J+1}{2i+1}\left|e^{i\delta_C}\sin\delta_C - e^{2i\delta_C}\frac{\Gamma_{\lambda C}/2}{E-E_\lambda+(i/2)\Gamma_\lambda}\right|^2 \tag{2.18}$$

Introducing the resonant phase angle γ_λ,

$$\tan\gamma_\lambda \equiv \frac{\Gamma_\lambda}{2(E-E_\lambda)}$$

(2.18) becomes

$$\sigma_C = \frac{4\pi}{k^2}\frac{2J+1}{2i+1}\left|e^{2i\delta_C}\left(\sin\delta_C e^{-i\delta_C} - \frac{\Gamma_{\lambda C}}{\Gamma_\lambda}\sin\gamma_\lambda e^{-i\gamma_\lambda}\right)\right|^2 \tag{2.19}$$

The simplest situation occurs when only the elastic channel is open. This,

together with the initial assumptions, has the consequences $\Gamma_{\lambda C} = \Gamma_\lambda$ and δ_C real. Then (2.19) becomes

$$\sigma_C = \frac{4\pi}{k^2}\frac{2J+1}{2i+1}|\sin\delta_c e^{-i\delta_c} - \sin\gamma_\lambda e^{-i\gamma_\lambda}|^2 \tag{2.20}$$

It is immediately clear that completely destructive interference occurs when

$$\gamma_\lambda = \delta_C \qquad \sigma_C(\alpha,\alpha) = 0$$

On the other hand, a maximum occurs when

$$\gamma_\lambda = \frac{\pi}{2} + \delta_C$$

with a maximum cross section

$$[\sigma_C(\alpha,\alpha)]_{\max} = \frac{4\pi}{k^2}\frac{2J+1}{2i+1} \tag{2.21}$$

In terms of the energy E we have

$$E = E_\lambda + \frac{\Gamma_\lambda}{2}\cot\delta_C \qquad \text{for the minimum value of } \sigma_C(\alpha,\alpha) = 0$$

and (2.22)

$$E = E_\lambda - \frac{\Gamma}{2}\tan\delta_C \qquad \text{for the maximum value of } \sigma_C(\alpha,\alpha)$$

We see that the effect of the interference is to shift the maximum and introduce a minimum, with the scale of these shifts given by Γ_λ. For no potential scattering term, that is, no interference, $\delta_C = 0$, the maximum is not shifted while the minimum is at infinity. For δ_C small, the maximum is shifted to a lower (larger) energy for δ_C positive (negative) while the minimum appears on the other side of E_λ. On the other hand, when δ_C approaches $\pi/2$, that is, when the potential scattering resonates, the maximum disappears (i.e., moves off to infinite energy). The resonance now manifests itself by a minimum (in this case a zero) at $E = E_\lambda$. Figure 2.1 gives an example of a resonance with an interference minimum and Fig. 2.2 shows a resonance in which the potential scattering is very small, so that no interference phenomena occur.

If more than one channel is open, $\Gamma_{\lambda C} < \Gamma_\lambda$ and δ_C can be complex since there will be absorption from the elastic scattering channel denoted by C into reaction channels‡. Under these circumstances the cross section at the interference

‡By using the eigenphases for the prompt channels similar to the σ_μ of (III.2.45′), one can avoid complex phase shifts.

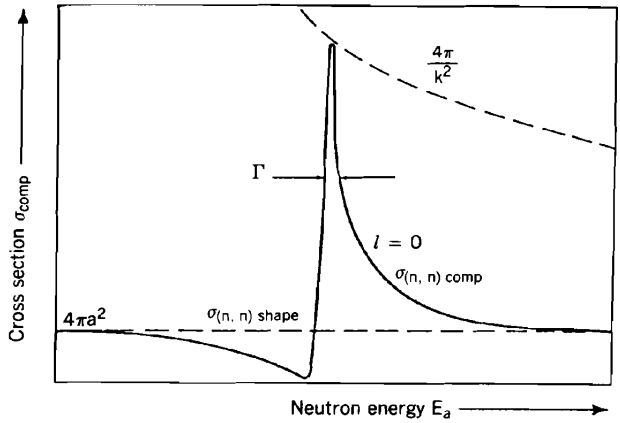

FIG. 2.1. Elastic scattering cross sections for S-wave neutrons near a resonance in the compound nucleus. The figure shows the relationship between the shape-elastic and the compound-elastic cross sections for a spinless target nucleus. [From Marmier and Sheldon (70).]

minimum will no longer be zero and the maximum will no longer be as large as that given by (2.20). The full formulas are given by Feshbach (60). As an example, we quote here the result for δ_C real:

$$\sigma_{\substack{\max \\ \min}}(\alpha,\alpha) = \frac{\pi}{k^2}\frac{2J+1}{2i+1}\left\{\left[1+\left(1-\frac{\Gamma_{\lambda C}}{\Gamma_\lambda}\right)^2 - 2\left(1-\frac{\Gamma_{\lambda C}}{\Gamma_\lambda}\right)\cos 2\delta_C\right]^{1/2} \pm \frac{\Gamma_{\lambda C}}{\Gamma_\lambda}\right\}^2 \tag{2.23}$$

The visibility of a resonance is reduced as $\Gamma_{\lambda C}$ becomes a smaller fraction of Γ_λ.

Note also that the elastic scattering resonance contributes only to the partial waves having a fixed J and Π. The cross section will contain the contributions for other values of J that generally will not resonate at E near E_λ [as assumed by (2.15)]. It will certainly be considerably easier to observe a resonance when the number of partial waves involved is few, as the nonresonant background tends to obscure the resonance structure.

As this discussion emphasizes, it is more difficult to observe resonance structure in the integrated cross section, particularly as the energy increases. To remove the effects of the nonresonant background and thus make the resonance more visible, it would be obviously helpful for the experiment to be designed so as to be more selective. Choosing a particular channel, for example, would be best. One common and important method looks at the reaction products, which because of selection rules and specificities originating in barrier penetration factors may have many fewer nonresonant background terms. An example is given in Fig. 2.3; the $^{12}C + {}^{12}C$ reaction shows many resonances detected by examining the γ-ray spectrum generated by reactions leading to the

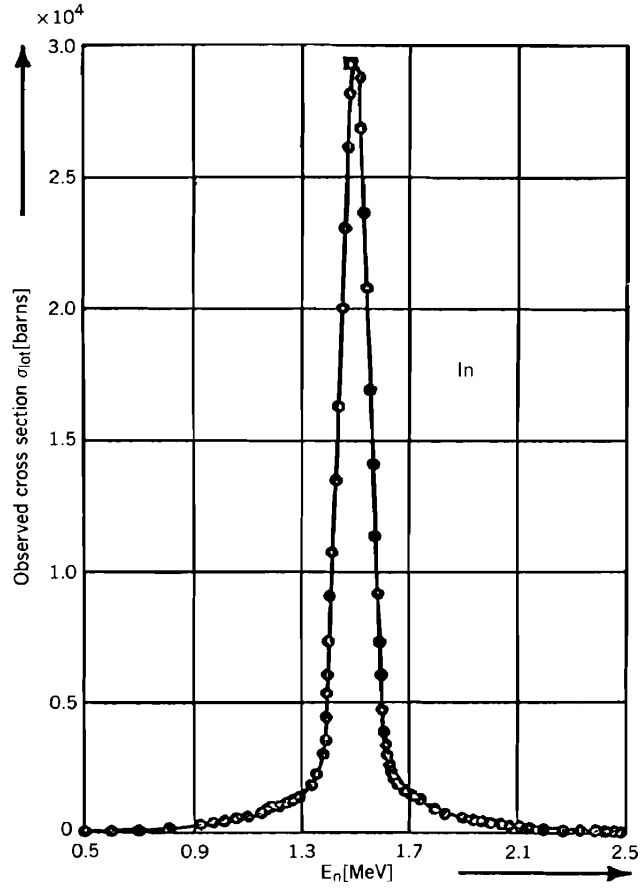

FIG. 2.2. Neutron total cross section for In. [Marmier and Sheldon (1969), taken from Landon and Sailor (55).]

states in ^{20}Ne and ^{23}Na. These resonances are well below the barrier and thus are not as readily detected in, say, elastic scattering, to cite an extreme example.

The angular distribution is much more sensitive than the integrated cross section to the presence of an isolated resonance. To demonstrate this, we take the simple case of an $s = 0$ initial system and an $s = 0$ final system. An example is the elastic scattering of α-particles (or pions or kaons) by a spin-zero nucleus. Then, as one can verify directly from (1.9),

$$l_1 = l'_1 = J_1 \qquad l_2 = l'_2 = J_2 \tag{2.24}$$

As one can directly show from (1.5) using (1.9) and, from deShalit and Feshbach (74), (A.2.96) and (A.2.35) deShalit and Feshbach (74)

$$\frac{d\sigma(\alpha', \alpha)}{d\Omega} = \frac{\pi^2}{k^2} |\sum (2l + 1) P_l(\cos \vartheta) \mathscr{T}_{\alpha'\alpha}(l)|^2 \tag{2.25}$$

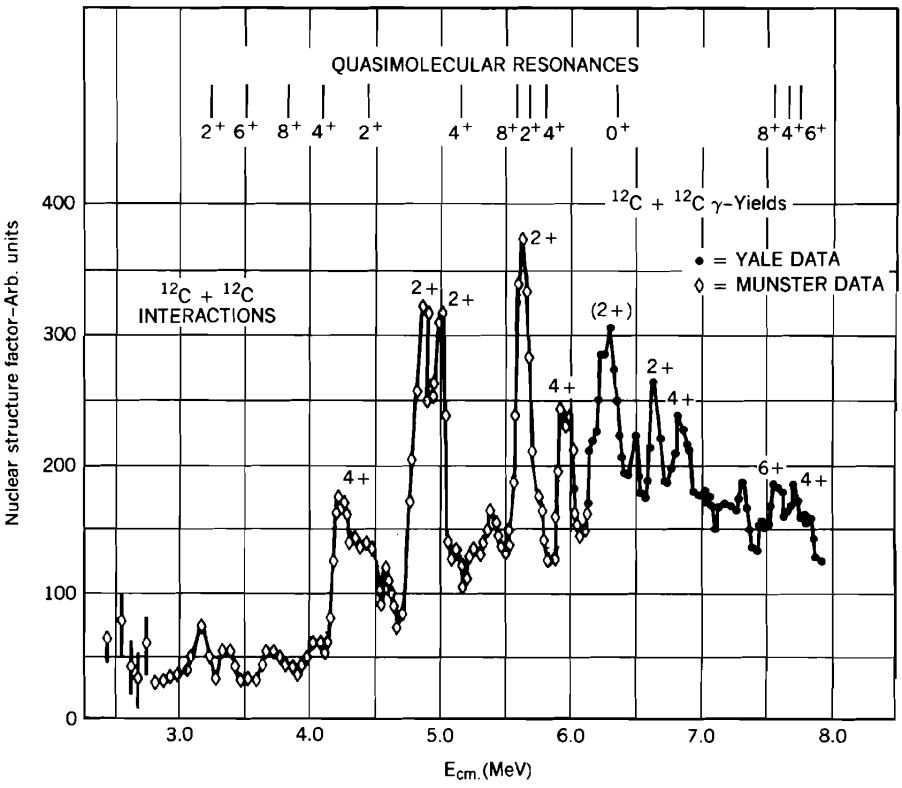

FIG. 2.3. Resonances in the $^{12}C+^{12}C$ reaction [From Erb and Bromley (85).]

where we have abbreviated $\mathscr{T}_{\alpha'\alpha}(l0;l0;l\Pi)$ by $\mathscr{T}_{\alpha'\alpha}(l)$. Of course, one can derive this result directly rather than as a special case of (1.5). Let the resonance occur for $l=J$. Then

$$\frac{d\sigma(\alpha',\alpha)}{d\Omega}=\frac{\pi^2}{k^2}|\mathscr{T}^{(P)}_{\alpha'\alpha}+(2J+1)P_J(\cos\vartheta)\mathscr{T}^{(R)}_{\alpha',\alpha}(J)|^2 \tag{2.26}$$

The first term is just the prompt term ("potential" scattering in the elastic case), the second the resonance term. We see that the interference occurs now between the full potential scattering amplitude and the resonant amplitude. This combination will have an interference minimum and a maximum whose positions will vary with angle. It is often the case, particularly at the higher energies, that the prompt amplitude is very small at back angles. In that event, the resonant term will be very prominent in this angular region and the angular distribution will vary like $(P_J)^2$. More generally, an analysis of the angular distribution into partial waves will reveal the resonance. When the channel spins are not zero, extracting the resonance amplitude from the angular distribution might again prove difficult. However, in these cases one can turn

to the polarizations and their angular distributions (if the data are available!) for the needed additional information.

Interference, constructive and destructive, as a consequence of the existence of both a prompt amplitude, (2.14), and a resonating reaction amplitude, (2.8), can occur in reactions as well as elastic scattering. Its strength depends on the relative magnitude of each of the contributing terms, that is, on $g_{c'\lambda}g_{c\lambda}/\Gamma_\lambda$ of (2.8) and on $A_{c'c}(J\Pi)$ of (2.14). Again because of the general tendency of the prompt amplitude eventually to decrease sharply as the angle increases, resonance structure should be more visible at back angles, while interference phenomena should be significant in the intermediate angular region lying between the forward angular region, where the dominant contribution to the differential cross section is from the prompt amplitude and the backward angular region dominated by the resonance reaction.

One should note that because the interference depends on the strengths of the prompt and resonant amplitudes and because these vary with the exit channel, the locations in energy of the interference maximum and minimum will generally vary with channel. The maximum will not be at E_λ; it may differ from that value by the order of Γ_λ and in extreme cases by more. The customary procedure for the identification of a resonance by observing its presence in each channel must take this possibility into account.

3. PROPERTIES OF THE WIDTHS; THRESHOLD BEHAVIOR OF CROSS SECTIONS; CUSPS

The width of a resonance is given [see (III.2.13)] by

$$\Gamma_{\lambda c} = 2\pi|\langle\Phi_\lambda|H_{QP}\chi_c^{(+)}\rangle|^2 \qquad \text{(III.2.13)}$$

The value of $\Gamma_{\lambda c}$ depends on the overlap of the channel wave function $\chi_c^{(+)}$ with Φ_λ and H_{QP}. Roughly speaking, this is increased if $\chi_c^{(+)}$ has an appreciable amplitude within the nucleus, that is, within the nuclear volume or on the nuclear surface, according to the nature of the reaction. In other words, the size of $\Gamma_{\lambda c}$ will depend on the probability that the incident wave will penetrate into the nucleus or, equivalently, the probability that the prompt reaction wave can emerge. The barriers that can reduce these probabilities are the angular momentum and Coulomb barriers referred to in Chapter I. The effect of these barriers is largely independent of the nuclear interaction and depends critically on the system's energy, size and the charge of the projectile and target. The angular momentum barrier is important near the threshold for the reaction. The reduction that the Coulomb barrier produces is important for energies near to and below the height of the barrier. Both of these effects can produce a rapid energy dependence of $\Gamma_{\lambda c}$. It would thus be useful to factor these effects out of $\Gamma_{\lambda c}$ so that the remainder will more truly reflect nuclear properties. This factorization cannot be unique.

In this volume we adopt the transmission factor in the channel cT_c, as a measure of these effects:

$$\Gamma_{\lambda c} \sim T_c \tag{3.1}$$

where T_c is defined by

$$T_c = 1 - \sum_{c'} |\langle S_{cc'} \rangle|^2 \tag{3.2}$$

$S_{cc'}$ is the S matrix, c and c' denoting open channels, while $\langle S_{cc'} \rangle$ is its energy average. The motivation for this choice can be seen most easily by considering the single-channel case, that is, when χ_c is a single-channel wave function. The averaged S can be obtained from the corresponding optical model wave function $\langle \chi_c \rangle$. In Chapter V (p. 367) we show that

$$T_c = 4k \int \langle \chi_c^* \rangle \left(\frac{-2\mu}{\hbar^2} W \right) \langle \chi_c \rangle r^2 \, dr \tag{3.3}$$

where W is the imaginary part of the complex optical potential. In (3.3) $\langle \chi_c \rangle$ is normalized to have unit amplitude at infinity. Since the angular momentum and Coulomb barriers enter in an identical way for the equations satisfied by χ_c and $\langle \chi_c \rangle$, the behavior of T_c and $\Gamma_{\lambda c}$ should be similar. Obviously, T_c cannot reproduce the dependence of $\Gamma_{\lambda c}$ on λ. However, since W represents the absorptive effects of the reactions as well as the reduction in channel c because of coupling to other channels, T_c provides in a rough fashion a measure of the magnitude of $\Gamma_{\lambda c}$. This relationship is, in fact, demonstrated by (III.3.22′), where the absorption computed from the optical model, which is proportional to T_c, is found in first order to be proportional to the energy average, $\langle \Gamma_{\lambda c} \rangle$. For the present purposes it will suffice to record the approximate result,

$$T_c \simeq 2\pi \langle \omega_\lambda \rangle \langle \Gamma_{\lambda c} \rangle \tag{3.4}$$

where ω_λ is the density of levels of the λ type.

The properties of the transmission factor are listed in the Appendix to Chapter III. Drawing on these results, we find that

$$T_c(E) \sim k^{2l+1} C_l^2(\eta) \qquad \text{as } k \to 0 \tag{3.5}$$

where E is the energy of the relative motion of the two-particle system in channel c, k the wave number is the corresponding momentum divided by $\hbar$, and $l\hbar$ is the relative angular momentum of the two particles. The quantity η is the Coulomb parameter

$$\eta = \frac{zZe^2}{\hbar v} = \frac{zZ}{137\beta} \tag{3.6}$$

$$\beta = \frac{v}{c} = \frac{1}{21.7}\sqrt{\frac{E(\text{MeV})}{\mu}} \tag{3.7}$$

where v is the relative velocity corresponding to wave number k and μ is the reduced mass in channel c in units of the proton mass. The Coulomb factor C_l^2 is given by (I.8.6), which we repeat here:

$$C_l^2 = \frac{2^{2l}}{[(2l)!]^2}(l^2+\eta^2)[(l-1)^2+\eta^2]\cdots(1+\eta^2)C_0^2(\eta)$$

where

$$C_0^2(\eta) = \frac{2\pi\eta}{e^{2\pi\eta}-1} \tag{3.8}$$

A short table of C_0^2 is given in (Table I.8.2).

Because of the close relationship between T_c as given by (3.3) and $\Gamma_{\lambda c}$ as expressed by (3.1), it follows that the threshold behavior of $\Gamma_{\lambda c}$ is also given by (3.5), that is,

$$\Gamma_{\lambda c} \sim k^{2l+1}C_l^2(\eta) \tag{3.9}$$

From the analysis of Section 4 in Chapter III, an expression for T near a single-particle resonance [Eq. (III.4.52)] is available:

$$T_c = \frac{\Gamma_{SP}^{\uparrow}\Gamma_{SP}^{\downarrow}}{(E-\mathscr{E}_{SP})^2+\frac{1}{4}\Gamma_{SP}^2} \qquad \Gamma_{SP} = \Gamma_{SP}^{\uparrow}+\Gamma_{SP}^{\downarrow} \tag{3.10}$$

$\Gamma_{SP}^{\uparrow}$, the escape width from the resonance, is usually referred to in the literature as the single-particle width. It is the single-particle width in the absence of an interaction of the single channel with the compound nuclear channels. An estimate of the order of magnitude of T can be obtained from the results given in the Appendix to Chapter III for T in the resonance region for a square-well optical potential whose imaginary part is W_0. Then when the relative angular momentum is $l\hbar$, one finds that

$$\Gamma_{SP}^{\downarrow} \simeq 2W_0 \tag{3.11}$$

$$\Gamma_{SP}^{\uparrow} = \frac{2\hbar^2}{\mu R^2}kRs_l(kR) \tag{3.12}$$

where R is the radius of the potential and μ is the reduced mass. The function $s_l(kR)$ is given by

$$s_l(x) = \frac{1}{|w_l^{(+)}(x)|^2} \tag{3.13}$$

where $w_l^{(+)}$ is the outgoing wave solution of

$$\frac{d^2 w_l}{dx^2} + \left[1 - \frac{l(l+1)}{x^2} - \frac{2\eta}{x}\right] w_l = 0 \tag{3.14}$$

For uncharged particles ($\eta = 0$)

$$\begin{aligned} s_0 &= 1 \\ s_1 &= \frac{x^2}{1+x^2} \\ s_2 &= \frac{x^4}{9+3x^2+x^4} \\ s_3 &= \frac{x^6}{225+45x^2+6x^4+x^6} \end{aligned} \tag{3.15}$$

The barrier effects given by (3.5) are in (3.10) carried by the factor $\Gamma_{SP}^{\uparrow}$, as can readily be demonstrated using (3.12).

The various expressions for T_c are not needed for its numerical evaluation, as this can be easily obtained from the numerical integration of the optical model differential equation for the channel. They serve here to furnish some insight into the properties of T_c, which in turn gives the gross properties of the widths according to (3.1). We shall often write

$$\Gamma_{\lambda c} = \gamma_{\lambda c}^2 T_c \tag{3.16}$$

where $\gamma_{\lambda c}^2$ will carry the deviation of the dependence of $\Gamma_{\lambda c}$ from normal.

The threshold behavior, (3.5), is obviously of importance for channel C. It can also sharply influence the behavior in other channels. For example, consider the scattering in channel C given by (2.18):

$$\sigma_C = \frac{4\pi}{k^2}\left| e^{-i\delta_C} \sin\delta_C - \frac{\frac{1}{2}\Gamma_{C\lambda}}{E - E_\lambda + (i/2)\Gamma_\lambda}\right|^2 \tag{3.17}$$

in the case where two channels C and D can be opened, so that

$$\Gamma_\lambda = \Gamma_{C\lambda} + \Gamma_{D\lambda} \tag{3.18}$$

Suppose that channel D is closed below E_T, and for the sake of the example suppose that the value of l for channel D is zero, so that above threshold

$$\Gamma_\lambda = \Gamma_{C\lambda} + \sqrt{E - E_T} A_{D\lambda} \tag{3.19}$$

where $A_{D\lambda}$ is a finite constant at $E = E_T$. Below E_T

$$\Gamma_\lambda = \Gamma_{C\lambda} \tag{3.20}$$

It is now a simple exercise to verify that

$$\left(\frac{\partial \sigma_C}{\partial E}\right) \to \infty \qquad E \to E_T^{(+)}$$

while

$$\left(\frac{\partial \sigma_C}{\partial E}\right) \to \text{const} \quad E \to E_T^{(-)} \tag{3.21}$$

Hence σ will have a cusp in its dependence on the energy, as illustrated in Fig. 3.1. For larger values of l, singularities in σ_C will appear for higher derivatives (e.g., in the second derivative for $l = 1$), but these effects are much more difficult to discern.

Note. The effects of the angular momentum and Coulomb barrier are not restricted to resonance reactions but hold more generally. The matrix, $\mathscr{T}_{c'c}$, is given by

$$\mathscr{T}_{c'c} = \langle \Psi_{c'}^{(-)} | V \chi_c \rangle \tag{3.22}$$

so that the dependency of $|\mathscr{T}_{c'c}|^2$ on χ_c is similar to that of $\Gamma_{\lambda c}$. Hence

$$|\mathscr{T}_{c'c}|^2 \sim T_c \sim k^{2l+1} C_l^2(\eta) \qquad k \to 0 \tag{3.23}$$

where l is the orbital angular momentum in the c channel. From (1.6) it follows that

$$\sigma_{c'c} \sim k^{2l-1} C_l^2(\eta) \qquad k \to 0 \tag{3.24}$$

revealing the $1/v$ law for reactions induced by a neutral particle ($\eta = 0$) valid when $l = 0$.

The cusp described by (3.21) is also more general, not being restricted to resonance reactions. This fact may be made evident through the use of one of

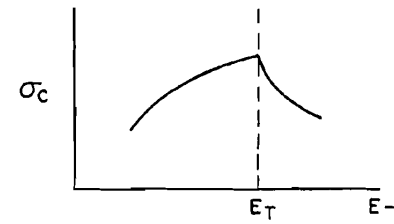

FIG. 3.1. Formation of a cusp in σ_c because of a threshold in another channel.

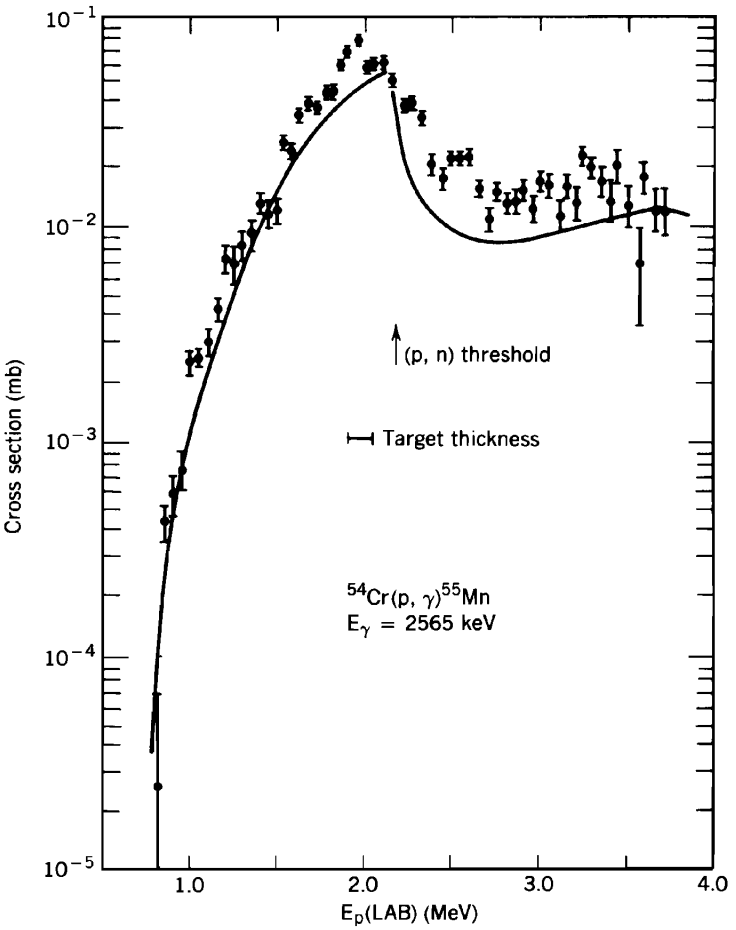

FIG. 3.2. Reaction showing cusp [From Zyskind, Davidson et al. (78).]

the conditions that follow from the unitarity of the S matrix:

$$\sum_d S_{cd}^* S_{cd} = 1 \tag{3.25}$$

Suppose, for example, that there are three channels c, c', c'', which must be considered, and moreover, suppose that there is an $l=0$ threshold in the c'' channel. We now look for the effect of this threshold on the c' channel, that is, on $|S_{cc'}|^2$, which is proportional to the cross section for the reaction $c \to c'$. From (3.25)

$$|S_{cc'}|^2 = |-|S_{cc}|^2 - |S_{cc''}|^2$$

The $l = 0$ threshold dependence of $|S_{cc''}|^2$ is given by the factor $\sqrt{E - E_T}$ for E greater than E_T, and by zero for E less than E_T. Therefore, $\partial |S_{cc'}|^2 / \partial E$ will have an infinite discontinuity at $E = E_T$ because of the $l = 0$ threshold in the c'' channel. Just such a cusp is shown in Fig. 3.2. The cusp in the $^{54}Cr(p,\gamma)^{55}Mn$ reaction is generated by the threshold in the $^{54}Cr(p,n)$ reaction (Zyskind, Davidson et al. (78)).

4. OVERLAPPING RESONANCES

The analysis of a cross section in terms of a prompt amplitude plus a resonant one can be readily extended to the case of several isolated (i.e., nonoverlapping), resonances. However, it should be noted that the results are not unique in the sense that they depend on the choice for H_{pp}, which in turn determines the prompt term. As was illustrated by several examples in Chapter III, H_{pp} is not unique, so that the prompt term can be the scattering from a hard sphere as in the Wigner–Eisenbud theory, or in another example it can be the amplitude deduced from an optical model potential. Consequently, the value of the widths Γ will vary with the choice of H_{pp}, although the reduced width of (3.16) will generally be less sensitive. This ambiguity reflects the latitude in the definition of what will be considered prompt and what will be considered delayed. It is essential that the presentation of an analysis of experimental results clearly state the choice made for the description of the prompt amplitude, that is, the choice of H_{pp}.

A related question asks how many resonance terms one should add on to the prompt term. Indeed, in some formalisms the number of terms is infinite. There is in some no prompt term initially. That term is recovered by summing over the "distant" resonances. This is, in fact, appropriate since the distant resonances are not resonances at all if by resonances we mean delay times, which are long compared to some appropriate characteristic time.

A simple illustration will clarify this remark. In potential scattering the characteristic time is a/v, where a is the range of the potential and v is the velocity of the incident particle inside the potential. Suppose that a pole of the S matrix occurs at $E - i\Gamma/2$. The delay time is then $\hbar/\Gamma$. If that delay time is less than a/v, the time required for the particle to cross the region in which the potential acts, the contribution of the pole term to the scattering amplitude is physically not a resonance. It is physically more correct to consider it as a contribution to the prompt amplitude. To complete this illustration, note that the poles of the S matrix for an attractive square-well potential, no matter how shallow, are infinite in number. In that case, it is mathematically possible to represent the scattering amplitude as a sum of contributions from each of these poles, but of course the resultant total amplitude shows no resonant structure if the well is sufficiently shallow.

These caveats have even more validity when the resonances are overlapping. Analysis of such data can and have been made using (III.2.23) or (III.2.47). In

the first of these, the transition matrix is written as follows:

$$\mathscr{T}_{fi} = \mathscr{T}_{fi}^{(P)} + \sum_{\mu} \frac{A_{fi}^{(\mu)}}{E - E_{\mu}} \tag{III.2.33}$$

As indicated by the earlier discussion the sum over μ contains a finite number of terms, say N. Because of the requirements of unitarity, the parameters $A_{fi}^{(\mu)}$ and E_{μ}, which are slowly varying functions of E, are not independent. To make one such relationship explicit, let

$$A_{fi}^{(\mu)} = \frac{1}{2\pi} e^{i(\delta_f + \delta_i)} e^{i\phi_{\mu}} g_{\mu f}(J\Pi) g_{\mu i}(J\Pi) \tag{4.1}$$

and define

$$\Gamma_{\mu} \equiv \sum_{k} \Gamma_{\mu k} \tag{4.2}$$

where

$$\Gamma_{\mu k} \equiv g_{\mu k}^2 \tag{4.3}$$

The reader should compare these definitions with (III.2.22)–(III.2.24) given in Section 2 of chapter III. With these definitions (III.2.33) becomes

$$\mathscr{T}_{fi} = \mathscr{T}_{fi}^{(P)} + \frac{1}{2\pi} e^{i(\delta_f + \delta_i)} \sum_{\mu} \frac{e^{i\phi_{\mu}} g_{\mu f}(J\Pi) g_{\mu i}(J\Pi)}{E - \mathscr{E}_{\mu} + (i/2)\Gamma_{\mu} + (i/2)\Gamma'_{\mu}} \tag{4.4}$$

where $\mathscr{E}_{\mu}$ is the real part of E_{μ}. The condition relating $A_{fi}^{(\mu)}$ and $\operatorname{Im} E_{\mu}$ given in the single-channel case by (III.2.37) becomes

$$\sum_{\mu} \Gamma'_{\mu} = 0 \tag{4.5}$$

so that the imaginary part of E_{μ} fluctuates about the isolated resonance value of (4.2).

Equation (4.5) is not the only relationship implied by unitarity. Despite the awkwardness of applying these conditions, (III.2.33) is often used in fitting experimental data.

Another procedure that automatically satisfies unitarity uses (III.2.47). In the single-channel case

$$\mathscr{T}_{fi} = \mathscr{T}_{fi}^{(P)} + S_{fi}^{(P)} \frac{\kappa}{1 + i\pi\kappa} \tag{III.2.48''}$$

where κ is given by the series

$$\kappa = \frac{1}{2\pi} \sum_{s} \frac{\gamma_s^2}{E - e_s} \tag{4.6}$$

The often used *R matrix* fit to resonance data is an example of the use of (III.2.48″). The parameters are γ_s and e_s.

In both methods there are two additional parameters which are not always explicitly mentioned. These are the range, δE, over which a fit is to be made, and the number of terms, N, in the series (4.4) or (4.6). These parameters are not independent. They should be determined by the usual statistical measure of the quality of a fit such as the χ^2 value. In particular, they should be chosen in such a way that the values of γ_s and e_s, for example, are stable against small changes in δE or N.

As the energy of the system increases, the spacing in energy of the resonances becomes smaller, the width of the resonance increases with the consequence that the resonances overlap more and more, and rather soon it becomes impossible to distinguish the individual resonances. Nevertheless, the structure in the energy dependences of the cross section does not immediately disappear. With sufficient energy resolution one observes rapid fluctuations in the energy dependence of the cross section. These are referred to as Ericson-fluctuations [Ericson (60c, 63); Brink and Stephen (63); Brink, Stephen, and Tanner (64)]. They have been observed in a wide variety of reactions.

Statistical measures are used to describe the Ericson-fluctuations. The simplest of these is the energy averaged cross section $\langle\sigma\rangle$, where the average of an energy-dependent quantity $F(E)$ is defined by

$$\langle F(E)\rangle = \int \rho(E, E_0) F(E_0)\, dE_0 \tag{4.7}$$

where

$$\int \rho(E, E_0)\, dE_0 = 1 \tag{4.8}$$

To proceed further it is useful to choose H_{PP} to be the optical potential [Kerman, Kwai, and McVoy (73)], for then, from the definition of the optical potential, it follows that in the decomposition of the $\mathscr{T}$ matrix into a prompt and fluctuating part (see Section 8 for further discussion)

$$\mathscr{T} = \mathscr{T}^{(P)} + \mathscr{T}^{(FL)} \tag{4.9}$$

$\mathscr{T}^{(FL)}$ satisfies

$$\langle \mathscr{T}^{(FL)}\rangle = 0 \tag{4.10}$$

It follows that the average cross section can be written as

$$\langle\sigma\rangle = \langle\sigma^{(P)}\rangle + \langle\sigma^{(FL)}\rangle = \sigma^{(P)} + \langle\sigma^{(FL)}\rangle \tag{4.11}$$

The second term does not vanish despite (4.10), since

$$\sigma^{(\mathrm{FL})} \sim |\mathscr{T}^{(\mathrm{FL})}|^2$$

The distribution of $\mathscr{T}^{(\mathrm{FL})}$ and $\sigma^{(\mathrm{FL})}$ about their mean values provides more detailed statistical information. For the distribution of $\mathscr{T}^{(\mathrm{FL})}$, the practice has been to appeal to the central limit theorem of the theory of probability [Feller (68)]. It will be recalled that this theorem states that if a quantity, call it x, is the sum of a large number of random contributions, then the probability $P(x)\,dx$ that x falls between x and $x + dx$ is given by

$$P(x) = \frac{1}{\sqrt{2\pi\langle x^2\rangle}} e^{-(1/2)(x^2/\langle x^2\rangle)} \tag{4.12}$$

where the average value of x, $\langle x\rangle$, is taken to be zero, and $\langle x^2\rangle$, the average value of x^2, is defined by

$$\langle x^2\rangle = \int_{-\infty}^{\infty} P(x)x^2\,dx \tag{4.13}$$

Following Ericson (63), we assume that both the real and imaginary parts of $\mathscr{T}$ are such random variables. If

$$\mathscr{T}^{(FL)} = \alpha + i\beta \tag{4.14}$$

then

$$P(\alpha) = \frac{1}{\sqrt{2\pi\langle\alpha^2\rangle}} e^{-(1/2)(\alpha^2/\langle\alpha^2\rangle)}$$

If, in addition, one assumes that

$$\langle\alpha^2\rangle = \langle\beta^2\rangle = a^2$$

one can write the joint probability $P(\alpha, \beta)$ as

$$P(\alpha, \beta) = \frac{1}{2\pi a^2} e^{-(1/2)(\alpha^2+\beta^2)/a^2} \tag{4.15}$$

It is now a simple matter to obtain the probability distribution for $\sigma^{(FL)}$ from the relation $\sigma^{(FL)} \sim (\alpha^2 + \beta^2)$. From (4.15),

$$P(\sigma^{(FL)}) = \frac{1}{\sqrt{\langle\sigma^{(\mathrm{FL})}\rangle}} e^{-\sigma^{(\mathrm{FL})}/\langle\sigma^{(\mathrm{FL})}\rangle} \tag{4.16}$$

where

$$\langle \sigma \rangle = \int P(\sigma)\sigma \, d\sigma \tag{4.17}$$

An experimental test of (4.16) is possible under the assumption that each observed value of $\sigma^{(FL)}$ is a member of the ensemble making up the distribution given by (4.16). In other words, by varying the energy, members of the ensemble are produced. Thus an energy average becomes identical with the ensemble average, a form of the ergodic theorem. An example of an experimental distribution constructed in this way is shown in Fig. 4.1. It will be seen that the probability distribution agrees with the simple result (4.16) rather well. The variance given by

$$\text{var} \equiv \frac{\langle \sigma^2 \rangle - \langle \sigma \rangle^2}{\langle \sigma \rangle^2}$$

equals unity for distribution equation (4.16). We note that the distribution given in Fig. 4.1 has a smaller variance. This can be consequence of the finite experimental energy resolution, which obviously will smooth the data by the rate of $(\Gamma/\Delta E)^2$, where ΔE is the resolution and Γ is the width of the fluctuation.

The ergodic hypothesis made above is not in fact correct, as is demonstrated by the existence of correlations in the fluctuations of the cross section and for that matter of the transition matrix, $\mathscr{T}$. At a particular angle θ at which the reaction product is observed, an autocorrelation function $C(\varepsilon, \theta)$ measuring the

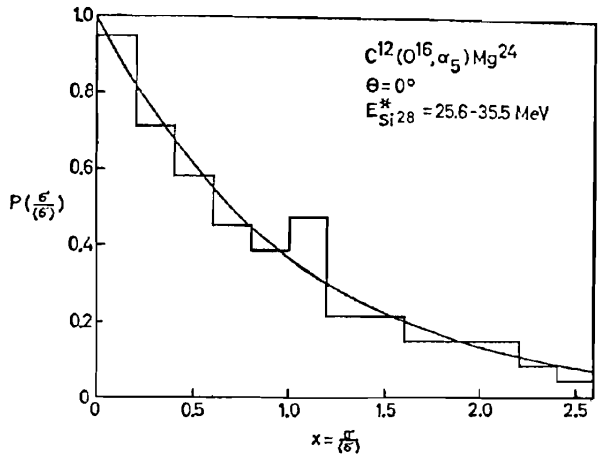

FIG. 4.1. Probability distribution of the differential cross section for ^{12}C (^{16}O, α_5) ^{24}Mg for the α_5 group leading to the 6.00-MeV excited state in ^{24}Mg. The excitation energy in the compound nucleus ^{28}Si is about 30 MeV [Halbert, Durham, Moak, and Zucker (64).] [From Ericson and Mayer-Kuckuk (66).].

correlations as a function of energy can be defined as follows:

$$C(\varepsilon,\theta)=\frac{\langle\sigma(E+\varepsilon)\sigma(E)\rangle-\langle\sigma\rangle^2}{\langle\sigma\rangle^2} \tag{4.18}$$

where σ is the differential cross section giving the angular distribution. Similarly, an amplitude correlation function, $c(\varepsilon,\theta)$, is given by

$$c(\varepsilon,\theta)=\frac{\langle f(E+\varepsilon)f^*(E)\rangle-|\langle f\rangle|^2}{\langle\sigma\rangle} \tag{4.19}$$

where

$$\sigma=|f|^2$$

It is generally assumed‡ that

$$\langle\sigma(E+\varepsilon)\rangle=\sigma(E)$$
$$\langle f(E+\varepsilon)\rangle=f(E)$$

If $\sigma(E+\varepsilon)$ and $\sigma(E)$ are uncorrelated, $\langle\sigma(E+\varepsilon)\sigma(E)\rangle$ will equal $\langle\sigma(E+\varepsilon)\rangle\langle\sigma(E)\rangle$ and $C(\varepsilon,\theta)$ will vanish. Deviations from zero indicate the presence of correlations.

We shall now write $C(\varepsilon,\theta)$ in terms of the prompt direct cross section and the fluctuating part as given by (4.11). From the assumption that $\sigma^{(P)}$ does not fluctuate, we have

$$\langle(\sigma^{(P)})^2\rangle=\langle\sigma^{(P)}\rangle^2 \tag{4.20}$$

Using this equation $C(\varepsilon,\theta)$ becomes

$$C(\varepsilon,\theta)=C(0,\theta)C^{(\mathrm{FL})}(\varepsilon,\theta) \tag{4.21}$$

where

$$C(0,\theta)=\frac{\langle(\sigma^{(\mathrm{FL})})^2\rangle-\langle\sigma^{(\mathrm{FL})}\rangle^2}{[\sigma^{(P)}+\langle\sigma^{(\mathrm{FL})}\rangle]^2} \tag{4.22}$$

and

$$C^{(\mathrm{FL})}(\varepsilon,\theta)=\frac{\langle\sigma^{(\mathrm{FL})}(E+\varepsilon)\sigma^{(\mathrm{FL})}(E)\rangle-\langle\sigma^{(\mathrm{FL})}\rangle^2}{\langle(\sigma^{(\mathrm{FL})})^2\rangle-\langle\sigma^{(\mathrm{FL})}\rangle^2} \tag{4.23}$$

‡This assumption is not necessary. One need only redefine $C(\varepsilon,\theta)$ as follows:

$$C(\varepsilon,\theta)=\frac{\langle\sigma(E+\varepsilon)\sigma(E)\rangle-\langle\sigma(E+\varepsilon)\rangle\langle\sigma(E)\rangle}{\langle\sigma(E+\varepsilon)\rangle\langle\sigma(E)\rangle}$$

$C^{(FL)}$ equals unity for $\varepsilon = 0$, and as ε becomes very large one can expect $\sigma^{(FL)}(E+\varepsilon)$ and $\sigma^{(FL)}(E)$ to be uncorrelated, so that $C^{(FL)}(\varepsilon, \theta)$ will approach zero for large values of ε.

Similar expressions can be obtained for $c(\varepsilon, \theta)$ with some simplfication since according to (4.10),

$$\langle f \rangle = 0$$

In particular,

$$c(\varepsilon, \theta) = \frac{\langle f^{(FL)}(E+\varepsilon) f^{(FL)*}(E) \rangle}{\langle \sigma \rangle} \tag{4.24a}$$

Note that

$$c(0, \theta) = \frac{\langle \sigma^{(FL)} \rangle}{\sigma^{(P)} + \langle \sigma^{(FL)} \rangle} = 1 - y \tag{4.24b}$$

where

$$y \equiv \frac{\sigma^{(P)}}{\langle \sigma \rangle}$$

In general, $C(\varepsilon, \theta)$ and $c(\varepsilon, \theta)$ are independent. However, under a sufficiently drastic approximation they can be related. Toward this end note that

$$\langle \sigma^{(FL)}(E+\varepsilon) \sigma^{(FL)}(E) \rangle = \langle f^{(FL)}(E+\varepsilon) f^{(FL)*}(E+\varepsilon) f^{(FL)}(E) f^{(FL)*}(E) \rangle \tag{4.25}$$

We now assume that only pair correlations are required to describe the right-hand side, so that

$$\begin{aligned} &\langle f^{(FL)}(E+\varepsilon) f^{(FL)*}(E+\varepsilon) f^{(FL)}(E) f^{(FL)*}(E) \rangle \\ &\quad \simeq \langle f^{(FL)}(E+\varepsilon) f^{(FL)*}(E+\varepsilon) \rangle \langle f^{(FL)}(E) f^{(FL)*}(E) \rangle \\ &\qquad + \langle f^{(FL)}(E+\varepsilon) f^{(FL)*}(E) \rangle \langle f^{(FL)*}(E+\varepsilon) f^{(FL)}(E) \rangle \\ &\quad = \langle \sigma^2 \rangle [1 + |c(\varepsilon, \theta)|^2] \end{aligned} \tag{4.26}$$

It should be noted that third-order terms such as $\langle f^{(FL)}(E+\varepsilon) f^{(FL)*}(E+\varepsilon) f^{(FL)}(E) \rangle \langle f^{(FL)*}(E) \rangle$ vanish in any event in virtue of (4.10). In deriving (4.26) we have also assumed that $\langle f^{(FL)}(E+\varepsilon) f^{(FL)}(E) \rangle$ is zero. This follows from (4.10) if that equation is valid because of the random phases of the components of $f^{(FL)}$. It is thus indicated that the major error in the derivation of (4.26) is the possible presence of a quadrilinear correlation which cannot be expressed, as in (4.26), in terms of lower-order correlations.

It immediately follows from (4.26) that

$$C(\varepsilon, \theta) = |c(\varepsilon, \theta)|^2 \tag{4.27}$$

Although $c(\varepsilon, \theta)$ can and has been measured directly [Feshbach and Yennie (62)], it is considerably simpler experimentally to measure $C(\varepsilon, \theta)$.

Before we look at some of the experimental data, it is useful to present a theoretical estimate of $c(\varepsilon, \theta)$. Toward this end we use expression (III.2.33) quoted earlier:

$$\mathscr{T}^{(\mathrm{FL})}(E) = \sum_{\mu} \frac{A^{(\mu)}}{E - \mathscr{E}_{\mu} + (i/2)\Gamma} \tag{4.28}$$

We have dropped the subscripts f and i, which are to be understood, and the simplifying approximation that the imaginary part of the poles, E_{μ}, is independent of μ and equal to $\Gamma/2$ has been made. We now wish to evaluate

$$\langle \mathscr{T}^{(\mathrm{FL})}(E+\varepsilon)\mathscr{T}^{(\mathrm{FL})*}(E)\rangle = \sum_{\mu,\nu} \left\langle \frac{A_{\mu}A_{\nu}^{*}}{[E+\varepsilon-\mathscr{E}_{\mu}+(i/2)\Gamma][E-\mathscr{E}_{\nu}-(i/2)\Gamma]} \right\rangle \tag{4.29}$$

We make the assumption that the important contributions to the sum occur when $\mu = \nu$. The other terms are small because they will generally have phases which if there are enough terms in the sum will take on all possible values. The net effect is a considerable cancellation. In the limit that we take here that the cancellation is complete, this assumption is known as the random phase assumption[‡]. Under this assumption

$$\langle \mathscr{T}^{(\mathrm{FL})}(E+\varepsilon)\mathscr{T}^{(\mathrm{FL})*}(E)\rangle = \sum_{\mu} \left\langle \frac{|A_{\mu}|^{2}}{[E+\varepsilon-\mathscr{E}_{\mu}+(i/2)\Gamma][E-\mathscr{E}_{\mu}-(i/2)\Gamma]} \right\rangle$$

Neglecting the energy dependence of A_{μ} and $\mathscr{E}_{\mu}$, the energy average of this quantity can be readily computed[§] with the result that

$$c(\varepsilon, \theta) = c(0, \theta)\frac{i\Gamma}{\varepsilon + i\Gamma} \tag{4.30}$$

[‡]More explicitly if ϕ_{μ} is the phase of A_{μ}, the right-hand side of (4.28) can be written

$$\sum_{\mu,\nu} e^{i(\phi_{\mu}-\phi_{\nu})} \frac{|A_{\mu}A_{\nu}^{*}|}{[E+\varepsilon-\mathscr{E}_{\mu}+(i/2)\Gamma][E-\mathscr{E}_{\nu}-(i/2)\Gamma]}$$

If we now assume that ϕ_{μ} and ϕ_{ν} are chosen from an ensemble of random numbers, the ensemble average of this quantity will contain only the $\phi_{\mu} = \phi_{\nu}$ terms, the remaining vanishing. Finally, one assumes that the ensemble and energy averages (i.e., the ergodic theorem) are identical.

[§]The calculation proceeds as follows:

$$\left\langle \frac{1}{[E+\varepsilon-\mathscr{E}_{\mu}+(i/2)\Gamma][E-\mathscr{E}_{\mu}-(i/2)\Gamma]} \right\rangle = \frac{1}{2\Delta}\int_{E_0-\Delta}^{E_0+\Delta} \frac{dE}{[E+\varepsilon-\mathscr{E}_{\mu}+(i/2)\Gamma][E-\mathscr{E}_{\mu}-(i/2)\Gamma]}$$

(Continued)

and

$$C(\varepsilon, \theta) = C(0, \theta) \frac{\Gamma^2}{\varepsilon^2 + \Gamma^2} \tag{4.31}$$

The width, Γ, scales the rate at which $C(\varepsilon, \theta)$ goes to zero with increasing ε. The value of $\hbar/\Gamma$ measures the time during which the compound nuclear system, formed by the projectile and target nucleus, lives. In contrast to the compound nuclear resonance, for which $\hbar/\Gamma$ gives the lifetime of a well-defined state, there is no well-defined state with a width Γ. Rather, because the resonances overlap, the system moves from resonance to resonance before finally breaking up into the final observed products. The quantity $\hbar/\Gamma$ measures the time for this process, and thus it would be most appropriate to refer to it as the *interaction* time. The quantity Γ is called the *coherence energy*.

The special nature of the form used for $\mathscr{T}^{(\mathrm{FL})}$ should be remarked upon. In the first place, the correlations between the coefficients $A^{(\mu)}$, the widths Γ, and the energies $\mathscr{E}_\mu$ because of unitarity have been neglected. More important, perhaps, is the neglect of effects of intermediate structure signaling the presence of doorway states. These will introduce another scale in addition to Γ, of the order of Γ_d, the average width of doorway states. Pappalardo (64) has suggested that one could search for doorway states by looking for this second scale factor in the autocorrelation function, as indicated in Fig. 4.2, which presents a highly idealized situation. As indicated in the figure, the small ε behavior (dashed line) is dominated by Γ and the large ε dependence is governed by Γ_d.

The existence of these fluctuation effects was predicted by Ericson (60c). It was first demonstrated by Colli, Facchini, and their collaborators (59). Some experimental results obtained by von Witsch, von Brentano, Meyer-Kuckuk, and Richter (66) using the $^{37}\mathrm{Cl}(p, \alpha)^{34}\mathrm{S}$ are shown in Figs. 4.3 and 4.4. In Fig. 4.3 we see the excitation functions for this reaction at 12 scattering angles taken with an energy resolution of $\Delta E \lesssim 5$ keV. The presence of fluctuations is clearly indicated. In Fig. 4.4 the autocorrelation function is plotted for three separate

where $\Delta \gg \varepsilon$. Let $x = (2/\Gamma)E$. Then the integral becomes

$$\frac{\Gamma}{\Delta} \int_{x_0 - (2/\Gamma)\Delta}^{x_0 + (2/\Gamma)\Delta} dx \frac{1}{(x + (2\varepsilon/\Gamma) - x_\mu + i)(x - x_\mu - i)}$$

If now it is assumed that the averaging interval 2Δ is much larger than Γ, the limits of the integral can be approximated by $\pm \infty$ and the integral evaluated by the calculus of residues, for example, to give

$$\frac{\pi i \Gamma}{\Delta} \frac{1}{i + \varepsilon/\Gamma}$$

from which (4.30) follows.

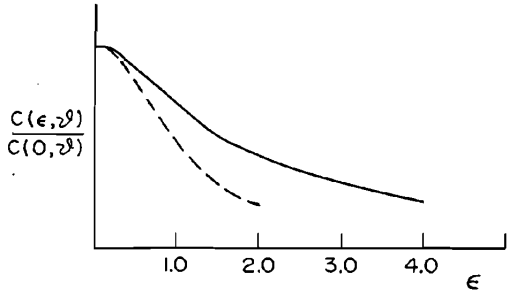

FIG. 4.2. Autocorrelation function in the presence of a doorway state.

angles. It will be observed that after an initial decrease as predicted by (4.31), $C(\varepsilon, \theta)$ fluctuate about the zero value. These fluctuations are referred to as *finite range deviations* (FRDs) and arise from the fact that a finite energy range was used in making the averages and correlations. The requisite corrections have been developed by Böhning (66). Fitting the small ε part of the results in Fig. 4.4 gives a mean value of Γ of about 18 keV.

On examining Fig. 4.3, it is quite clear that there is considerable angular correlation. For example, the peak at about 11.5 MeV proton energy at the laboratory angle $\theta = 175°$ also appears at 170°, 162°, and 157°. Angular correlations are to be expected simply from the complexity theorem mentioned in Chapter I and by (1.10). This states that if there are maximum values of the orbital angular momentum in either the entrance or exit channel, there is a

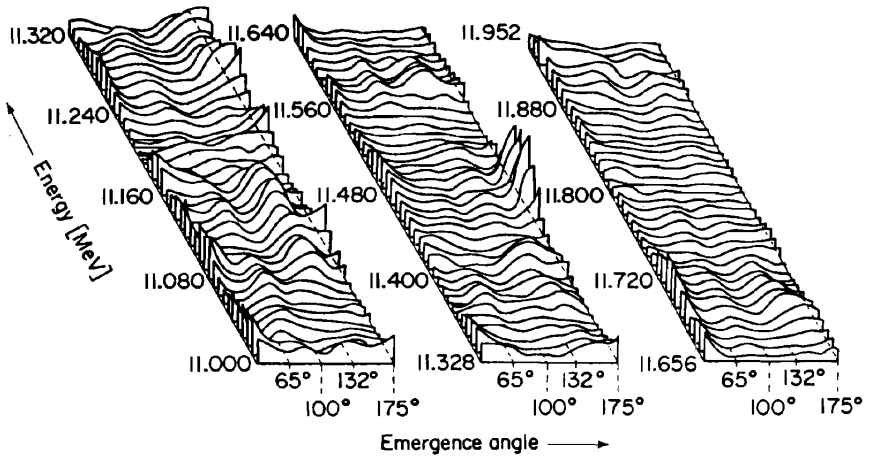

FIG. 4.3. Three-dimensional representation of the variation of the angular distribution of the α-particles emerging from the reaction $^{37}Cl(p, \alpha)^{34}S$ and proceeding to the ground state of ^{34}S, shown as a function of energy between 11.000 and 11.952 MeV in steps of 0.008 MeV [von Witsch, von Brentano et al. (66).]. [From Marmier and Sheldon (70).]

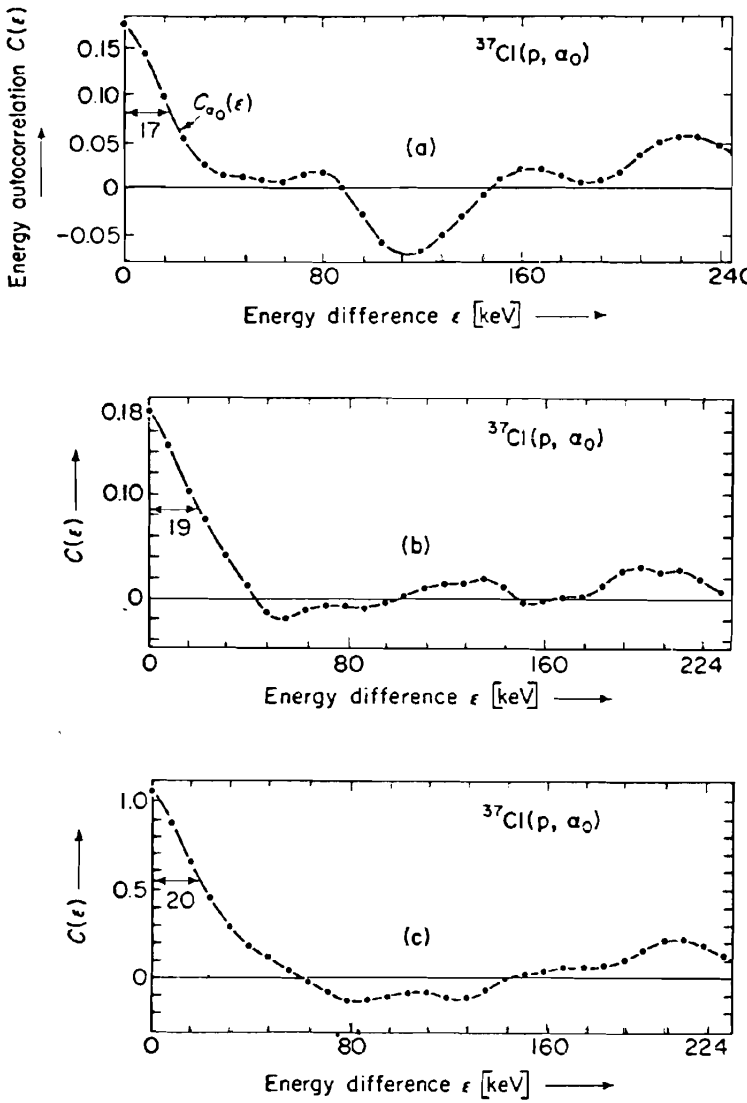

FIG. 4.4. Energy autocorrelation functions $C(\varepsilon)$ plotted as a function of the energy difference ε for (*a*) $\theta = 33°$, (*b*) $\theta = 80°$, (*c*) $\theta = 175°$ (CM) in the case of the $^{37}Cl(p, \alpha_0)^{34}S$ reaction proceeding to the ground state of ^{34}S. The coherence energy Γ can be derived from the width at half-height of the first peak; the results indicate that $\Gamma = 18$ keV, which corresponds to a mean lifetime for the compound nucleus $^{38}Ar^*$ of $\tau = \hbar/\bar{\Gamma} = 3.7 \times 10^{-20}$ s [von Witsch, von Brentano, et al (66).]. [From Marmier and Sheldon (70).]

maximum value of the order, L, of the Legendre polynomial P_L required to describe the angular distribution of the reaction. Well above the Coulomb barrier, these maxima values are set by the angular momentum barrier. If the momentum change is q, then

$$\frac{qR}{\hbar} \simeq l_{\max}\theta \approx 1 \tag{4.32}$$

Experimental verification of the validity of this remark has been given by Dearnley, Gibbs, Leachman, and Rogers (65).

We observe that there are two causes of angular fluctuations. One, just discussed, is a consequence of the finite size of the nuclear system. The second, which originates in the energy fluctuations, affects the differential cross section $d\sigma/d\Omega$. The appropriate correlation function is defined as follows:

$$C(\theta,\theta') = \frac{\langle (d\sigma^{(\mathrm{FL})}/d\Omega)(d\sigma^{(\mathrm{FL})}/d\Omega')\rangle - \langle d\sigma^{(\mathrm{FL})}/d\Omega\rangle\langle d\sigma^{(\mathrm{FL})}/d\Omega'\rangle}{\langle d\sigma/d\Omega\rangle\langle d\sigma/d\Omega'\rangle} \tag{4.33}$$

The averages in (4.33) are energy averages. This correlation function can be evaluated using the expression for the $\mathscr{T}$ matrix, (1.5). We shall not carry that calculation out but will leave it as an exercise for the reader who may be helped by the following derivation of $\langle d\sigma/d\Omega\rangle$. According to (1.5),

$$\langle d\sigma^{(\mathrm{FL})}/d\Omega\rangle = \frac{4\pi^3}{k^2}\frac{1}{(2i+1)(2I+1)}\sum (l_1 s J_1 \| Y_L \| l_2 s J_2)(l_1' s' J_1 \| Y_L \| l_2' s_2' J_2)$$
$$\times \langle \mathrm{Re}[\mathscr{T}^{(\mathrm{FL})}(l_1', s'; l_1 s; J, \Pi_1)\mathscr{T}^{(\mathrm{FL})*}(l_2', s'; l_2 s; J_2 \Pi_2)\rangle P_L(\cos\theta) \tag{4.34}$$

To evaluate the average we make use of the random-phase approximation, which in the present context takes the form

$$\langle \mathrm{Re}(\mathscr{T}^{(\mathrm{FL})}\mathscr{T}^{(\mathrm{FL})*})\rangle = \delta(l_1', l_2')\delta(l_1, l_2)\delta(J_1, J_2)\delta(\Pi_1, \Pi_2)\langle |\mathscr{T}^{(\mathrm{FL})}(l_1' s'; l_1, s; J_1 \Pi_1)|^2\rangle$$
$$\left\langle \frac{d\sigma^{(\mathrm{FL})}}{d\Omega} \right\rangle = \frac{4\pi^3}{k^2}\frac{1}{(2I+1)(2i+1)}\sum (lsJ \| Y_L \| lsJ)(l's'J \| Y_L \| l's'J)$$
$$\times \langle |\mathscr{T}^{(\mathrm{FL})}(l's'; ls; J\Pi)|^2\rangle P_L(\cos\theta) \tag{4.35}$$

From the properties of the reduced matrix elements of Y_L, it follows that L is even, so that $\langle d\sigma^{(\mathrm{FL})}/d\Omega\rangle$ is symmetric about 90°. Later in this chapter we describe how to evaluate $\langle |\mathscr{T}^{(\mathrm{FL})}|^2\rangle$ using the statistical theory of nuclear reactions.

5. LEVEL DENSITY‡

In considering reactions that lead to highly excited states of residual nuclei, it is usually neither practical nor desirable to observe the cross sections for the excitation of a particular state. Generally, the experimental energy resolution, ΔE, is not sufficiently small to permit the selection of a given final state or to go on to define its properties such as spin, parity, moments, and so on. Under these circumstances the summation in the expression for the cross section

$$\sigma = \frac{4\pi^3}{k^2} \sum_f |\mathscr{T}_{fi}|^2 \tag{5.1}$$

where f designates the final states of the system contained in the energy interval ΔE, is replaced by an integral as follows:

$$\sigma = \frac{4\pi^3}{k^2} \int dE_f \omega(E_f) |\mathscr{T}_{fi}|^2 \tag{5.2}$$

Here $\omega(E_f)$ is the level density of the residual nucleus. The quantity $\omega(E)\,dE$ gives the number of levels between E and $E + dE$. It is, of course, possible to partition the density further by asking, for example, for the density of levels with a given quantum number, such as the spin, J, or with a given set of quantum numbers, J, Π, T, and so on.

We shall also be interested in the density of levels at a particular energy of excitation of the compound nucleus. Except for a relatively small energy range, in which the resonances can be individually observed, it is generally not possible to determine the properties of the individual resonances, and a more global approach in which the occurrence of resonances is given by a level density is preferred.

In both cases, density of levels in the compound or in the residual nucleus, the energy spectrum is taken to be discrete. This certainly can be the case for the residual nucleus. For the compound nucleus, the levels are taken to be the levels of the states of the system in what was designated in Chapter III as the $\mathscr{Q}$ space. This Hilbert space is defined as containing those states in which no part of the system is in the continuum, so that $\mathscr{Q}$ is the closed-channel subspace. Because of this restriction, the energies of the $\mathscr{Q}$ space form a discrete spectrum even though the energy of the system is positive. The levels in $\mathscr{Q}$ space become observable resonances with finite widths, when one includes the effect of the coupling to the open-channel subspace designated by $\mathscr{P}$.

For a discrete energy spectrum with energies ε_j, the level density $\omega(E)$ is given exactly by

$$\omega(E) = \sum_j \delta(E - \varepsilon_j) \tag{5.3}$$

‡Ericson (60c); Bloch (69, 72); Huizenga and Moretto (72); Huizenga (72).

where

$$\int_{E_2}^{E_1} \omega(E)\,dE = N(E_1) - N(E_2) \tag{5.4}$$

$N(E)$ gives the total number of levels with energies less than E.

Equation (5.3) is exact. Using an integral representation of ω which follows from (5.3), it will be possible in the limit of large E to obtain a continuous approximation to the series of delta functions. Toward this end introduce the Fourier representation of $\delta(E-\varepsilon_j)$:

$$\delta(E-\varepsilon_j) = \frac{1}{2\pi}\int_{-\infty}^{\infty} e^{-i\kappa(E-\varepsilon_j)}\,d\kappa$$

so that

$$\omega(E) = \frac{1}{2\pi}\int_{-\infty}^{\infty} e^{-i\kappa E}\left(\sum_j e^{i\kappa\varepsilon_j}\right)d\kappa$$

Letting $\kappa = i\beta$,

$$\omega(E) = \frac{1}{2\pi i}\int_{-i\infty}^{i\infty} e^{\beta E} Z(\beta)\,d\beta \tag{5.5}$$

where $Z(\beta)$ is the partition sum:

$$Z(\beta) = \sum_j e^{-\beta\varepsilon_j} = \mathrm{tr}(e^{-\beta H}) \tag{5.6}$$

the trace is restricted to the states in $\mathcal{Q}$. The partition sum is a familiar object in statistical mechanics and one is tempted to relate the integration variable, β, with the inverse of the temperature. That would be the case if the system were in contact with a heat bath and if one could describe the excited nucleus as an equibrated system.

In the limit of large E, the method of steepest descents [Morse and Feshbach ((53), 437 et seq.)] can be used to obtain an approximate evaluation of the integral in (5.5). Rewriting the integrand as $\exp[\beta E + \ln Z(\beta)]$, we expand the bracketed expression around the saddle point, β_0, defined to be a point at which the derivative of $\beta E + \ln Z(\beta)$ with respect to β is zero.

$$E + \frac{d\ln Z(\beta)}{d\beta} = 0 \qquad \text{at } \beta = \beta_0$$

The integral for $\omega(E)$ is then approximately given by

$$\omega(E) = \frac{1}{2\pi} e^{\beta_0 E} Z(\beta_0)\int_{-\infty}^{\infty} \exp\left[-\frac{1}{2}\left|\frac{d^2\ln Z}{d\beta_0^2}\right|(\beta-\beta_0)^2\right]d\beta$$

where we have assumed it to be possible to deform the path of integration from the pure imaginary axis to the real one in the neighborhood of $\beta = \beta_0$. Hence

$$\omega \simeq \left[\frac{1}{2\pi|d^2 \ln Z/d\beta_0^2|}\right]^{1/2} e^{\beta_0 E} Z(\beta_0) = \left[\frac{1}{2\pi|dE/d\beta_0|}\right]^{1/2} e^{\beta_0 E} Z(\beta_0) \tag{5.7}$$

This result, providing a continuous function approximating the ω that is given in (5.3) by a series of δ functions, can be valid only for sufficiently large energy E. The energy interval around E over which expression (5.3) has been effectively averaged to obtain (5.7) should contain a sufficiently large number of levels.

Problem. Show that

$$E = \frac{\sum \varepsilon_j e^{-\beta_0 \varepsilon_j}}{\sum e^{-\beta_0 \varepsilon_j}} \equiv \langle \varepsilon_j(\beta_0) \rangle \tag{5.8}$$

and

$$\frac{d^2 \ln Z}{d\beta_0^2} = \langle \varepsilon_j^2 \rangle - \langle \varepsilon_j \rangle^2 \tag{5.9}$$

where

$$\langle \varepsilon_j^2 \rangle = \frac{\sum \varepsilon_j^2 e^{-\beta_0 \varepsilon_j}}{\sum e^{-\beta_0 \varepsilon_j}} \tag{5.10}$$

Equation (5.7) for ω does not explicitly take into account constraints that can be imposed on the system because of conservation conditions. For example, one might ask for the level density for a system consisting of a given number, N, of nucleons, or for a system whose angular momentum is J, and so on. In what follows we generalize the discussion leading to (5.7) asking for the density $\omega(E, N)$.

The density $\omega(E, N)$ is given by

$$\omega(E, N) = \sum_{j,\nu} \delta(\nu - N)\delta(E - \varepsilon_j(\nu)) \tag{5.11}$$

where, as indicated, ε_j is a function of the number of nucleons. Introducing the Fourier integral representation of the δ functions, one is immediately led to the analog of (5.5):

$$\omega(E, N) = \frac{1}{(2\pi i)^2} \int_{-i\infty}^{i\infty} d\beta_1 \int_{-i\infty}^{i\infty} d\beta_2 Z(\beta_1, \beta_2) e^{\beta_1 E - \beta_2 N} \tag{5.12}$$

where

$$Z(\beta_1, \beta_2) = \sum_{j,\nu} e^{\beta_2 \nu - \beta_1 \varepsilon_j(\nu)} \tag{5.13}$$

The method of steepest descents applied to the integral in (5.12) yields

$$\omega(E, N) = \frac{1}{2\pi |\det L|^{1/2}} Z(\beta_1^{(0)}, \beta_2^{(0)}) e^{\beta_1^{(0)} E - \beta_2^{(0)} N} \tag{5.14}$$

where the saddle-point values of β_1 and $\beta_2, \beta_1^{(0)}$ and $\beta_2^{(0)}$, respectively, are determined by the equations

$$E + \frac{\partial}{\partial \beta_1} \ln Z(\beta_1^{(0)}, \beta_2^{(0)}) = 0 \tag{5.15}$$

$$N - \frac{\partial}{\partial \beta_2} \ln Z(\beta_1^{(0)}, \beta_2^{(0)}) = 0 \tag{5.16}$$

and

$$L_{ij} = \frac{\partial^2 \ln Z(\beta_1, \beta_2)}{\partial \beta_i \partial \beta_j} \tag{5.17}$$

A. The Level Density for the Independent Particle Model

Let us suppose that N nucleons move independently in an average one-body potential [see Chapter V) in deShalit and Feshbach (74)]. Suppose, moreover, that the one-body energy levels in this potential are given by $\varepsilon_1, \varepsilon_2, \ldots$. Because of the Pauli exclusion principle, the number of nucleons in each level is either zero or 1, where we are using the m-representation [deShalit and Feshbach (74, p. 221)]. Then

$$\Sigma n_s = N \tag{5.18}$$

$$\sum n_s \varepsilon_s = E \tag{5.19}$$

The partition sum, (5.13), is

$$Z(\beta_1, \beta_2) = \sum_{\text{all } n_s} \exp[\beta_2 \sum n_s - \beta_1 \sum n_s \varepsilon_s] = \sum_{\text{all } n_s} \exp\left[\sum_s (\beta_2 - \beta_1 \varepsilon_s) n_s\right] \tag{5.20}$$

or

$$Z(\beta_1, \beta_2) = \prod_s (1 + e^{(\beta_2 - \beta_1 \varepsilon_s)}) \tag{5.21}$$

Further development requires assumptions regarding ε_s. We shall assume that

the spectrum ε_s can be replaced by a smoothly varying continuous spectrum as indicated by the Fermi-gas model [see Chapter II in deShalit and Feshbach (74)]. Then

$$\ln Z(\beta_1, \beta_2) = \sum_s \ln(1 + e^{(\beta_2 - \beta_1 \varepsilon_s)}) \rightarrow \int_{\varepsilon_0}^{\infty} \omega(\varepsilon) \ln(1 + e^{(\beta_2 - \beta_1 \varepsilon)})\, d\varepsilon \tag{5.22}$$

where ε_0 is the smallest value of ε_s. This integral will be evaluated for large β_2 and β_1. The validity of this assumption will be justified *a posteriori*. Under these circumstances the exponential, $\exp(\beta_2 - \beta_1 \varepsilon)$, will for small or negative values of ε, be much larger than unity, so that the logarithm in (5.22) is approximately equal to $\beta_2 - \beta_1 \varepsilon$. For large values of ε, the exponential will be negligible and the logarithm will tend to zero. The drop to zero occurs precipitously for large values of β_2 and β_1, at

$$\varepsilon_F \equiv \frac{\beta_2}{\beta_1} \tag{5.23}$$

As the notation indicates, for the saddle-point values of β_2 and β_1, the ratio equals the Fermi energy.

In this limit

$$\ln Z \underset{\beta_2, \beta_1 \gg 1}{\longrightarrow} F^{(\infty)} \equiv \int_{\varepsilon_0}^{\varepsilon_F} \omega(\varepsilon)(\beta_2 - \beta_1 \varepsilon)\, d\varepsilon$$

or

$$F^{(\infty)} = \beta_2 N(\varepsilon_F) - \beta_1 W(\varepsilon_F) \tag{5.24}$$

where

$$N(\varepsilon_F) \equiv \int_{\varepsilon_0}^{\varepsilon_F} \omega(\varepsilon)\, d\varepsilon \tag{5.25a}$$

gives the number of single-particle states up to ε_F, while

$$W(\varepsilon_F) \equiv \int_{\varepsilon_0}^{\varepsilon_F} \varepsilon \omega(\varepsilon)\, d\varepsilon \tag{5.25b}$$

gives the total energy of these states.

The next order is obtained by evaluating

$$\ln Z - F^{(\infty)} = \int_{\varepsilon_F}^{\infty} \omega(\varepsilon) \ln(1 + e^{\beta_2 - \beta_1 \varepsilon})\, d\varepsilon + \int_{\varepsilon_0}^{\varepsilon_F} \omega(\varepsilon) \ln(1 + e^{-\beta_2 + \beta_1 \varepsilon})\, d\varepsilon$$

In the first integral let $\beta_1\varepsilon - \beta_2 = x$ and in the second $\beta_2 - \beta_1\varepsilon = x$. Then

$$\ln Z - F^{(\infty)} = \frac{1}{\beta_1}\int_0^\infty \omega\left(\frac{x}{\beta_1} + \varepsilon_F\right)\ln(1 + e^{-x})\,dx + \frac{1}{\beta_1}\int_0^{\beta_2 - \beta_1\varepsilon_0} \omega\left(-\frac{x}{\beta_1} + \varepsilon_F\right)\ln(1 + e^{-x})\,dx$$

As β_1 increases, taking ε_0 to be negative, to $O(1/\beta_1)$, one obtains

$$\ln Z - F^{(\infty)} \simeq \frac{2\omega(\varepsilon_F)}{\beta_1}\int_0^\infty \ln(1 + e^{-x})\,dx = \frac{(\pi^2/6)\omega(\varepsilon_F)}{\beta_1}$$

Combining this with (5.24) for $F^{(\infty)}$ yields

$$\ln Z \simeq \beta_2 N(\varepsilon_F) - \beta_1 W(\varepsilon_F) + \frac{(\pi^2/6)\omega(\varepsilon_F)}{\beta_1} \qquad \varepsilon_F \equiv \frac{\beta_2}{\beta_1} \tag{5.26}$$

This result can now be substituted in (5.15) and (5.16), determining the saddle-point values of $\beta_1^{(0)}$ and $\beta_2^{(0)}$. Take, for example, (5.1):

$$N = \frac{\partial \ln Z}{\partial \beta_2} \simeq N(\varepsilon_F) + \frac{\pi^2}{6\beta_1^2}\omega'(\varepsilon_F)$$

For large values of β_1 and smooth single-level density ω,

$$N \simeq N(\varepsilon_F) \tag{5.27}$$

so that indeed ε_F is, to this approximation, the Fermi energy. In the same approximation, (5.16),

$$E = W(\varepsilon_F) + \frac{\pi^2}{6}\frac{\omega(\varepsilon_F)}{\beta_1^2} + \text{terms in } \omega'(\varepsilon_F) + \cdots \tag{5.28}$$

Since $W(\varepsilon_F)$ is the energy of the Fermi gas in its ground state, the excitation energy U is given by

$$U = \frac{\pi^2}{6}\frac{\omega(\varepsilon_F)}{\beta_1^2} \tag{5.29}$$

The two equations $\beta_2/\beta_1 = \varepsilon_F$ and (5.29) then determine both β_2 and β_1.

We also need to compute the determinant L, whose elements are given by (5.17). The second derivatives are readily calculated in the limit of β_1 and β_2

large from (5.26) bearing in mind that $\varepsilon_F = \beta_2/\beta_1$. One obtains

$$\frac{\partial^2 \ln Z}{\partial \beta_1^2} = \frac{\omega(\varepsilon_F)}{\beta_1} \qquad \frac{\partial^2 \ln Z}{\partial \beta_1^2} = \left(\frac{\pi^2}{3} + \beta_2^2\right)\frac{\omega(\varepsilon_F)}{\beta_1^3}$$

$$\frac{\partial^2 \ln Z}{\partial \beta_1 \partial \beta_2} = -\frac{\beta_2}{\beta_1^2}\omega(\varepsilon_F)$$

so that

$$\det L = \frac{\pi^2}{3}\left(\frac{\omega(\varepsilon_F)}{\beta_1^2}\right)^2$$

It is now possible to evaluate the right-hand side of (5.14) to obtain $\omega(E, N)$. The result[‡] is [Bethe (37)]

$$\omega(U, N) \simeq \frac{1}{\sqrt{48}U}\exp\left(\frac{\pi^2\omega}{3\beta_1}\right)^{1/2} = \frac{1}{\sqrt{48}U}\exp\left[2\sqrt{\frac{\pi^2\omega(\varepsilon_F)U}{6}}\right] \tag{5.30}$$

where for convenience we have changed the independent variable from E to U. This form is commonly used in the semiempirical description of the density of levels to be discussed. The constant $1/\beta_1$ plays the role of a temperature, t, so that (5.29) relates the temperature and the excitation energy[§]:

$$U = at^2 \tag{5.31}$$

where the Fermi-gas model gives

$$a = \frac{\pi^2\omega(\varepsilon_F)}{6}$$

[‡]Morrison (53) has compared this result and that obtained by Hardy and Ramanujan (18) for the different ways, $p(n)$, to form a given number n by any of the possible sums of smaller integers. For large n they find that

$$p(n) = \frac{1}{\sqrt{48}n}\exp\left[2\left(\frac{\pi^2}{6}n\right)^{1/2}\right]$$

The reader is invited to consider the relationship of this result and (5.30).

[§]A statistical-mechanical definition of temperature T is

$$T^{-1} = \frac{1}{\omega}\frac{\partial \omega}{\partial E} = -\frac{1}{U} + \sqrt{\frac{c}{U}}$$

or approximately,

$$U = c\left(T - \frac{1}{c}\right)^2$$

or

$$t = \left[\frac{6U}{\pi^2 \omega(\varepsilon_F)}\right]^{1/2}$$

Problem. Using (5.21) and $N = \partial \ln Z/\partial \beta_2$, show that

$$N = \sum \frac{1}{1 + e^{\beta_1(\varepsilon_s - \varepsilon_F)}} = \sum \bar{n}(\varepsilon_s)$$

where $\bar{n}(\varepsilon_s)$ is the average occupation number of the one-body state with energy ε_s. Using the continuous approximation for the spectrum of ε_s [see (5.22)], this becomes

$$N = \int_0^\infty \frac{d\varepsilon \omega(\varepsilon)}{1 + e^{\beta_1(\varepsilon - \varepsilon_F)}} = \int_{\varepsilon_0}^\infty d\varepsilon\, \omega(\varepsilon)\bar{n}(\varepsilon)$$

See Fig. 5.1 for a plot of $\bar{n}(\varepsilon)$. Using the approximation developed following (5.22), show that $N = N(\varepsilon_F)$. Show that the number of particles excited above ε_F is

$$\frac{(\ln 2)\omega}{\beta_1}$$

Thus the average number of degrees of freedom (particles plus holes) excited when the excitation energy is U is given by

$$n_s = \frac{(2 \ln 2)\omega}{\beta_1}$$

or

$$n_{\text{exc}} = 2 \ln 2 \sqrt{\frac{6U\omega(\varepsilon_F)}{\pi^2}} \tag{5.32}$$

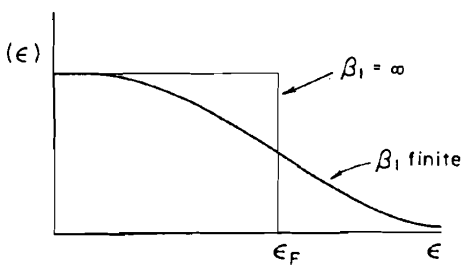

FIG. 5.1. Average occupation number, $\bar{n}(\varepsilon)$ of a one-body state with energy ε for two values of β_1.

If we write the exponent in (5.30) as $2\sqrt{aU}$,

$$n_{\text{exc}} = \frac{12 \ln 2}{\pi^2} \sqrt{aU} = 0.84 \sqrt{aU} \simeq 0.3 \sqrt{AU_{\text{MeV}}}$$

where we have used the empirical $a = A/8$.

It is, of course, clear that (5.30) is incorrect near U equal to zero, that is, when the excitation energy goes to zero, and is applicable only for sufficiently large values of U and N. A comparison of (5.30) with an exact calculation of the density of levels when the single-particle levels are equidistantly spaced is shown on Fig. 5.2. Except at small values of the excitation energy, the agreement is excellent.

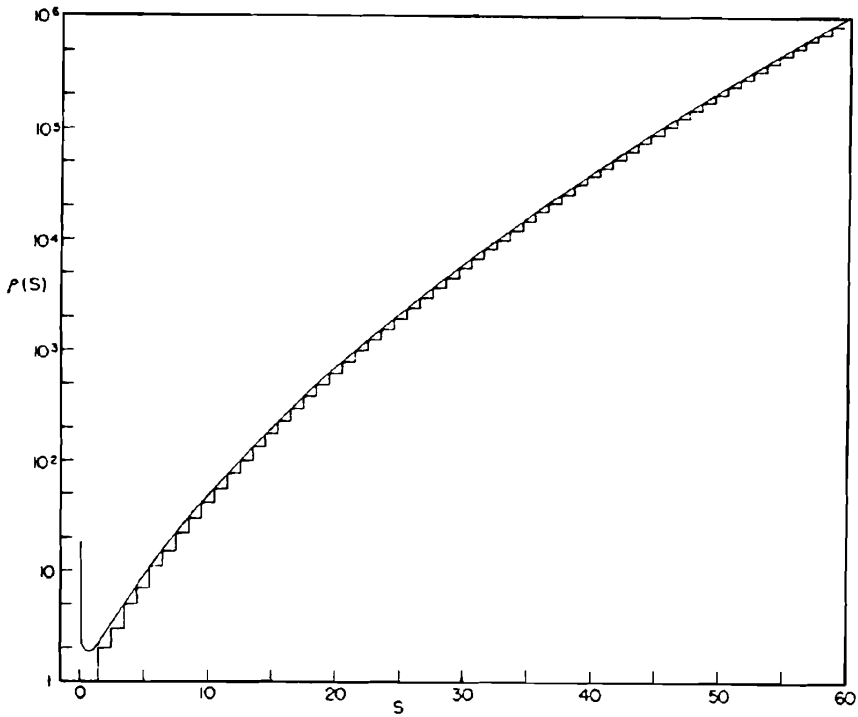

FIG. 5.2. Exact level density per unit single particle spacing for a Fermi system of one kind of particles with equidistant single-particle levels versus excitation energy s in units of this spacing. The solid smooth curve is the approximate solution, (5.30). [From Ericson (60).]

Fluctuations. If these results gave an exact evaluation of the expression (5.11) for $\omega(E, N)$ the value of $(\bar{N})^2$ and of $\overline{N^2}$ would be equal, where

$$\bar{N}\omega(E, N) = \sum_{j,\nu} \nu\delta(\nu - N)\delta(E - \varepsilon_j(\nu))$$

and

$$\overline{N^2}\omega(E, N) = \sum_{j,\nu} \nu^2\delta(\nu - N)\delta(E - \varepsilon_j(\nu))$$

A measure of the accuracy of these calculations is then furnished by the fluctuation defined by

$$\left[\frac{\overline{N^2} - \bar{N}^2}{(\bar{N})^2}\right]^{1/2} = \left[\frac{\overline{(N - \bar{N})^2}}{\bar{N}^2}\right]^{1/2} \equiv \frac{\Delta N}{\bar{N}}$$

From (5.12) and (5.13) we see that

$$\bar{N} = \frac{\int d\beta_1 \int d\beta_2 [\partial Z(\beta_1, \beta_2)/\partial\beta_2] e^{\beta_1 E - \beta_2 N}}{\int d\beta_1 \int d\beta_2 Z(\beta_1, \beta_2) e^{\beta_1 E - \beta_2 N}}$$

Evaluating Z and $\partial Z/\partial\beta_2$ at the saddle point gives the result

$$\bar{N} \simeq \frac{\partial \ln Z(\beta_1, \beta_2)}{\partial\beta_2} \qquad \text{at } \beta_1 = \beta_1^{(0)}, \beta_2 = \beta_2^{(0)}$$

in agreement with (5.16).

The value of $\overline{N^2}$ is similarly given by

$$\overline{N^2} = \frac{\partial^2 Z(\beta_1, \beta_2)/\partial\beta_2^2}{Z(\beta_1, \beta_2)}$$

so that

$$\overline{N^2} - \bar{N}^2 = \frac{\partial^2 \ln Z(\beta_1, \beta_2)}{\partial\beta_2^2}$$

The independent particle model [see below (5.29)] gives

$$\overline{N^2} - \bar{N}^2 = (\Delta N)^2 = \frac{\omega(\varepsilon_F)}{\beta_1}$$

or using (5.29),

$$(\Delta N)^2 = \left[\frac{6U\omega(\varepsilon_F)}{\pi^2}\right]^{1/2}$$

Inserting the Fermi-gas model value for ω,

$$\omega = \frac{3N}{2\varepsilon_F}$$

one obtains

$$(\Delta N)^2 = \left(\frac{9UN}{\pi^2 \varepsilon_F}\right)^{1/2}$$

Introducing u, the excitation energy per nucleon (and replacing $9/\pi^2$ by 1)

$$u = \frac{U}{N}$$

one finally obtains

$$\frac{\Delta N}{N} \simeq N^{-1/2}\left(\frac{u}{\varepsilon_F}\right)^{1/4}$$

indicating the error is least for heavier nuclei and smaller excitation energies. For a further discussion, see Feshbach (88).

B. Angular Momentum Distribution

The level density, $\omega(E, N)$, (5.30), derived just above, takes account of all states regardless of their angular momentum. Because of the important role played by angular momentum barriers as discussed briefly in Section 4, we shall find knowledge of the level density for levels with energy E *and* with angular momentum J, $\omega(E, N, J)$, essential for the interpretation of nuclear reactions.

In the procedure developed by Bloch (54), one adds to the constraints that the total number of particles be N and that the total energy be E, the constraint that the projection of the total angular momentum along an axis be M; that is, in addition to the conditions given by (5.18) and (5.19), we add

$$M = \sum n_s m_s$$

The resulting level density is $\omega(E, N, M)$. The density we seek $\omega(E, N, J)$ is then given by

$$\begin{aligned}\omega(E, N, J) &= \omega(E, N, M = J) - \omega(E, N, M = J + 1) \\ &\simeq -\left(\frac{\partial \omega(E, N, M)}{\partial M}\right)_{M = J + 1/2}\end{aligned} \tag{5.33}$$

We begin by forming the partition function Z, which will now depend on

three parameters $\beta_1, \beta_2, \beta_3$:

$$Z(\beta_1, \beta_2, \beta_3) = \sum \exp(\beta_2 \nu + \beta_3 M_s(\nu) - \beta_1 \varepsilon_s(\nu))$$

Applying the method of steepest descents [see (5.12)] yields

$$\omega(E, N, M) = \frac{1}{(2\pi)^{3/2} |\det L|^{1/2}} Z(\beta_1^{(0)}, \beta_2^{(0)}, \beta_3^{(0)}) e^{\beta_1^{(0)} E - \beta_2^{(0)} N - \beta_3^{(0)} M} \tag{5.34}$$

where $\beta_i^{(0)}$, the saddle-point values of β_i, satisfy (5.15) through (5.17) and the additional equation

$$\frac{\partial \ln Z}{\partial \beta_3} = M \tag{5.35}$$

The generalization of (5.22) becomes

$$\ln Z = \sum_m \int \omega(\varepsilon, m) \ln(1 + e^{\beta_3 m + \beta_2 - \beta_1 \varepsilon}) \, d\varepsilon \tag{5.36}$$

where $\omega(\varepsilon, m)$ is the single-particle level density for particles of energy ε and projected angular momentum m. The evaluation of the integral in (5.36) proceeds according to method described above following (5.23). One obtains

$$\ln Z = \sum_m \left\{ (\beta_2 + \beta_3 m) N_m(\varepsilon_F(m)) - \beta_1 W_m(\varepsilon_F(m)) + \frac{\pi^2}{6} \frac{\omega(\varepsilon_F(m), m)}{\beta_1} \right\} \tag{5.37}$$

where

$$N_m(\varepsilon_F(m)) = \int_{\varepsilon_0}^{\varepsilon_F(m)} \omega(\varepsilon, m) \, d\varepsilon \tag{5.38a}$$

$$W_m(\varepsilon_F(m)) = \int_{\varepsilon_0}^{\varepsilon_F(m)} \varepsilon \omega(\varepsilon, m) \, d\varepsilon \tag{5.38b}$$

where the Fermi energy $\varepsilon_F(m)$ is defined by

$$\varepsilon_F(m) \equiv \frac{\beta_2 + \beta_3 m}{\beta_1} \tag{5.39}$$

We now define a Fermi energy independent of m, ε_F, by averaging $\varepsilon_F(m)$ over m:

$$\varepsilon_F \equiv \frac{\beta_2 + \beta_3 \bar{m}}{\beta_1} \tag{5.40}$$

where

$$\bar{m} = \frac{\sum m\omega(\varepsilon_F(m), m)}{\sum \omega(\varepsilon_F(m), m)}$$

or using

$$\omega(\varepsilon_F) = \sum_m \omega(\varepsilon_F(m), m) \tag{5.41}$$

$$\bar{m} = \frac{\sum m\omega(\varepsilon_F(m), m)}{\omega(\varepsilon_F)} \tag{5.42}$$

Similarly,

$$\overline{m^2} = \frac{\sum m^2\omega(\varepsilon_F(m), m)}{\omega(\varepsilon_F)} \tag{5.43}$$

Finally, the functions N and W of the preceding section are given by

$$N(\varepsilon_F) = \sum_m N_m(\varepsilon_F) \tag{5.44}$$

and

$$W(\varepsilon_F) = \sum_m W_m(\varepsilon_F) \tag{5.45}$$

Inserting these relations into (5.37) yields

$$\ln Z = \beta_2 N(\varepsilon_F) + \beta_3 M(\varepsilon_F) - \beta_1 W(\varepsilon_F) + \frac{1}{2\beta_1}\omega(\varepsilon_F)\left[\frac{\pi^2}{3} + \beta_3^2(\overline{m^2} - \bar{m}^2)\right] \tag{5.46}$$

where a Taylor expansion of $N_m(\varepsilon_F(m)$ to first order and $W_m(\varepsilon_F(m))$ to second order has been used:

$$N_m(\varepsilon_F(m)) = N_m\left(\frac{\beta_3 m + \beta_2}{\beta_1}\right) \simeq N_m(\varepsilon_F) + \frac{\beta_3}{\beta_1}(m - \bar{m})\omega(\varepsilon_F(m), m)$$

Terms up to $\omega(\varepsilon_F(m), m)$, but not including its derivatives, have been taken into account.

Using the conditions (5.15), (5.16), and (5.35), one obtains

$$\begin{aligned} E &= W(\varepsilon_F) + \frac{\omega(\varepsilon_F)}{2\beta_1^2}\left[\frac{\pi^2}{3} + \beta_3^2(\overline{m^2} - \bar{m}^2)\right] \\ N &= N(\varepsilon_F) \\ M &= M(\varepsilon_F) + \frac{\beta_3\omega(\varepsilon_F)}{\beta_1}(\overline{m^2} - \bar{m}^2) \end{aligned} \tag{5.47}$$

The last equation can be solved for β_3 and the result introduced into (5.46) as follows:

$$\beta_3 = \frac{\beta_1 \Delta M}{\omega(\varepsilon_F)(\overline{m^2} - \bar{m}^2)}$$

$$\Delta M \equiv M - M(\varepsilon_F)$$

and

$$U = E - W(\varepsilon_F) = \frac{\pi^2}{6\beta_1^2}\omega(\varepsilon_F) + \frac{\frac{1}{2}(\Delta M)^2}{\mathscr{I}} \tag{5.48}$$

$$\mathscr{I} \equiv \omega(\varepsilon_F)(\overline{m^2} - \bar{m}^2) \tag{5.49}$$

The second term in (5.48) can be interpreted as the rotation kinetic energy of excitation, where $\mathscr{I}$ is the moment of inertia about the axis upon which the angular momentum is projected, an identification that requires justification.

Problem. Prove that $\mathscr{I}$ approximately equals the rigid moment of inertia for a spherical nucleus. Use

$$\omega(\varepsilon_F) = \frac{3}{2}\frac{A}{\varepsilon_F} \tag{5.50}$$

and

$$\overline{m^2} \simeq \overline{(xp_y - yp_x)^2}$$

It is now a straightforward calculation to obtain the level density by using the results above in (5.34). We find that

$$\omega(E, N, M) = \frac{1}{(2\pi)^{3/2}[(\pi^2/3)(\omega(\varepsilon_F)/\beta_1^2)^2(\mathscr{I}/\beta_1)]^{1/2}} \exp\left[\frac{\pi^2}{3}\frac{\omega(\varepsilon_F)}{\beta_1}\right] \tag{5.51}$$

Inserting the value of β_1 from (5.48) and differentiating the result according to (5.33) to obtain $\omega(E, N, J)$, one obtains

$$\omega(U, N, J) = \frac{2J+1}{2} \frac{\omega(U - \mathscr{R}, N)}{[2\pi\mathscr{I}^3((6/\pi^2\omega(\varepsilon_F))(U - \mathscr{R}))^{3/2}]^{1/2}} \tag{5.52}$$

where again the independent variable E has been replaced by U. In this equation, $\omega(U, N)$ is given by (5.30), and

$$\mathscr{R} = \frac{(J + \frac{1}{2})^2}{2\mathscr{I}} \tag{5.53}$$

is the rotational energy. In obtaining (5.52), $M(\varepsilon_F)$ has been placed equal to zero, as would be the case when the ground-state spin is zero. Note again that this expression fails when U equals $\mathscr{R}$, that is, on the Yrast line.‡

When $\mathscr{R}$ is small compared to U, that is, away from the Yrast line, we can expand (5.52) about $\mathscr{R} = 0$ to obtain

$$\omega(U, N, J) = \frac{2J+1}{\sqrt{8\pi\sigma^3}} \omega(U, N) e^{-[J+(1/2)]^2/2\sigma^2} \tag{5.54}$$

where [see below (5.32)]

$$\sigma^2 \equiv \mathscr{I}\left(\frac{6U}{\pi^2 \omega(\varepsilon_F)}\right)^{1/2} = \mathscr{I}\left(\frac{U}{a}\right)^{1/2} \tag{5.55}$$

Problem. Prove that

$$\sum_J (2J+1)\omega(E, N, J) \to \int_0^\infty dJ(2J+1)\omega(U, N, J) = \omega(U, N)$$

Problem. Show from (5.51) that

$$\omega(U, N, M) = \frac{1}{\sqrt{2\pi}} \frac{\omega(U - \frac{1}{2}(\Delta M^2/\mathscr{I}), N)}{[\mathscr{I}((6/\pi^2\omega(\varepsilon_F))(U - \frac{1}{2}(\Delta M^2/\mathscr{I}))^{1/2}]^{1/2}}$$

In the limit of $\frac{1}{2}(\Delta M)^2/\mathscr{I} \ll U$,

$$\omega(U, N, M) = \frac{1}{\sqrt{2\pi}\sigma} \omega(U, N) e^{-(\Delta M)^2/2\sigma^2} \tag{5.54'}$$

Thus in this approximation the angular momentum distribution is a Gaussian with a root-mean-square derivation, σ, given by (5.55), which increases with increasing excitation energy. One can expect [see (3.4)] that the absorption cross section will decrease when J exceeds σ. This is simply the statement that it will be much less probable for the angular momenta of the individual nucleons to line up to obtain a given J as J increases. However, the probability improves if the excitation energy increases since a greater variation in the values of the angular momenta for the individual nucleons occurs.

‡The Yrast line is defined as the curve in the (U, J) plane giving the lowest possible value of J for a given value of U.

C. Rotational Nuclei

In addition to the total angular momentum I, the state of rotational nuclei are characterized by the quantum number K [see (VI.3.30) in deShalit and Feshbach (74)], the projection of I on the body-fixed axis of symmetry, assuming axially symmetric nuclear deformation. We can now ask for the density of levels with a given I and K.

Since K is a projection, approximation (5.54) can be used:

$$\omega(U, N, K) = \frac{1}{\sigma_k \sqrt{2\pi}} \omega(U, N) \exp\left(-\frac{K^2}{2\sigma_K^2}\right) \tag{5.56}$$

where σ_K is given by (5.55), employing for $\mathscr{I}$ the moment of inertia about the symmetry axis. The density of levels for a given value of I is then obtained by summing:

$$\omega(U, N, I) = \tfrac{1}{2} \sum_{K=-I}^{I} \omega(U - \mathscr{R}(K, I), N, K) \tag{5.57}$$

where $\mathscr{R}$ is the rotational energy associated with rotation about the axes perpendicular to the symmetry axis [see (VI.2.12) in deShalit and Feshbach (74)]:

$$\mathscr{R} = \frac{1}{2\mathscr{I}_\perp}[(I)(I+1) - K^2]$$

and $\mathscr{I}_\perp$ is the appropriate moment of inertia. The factor of $\frac{1}{2}$ takes into account the fact that the sum includes both K and $-K$. Inserting this value for $\mathscr{R}$ and using the approximation $\mathscr{R} \ll U$ yields

$$\omega(U, N, I) = \frac{1}{\sqrt{8K}\sigma_K} \omega(U, N) \sum_{K=-I}^{I} e^{-(1/2\sigma_\perp^2)(I)(I+1) - (1/2)(1/\sigma_K^2 - 1/\sigma_\perp^2)K^2} \tag{5.58}$$

where $\sigma_\perp^2$ is given by (5.55) with $\mathscr{I}$ replaced by $\mathscr{I}_\perp$. The factor multiplying K^2 in the exponent depends on the difference $(1/\mathscr{I}_K - 1/\mathscr{I}_\perp)$. In a rigid body in the shape of a prolate spheroid,

$$\mathscr{I}_K = \mathscr{I}_{\text{sph}}(1 - \tfrac{2}{3}\delta) \qquad \mathscr{I}_\perp = \mathscr{I}_{\text{sph}}(1 + \tfrac{1}{3}\delta) \tag{5.59}$$

where δ is the eccentricity parameter [see deShalit and Feshbach (74, p. 416)] and $\mathscr{I}_{\text{sph}}$ is the moment of inertia of a rigid sphere of radius R_0 where R_0 is the mean radius [see deShalit and Feshbach (74, p. 415)]. Then

$$\frac{1}{\mathscr{I}_K} - \frac{1}{\mathscr{I}_\perp} = \frac{1}{\mathscr{I}_{\text{sph}}} \frac{\delta}{(1 - \frac{2}{3}\delta)(1 + \frac{1}{3}\delta)}$$

A contribution to the energy of rotation coming from rotation about the symmetry axis is possible only at excitations sufficiently great that pairing effects are reduced. Under these circumstances, the superfluidity [see deShalit and Feshbach (74, p. 568)] thought to be responsible for condition equation (VI.4.1) in deShalit and Feshbach will be correspondingly less and this moment of inertia, $\mathcal{I}_K$, will approach the rigid value, (5.59). More explicitly, if the average number of unpaired particles is ν and the average value of K^2 for one particle is K_1^2, then

$$\sigma_K^2 = \nu K_1^2 = \mathcal{I}_K \left[\frac{6U}{\pi^2 \omega(\varepsilon_F)} \right]^{1/2}$$

At low energies the number of unpaired particles goes rapidly to zero, so that $\mathcal{I}_K$ is reduced from its rigid value, which applies at sufficiently large excitation energies.

The angular distribution of fission fragments depends on the K dependence of $\omega(U, N, I)$, permitting a determination of $\mathcal{I}_K$ from experiment. [See Reising, Bate, and Huizenga (66) and Bohr and Mottelson (75, p. 619); see also Huizenga, Behkamu, et al. (74) and Dφssing and Jensen (74).]

D. Isospin Distribution

The results obtained for the angular momentum distribution, in particular (5.54'), can be quickly adapted to this problem. The level density $\omega(U, N, T_3)$, giving the density of levels at an excitation energy U, number of particles N, and isospin component T_3 [$\equiv \frac{1}{2}(Z - N)$], is

$$\omega(U, N, T_3) = \frac{1}{\sigma_\tau \sqrt{2\pi}} \omega(U, N) \exp\left(-\frac{T_3^2}{2\sigma_\tau^2} \right) \tag{5.60}$$

where

$$\sigma_\tau^2 = (\overline{m_\tau^2} - \bar{m}_\tau^2) \left[\frac{6\omega(\varepsilon_F)U}{\pi^2} \right]^{1/2}$$

Of course, $\bar{m}_\tau^2 = \frac{1}{4}$. Near the Fermi energy,

$$\bar{m}_\tau = \frac{1}{2} \frac{\omega_P(\varepsilon_F) - \omega_N(\varepsilon_F)}{\omega_P(\varepsilon_F) + \omega_N(\varepsilon_F)}$$

where ω_P and ω_N are the single-particle level density for protons and neutrons, respectively. Hence

$$\sigma_\tau^2 = \left[\frac{6\omega(\varepsilon_F)U}{\pi^2} \right]^{1/2} \frac{\omega_N(\varepsilon_F)\omega_P(\varepsilon_F)}{[\omega_N(\varepsilon_F) + \omega_P(\varepsilon_F)]^2} \tag{5.61}$$

where

$$\omega(\varepsilon_F) = \omega_N(\varepsilon_F) + \omega_P(\varepsilon_F)$$

Equation (5.60) becomes

$$\omega(U, N, T_3) = \frac{6^{1/4}}{12}\omega(\varepsilon_F)\left[\frac{\omega^2(\varepsilon_F)}{\omega_N(\varepsilon_F)\omega_P(\varepsilon_F)}\right]^{1/2}[\omega(\varepsilon_F)U]^{-5/4} \times \exp\left[2\sqrt{\frac{\pi^2}{6}\omega(\varepsilon_F)U - \frac{T_3^2}{2\sigma_\tau^2}}\right] \tag{5.60'}$$

All the considerations above are based on the independent particle model of the model; that is, the Hamiltonian is assumed to be given by

$$H = \sum_s a_s^\dagger a_s \varepsilon_s \tag{5.62}$$

where $a_s^\dagger$ and a_s are the Fermion creation and destruction operators associated with a single-particle level of energy ε_s. In addition, it is assumed that single-particle level density is a smooth function of the single-particle energy. Under these circumstances the level density for the nucleus depends primarily on $\omega(\varepsilon_F)$, the single-particle density evaluated at the Fermi energy.‡

Improvements can be obtained by using a more realistic nuclear Hamiltonian and single-particle level density. For example, the single-particle levels of the independent particle shell model are bunched and the possibility of degeneracy is substantially different when a shell is, for example, half filled than when it is completely filled. The assumption of a smooth single particle density is not a good approximation under these conditions. Rosenzweig (57) has, for example, calculated the nuclear level density using a simple model that exhibits both the bunching and variation of degeneracy, characteristic of the shell model. In another, obvious improvement the interactions are taken into account. For example, Hartree–Fock single-particle levels can be inserted in (5.62). Proceeding further, the quasi-particle description of Chapter VII of deShalit and Feshbach (74), which should be especially advantageous in view of the strong dependence of $\omega(U)$ on $\omega(\varepsilon_F)$, can be used. H will now include both the single-particle energies and the pairing Hamiltonian [Moretto (72a, 72b)]. Finally, more sophisticated methods based on the Goldstone linked cluster expansion [Section VII.14 in deShalit and Feshbach (74)] could in principle be adapted for the calculation of nuclear level densities.

‡The saddle-point evaluation of the density of levels is an approximation to the exact density. The latter can be obtained for noninteracting nucleons by using the combinatorial method. This method amounts to finding the number of ways in which the nucleons can be distributed among the single-particle levels for a given energy of the nucleus. A systematic approach to this enumeration has been given by Hillman and Grover (69).

The results of these calculations are not readily summarized by an analytical expression. However, some features that can be readily understood qualitatively emerge. These have formed the basis of a semiempirical description of the nuclear level density.

The major effects of the residual interaction on the nuclear levels of the independent particle shell model include the lifting of degeneracies of that model and the motion of the energy levels to different values of the energy. Of particular importance for our discussion is the substantial descent of some levels, these thereby becoming either the ground state or lying much closer to the ground state. On the other hand, at relatively high excitation energies the motion of the levels does not result in any substantial change in the level density from that predicted by the independent particle model. The two spectra before and after the residual interaction is "turned on" are illustrated in Fig. 5.3. It is clear from the figure that one can use the independent particle model result for $\omega(U)$ for the spectrum of Fig. 5.3*b* for sufficiently large U if U is replaced by $U - \Delta$. In other words, one shifts the ground-state energy from which U is calculated to the value it has before the residual interaction is turned on. This is, of course, not an exact statement, since the differences in the spectra can hardly be expressed by means of only one parameter. However, by choosing an empirical value for Δ, one might expect to be able to match the spectrum of (b) at sufficiently large U. If $\omega_0(U)$ is the level density for the independent particle model, then for sufficiently large U, $\omega_0(U - \Delta)$ is the level density when interactions are taken into account.

This concept of a reference level, differing from the ground state, for the calculation of the effective excitation energy [Hurwitz and Bethe (51)] has been incorporated into (5.52) with Δ as well as a and σ as empirical parameters to be determined from experiment [Huizenga (72)]. The effect of pairing energy on level density can be included in this way. Recall from (II.3.1) in deShalit and Feshbach (74) that the pairing energy is taken to be zero for odd–even nuclei and is given by a positive function of Δ, $\delta(A)$, for odd–odd nuclei and by $-\delta(A)$ for even–even nuclei. Taking the same reference level, that is, the odd–even nucleus, Δ is given by $-\delta(A)$ for odd–odd nuclei and by $\delta(A)$ for even–even nuclei [Ericson (59)].

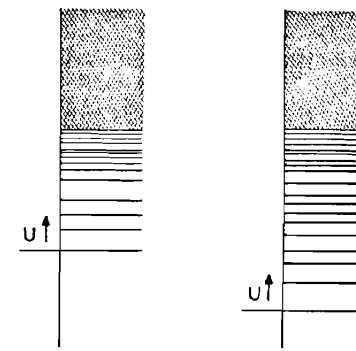

FIG. 5.3. Effect of the residual interactions on the distribution of the nuclear energy levels.

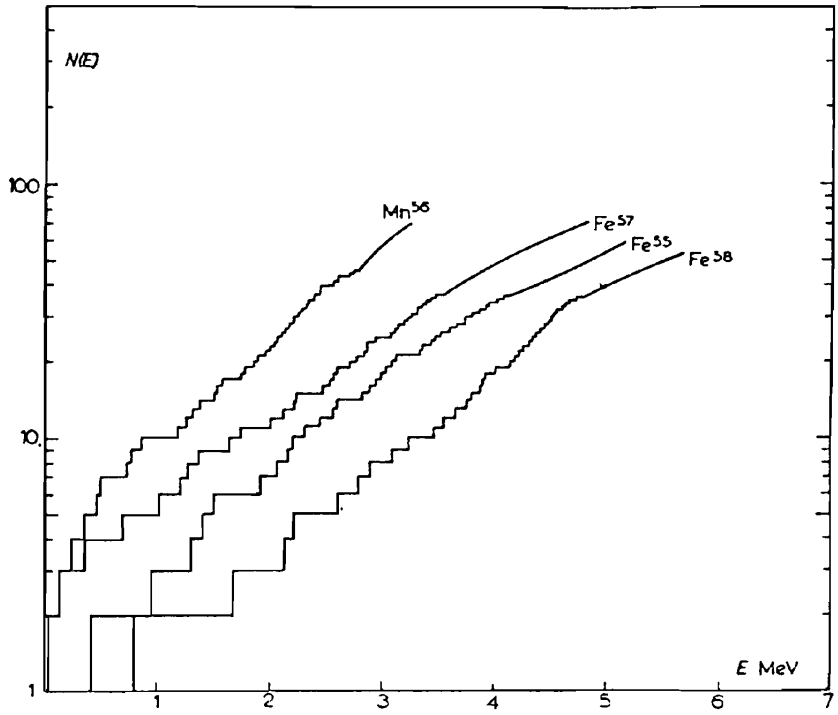

FIG. 5.4. Total number of states up to the excitation energy E for Mn^{56}, Fe^{55}, Fe^{57}, and Fe^{58} versus E. The resolution is somewhat higher in the case of Mn^{56} than for the rest. The figure compares the total numbers of states for even, odd, and odd-mass nuclei. [From Ericson (59).]

The odd–even effect is illustrated in Fig. 5.4, which gives the total number of states up to an excitation energy U for four nuclei: ^{56}Mn (odd, odd), ^{57}Fe (even, odd), ^{55}Fe (even, odd), and ^{58}Fe (even, even). As expected, the odd–odd nucleus has the greatest number of states, the even–even the fewest, while the even–odd nuclei fall in between. The shell model provides a reason that the number of states of ^{57}Fe is greater than that for ^{55}Fe for a given excitation energy; namely, ^{55}Fe has only one neutron outside the closed neutron shell at $N = 28$, while ^{57}Fe has three such neutrons. There is, therefore, a larger number of states that can be formed in ^{57}Fe than in ^{55}Fe.

More quantitatively, one might hope to use the experimental determinations of the level density to obtain the parameters a, σ, and Δ. The systematics of their dependence upon excitation energy, and the mass, Δ, and atomic number, Z, of the nucleus might then provide insights into the properties of excited nuclei. For the most part such systematic studies have not been carried out. Unfortunately, it is often the case that different expressions are used for ω so that the values of a and σ obtained are not immediately comparable.

A compilation [Facchini and Saetta-Memchella (68); Baba (70)] of the values

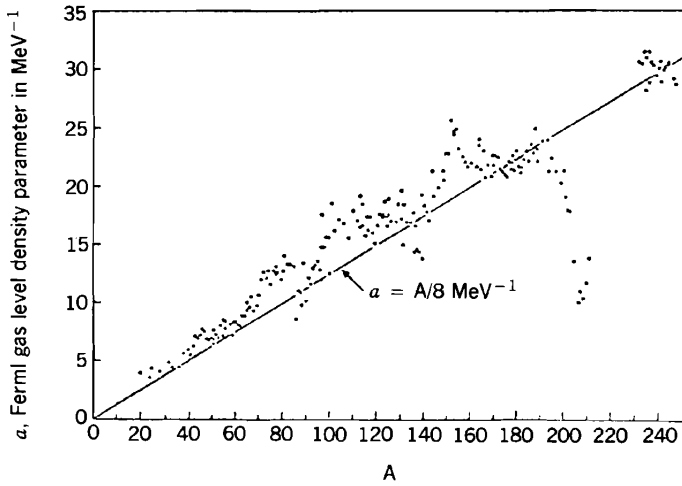

FIG. 5.5. Level density parameter a as a function of atomic mass A [Baba (70)]. [From Huizenga and Moretto (72).]

for a are shown in Fig. 5.5. To obtain these, σ, the spin-cut off parameter, was calculated from (5.55) using the rigid moments of inertia, and Δ was taken to be equal to the pairing energy values given by Gilbert and Cameron (65). We observe that these values of a are marked by substantial deviations from the expected linear dependence on A, (5.50), deviations that are especially large for nuclei near the closed shells. This can be related to the fact that the density of single-particle levels near the Fermi energy is markedly smaller for closed-shell nuclei. The correctness of this analysis is indicated by theoretical level density calculations using the single-particle levels provided by the Nilsson model [see Chapter VI in deShalit and Feshbach (74)] for nuclei close to the doubly magic nucleus ^{208}Pb. The results are shown in Fig. 5.6. As expected, ^{208}Pb has the smallest level density. The level densities for neighboring nuclei increase with increasing distance of the nuclei from ^{208}Pb.

The values of σ that are extracted from those experiments, particularly those sensitive to the value of the maximum angular momentum which can contribute to the reaction cross section, are shown in Fig. 5.7. The excitation energy, U, is approximately 8 MeV. The solid line that gives the value of σ computed using the rigid moment of inertia [Chang (70); Coceva, Corvi, Giacobbe, and Stefanson (72)] is in substantial agreement with the experimental results for $A \leqslant 110$. It is not possible to draw any conclusions for larger values of A in view of the little information available.

Theoretical values of the spin cutoff parameter, σ, have also been obtained using the Nilsson model. The results are shown in Fig. 5.8. The nuclei involved do not overlap with those experimentally observed in Fig. 5.7, but the comparison would suggest that the theoretical values will be too large.

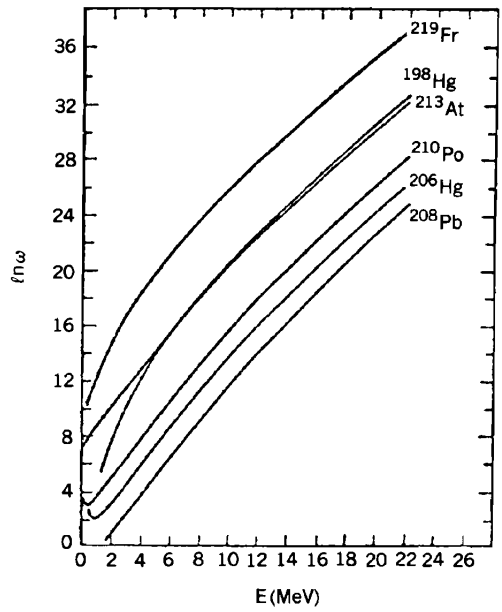

FIG. 5.6. Theoretical level densities as a function of excitation energy for nuclei in the neighborhood of the ^{295}Pb doubly closed shell. The Nilsson shell model has been used to obtain the spherical set of single particle levels [Moretto, Stella, and Carmella-Crespi (70).] [From Huizenga and Moretto (72).]

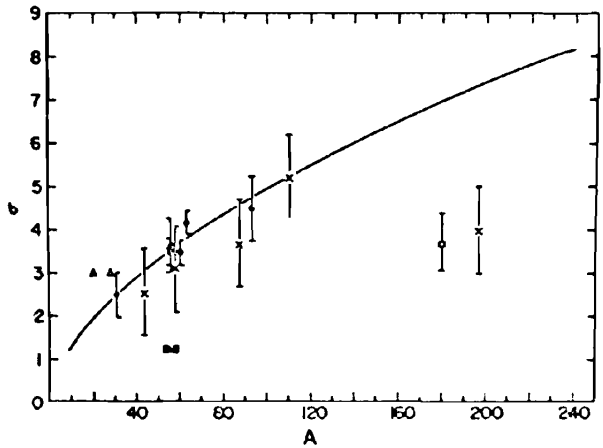

FIG. 5.7. Computation of values of σ. [From Huizenga (72).]

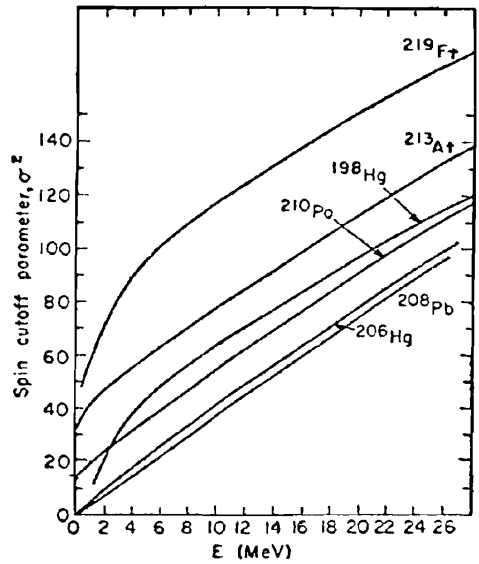

FIG. 5.8. Theoretical spin cutoff parameters σ^2 as a function of excitation energy for nuclei in the ^{205}Pb region. The calculations have been performed on the basis of the Nilsson diagram [Moretto, Stella, and Caramella-Crespi (70).] [From Huizenga and Moretto (72).]

The experimental results that form the basis of the foregoing comparisons with the theory are obtained from a variety of sources. The most obvious involves simply counting of the levels, which is possible only if they are isolated, as can be the case for low-energy neutron resonances. However, this procedure rapidly becomes impossible as the excitation energy increases. The primary method then exploits the dependence of reaction cross sections, total as well as differential, on the nuclear level density, as will be made evident in later sections of this chapter (see Section 7). For the present we illustrate the results that can be obtained by Fig. 5.9 for the case of ^{60}Ni.

French and his collaborators have developed a statistical method for determining the nuclear level density which is appropriate for the interacting shell model. In this model the wave functions for the system are assumed to be expressible in terms of the shell model single-particle wave functions. Moreover, a finite number of shells are assumed to be mixed by the residual interaction forming the shell model space. Thus the effective Hamiltonian is given by the finite matrix $\langle \Phi_j | H | \Phi_i \rangle$, in that shell model space where the set $\{\Phi_i\}$ are the independent-particle (i.e., noninteracting shell model), wave functions. The theory attempts to compensate for the effect of omission of the states outside the model space by using an adjusted ("renormalized") residual interaction. This procedure is in obvious difficulty when the actual interaction brings down into the energy domain of interest, states that have appreciable components not

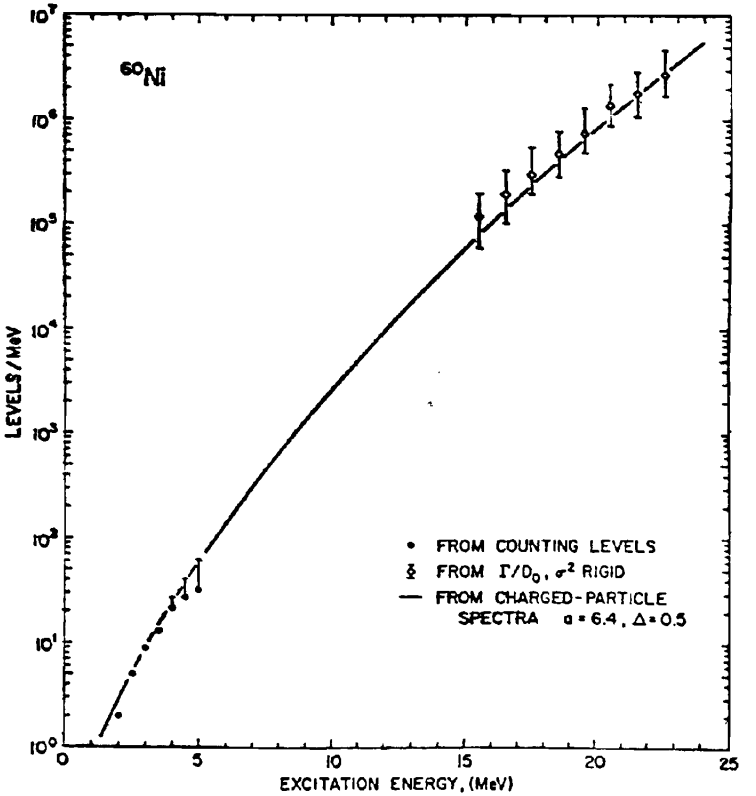

FIG. 5.9. Plot of the experimental level density of ^{60}Ni as a function of excitation energy [Lu, Vag, and Huizenga (72).] [From Huizenga and Moretto (72).]

included in the model space. These are referred to as *intruder* states. It should also be noted that even when the unrenormalized residual interaction is two-body, the renormalized interaction will generally contain many-body interactions as components. The energies of the system are given by the eigenvalues of the Hamiltonian $\langle \Phi_j | H | \Phi_i \rangle$. Generally, the diagonalization of such a matrix is a formidable numerical task. For instance, the $J = 3$, $T = 1$ matrix in the shell with 12 particles has the dimension of 6706, so that there are 2.25×10^6 different matrix elements and 6706 eigenvalues. If, however, the residual interaction is two-body, as is usually assumed [see Chapter V in deShalit and Feshbach (74)], the number of independent matrix elements is only 63. The two-body assumption is not generally correct, as the omission of states outside the model space rigorously requires the introduction of many-body forces, so that the number of independent matrix elements will be larger than 63. There is an upper bound to this number when the number of active particles is m, since then the many-body force is at most an m-body force.

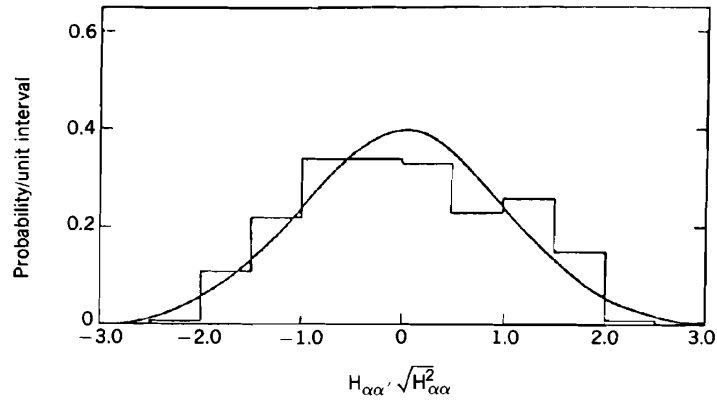

(*a*)

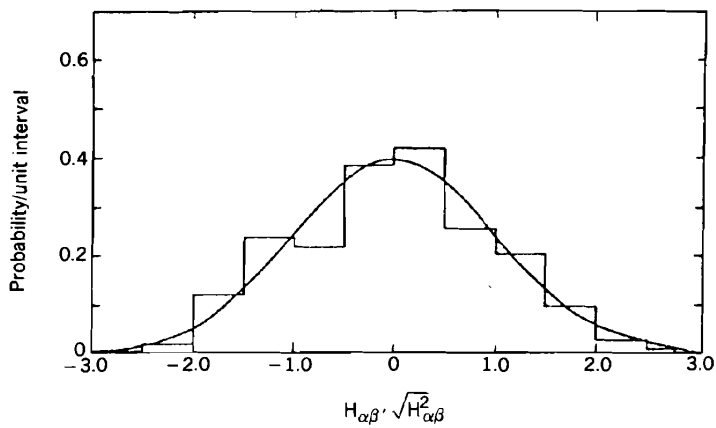

(*b*)

FIG. 5.10. (a) Plot of the distribution of 196 diagnonal nuclear shell model matrix elements from the work of D. Kurath. The solid curve is a simple normal distribution $(2\pi)^{-1/2}\exp(-H^2_{\alpha\alpha}/2\overline{H^2_{\alpha\alpha}})$ in which $H_{\alpha\alpha}$ is the diagnonal element minus the mean diagnonal element for each matrix. (b) Plot of the distribution of 675 off-diagonal matrix elements obtained in the work of D. Kurath. The solid curve is a simple normal distribution $(2\pi)^{-1/2}\exp(-H^2_{\alpha\beta}/2\overline{H^2_{\alpha\beta}})$ in which $H_{\alpha\beta}$ is the off-diagonal element; the mean value of the off-diagnonal elements is very close to zero. [From Porter and Rosenzweig (60).]

The statistical method adopted by French and Wong (70) and Bohigas and Flores (71) makes use of the empirical result (see Fig. 5.10) that the matrix elements of a short-range residual interaction are random. By this we mean that the distribution of values of the matrix elements when the excitation energy or the mass number of the nucleus is varied is Gaussian. A justification of this

result is indicated by the following plausible but hardly rigorous argument. In terms of $\phi_n(\mathbf{r})$, the single-particle shell model wave function, the matrix element of a two-body potential $v(\mathbf{r}, \mathbf{r}')$ is

$$\langle \phi_k \phi_l | v \phi_m \phi_n \rangle = \int \phi_k^*(\mathbf{r}) \phi_l^*(\mathbf{r}') v(\mathbf{r}, \mathbf{r}') \phi_m(\mathbf{r}) \phi_n(\mathbf{r}')\, d\mathbf{r}\, d\mathbf{r}' \tag{5.63}$$

For large quantum numbers (i.e., for reasonably high excitation energies) the ϕ_n's will have a large number of nodes. The overlap of these wave functions as they occur in (5.63) will generally yield a very irregular and complex dependence on $\mathbf{r}$ and $\mathbf{r}'$. Since v is short range, the matrix element of (5.63) is a sum of contributions that come from the regions in which the overlap is constructive. To the extent that these contributions are effectively random, the central limit theorem may be applied and the distribution of the matrix elements is Gaussian.

This empirical result suggests the following procedure. One can construct an ensemble of possible Hamiltonians with model shell space by choosing each of the independent matrix elements randomly (i.e., from a Gaussian distribution), and then solving the resulting secular equation for the energy eigenvalues of the system. By this means it would then be possible to develop an energy eigenvalue distribution. The fundamental assumption is then made that this distribution is identical with that which would be obtained from the energies of the levels in a given nucleus or from a variety of nuclei. This hypothesis is referred to as the ergodic hypothesis and is reminiscent of the hypothesis made in statistical mechanics, in which the time behavior of a system is related statistically to the properties of an ensemble of trajectories generated by random initial conditions.

An important simplification in the calculation of the distribution of energies can be obtained if one assumes that the distribution is Gaussian.

$$\omega(E) = \frac{1}{\sqrt{2\pi\lambda^2}} \exp\left[-\frac{(E-\varepsilon)^2}{2\lambda^2} \right] \tag{5.64}$$

where the average energy $\bar{E}$ is given by ε and the mean-square deviation $\overline{E^2} - \bar{E}^2$ by λ^2. The validity of (5.64) has been shown by numerical calculations as well as through an application of the central limit theorem [Mello (78)] when the number of particles is larger than two, when the interaction is two-body, or larger than k, when the interaction is k-body.

It is thus no longer necessary to diagonalize the Hamiltonian. One need only compute the mean energy and the dispersion using the expressions

$$\varepsilon = \frac{1}{d} \sum_i \langle \Phi_i | H \Phi_i \rangle$$

and

$$\lambda^2 = \frac{1}{d}\sum_i \langle \Phi_i | (\varepsilon - H)^2 \Phi_i \rangle = \frac{1}{d}\sum_i \langle \Phi_i | H^2 \Phi_i \rangle - \varepsilon^2 \tag{5.65}$$

or

$$\lambda^2 = \frac{1}{d}\sum_{i,j} |\langle \Phi_i | H \Phi_j \rangle|^2 - \varepsilon^2 \tag{5.66}$$

In these expressions d is the dimension of the space, while the matrix elements are linear combinations of randomly chosen quantities. Such a procedure was used by Ayik and Ginocchio (74) to compute the level densities for light nuclei. The orbital single-particle, wave functions of the $2s$, $1d$, and $f_{7/2}$ shell were used.

Some comment should be made with regard to the Gaussian form, (5.64). It differs sharply from the expression (5.30) obtained earlier, which showed an ever-increasing density of levels. The reduction in the level density at large E is a consequence of the use of a finite shell model space and is simply an expression of the fact that the energy eigenvalues in such a space will be bounded from above. The Gaussian, 5.64, is therefore meaningful only in the low-energy region, $E < \varepsilon$. The resulting form in this domain is not identical with (5.30). However, Ayik and Ginocchio's calculations take interactions and shell model effects into account.

6. SPACING OF ENERGY LEVELS; WIDTH DISTRIBUTIONS‡

The preceding discussion provides an overall broad view of the distribution of nuclear energy levels. We turn next to the description of local properties of the energy spectrum as posed by the question: What is the probability that the separation between two neighboring energy levels is s? Further specifications would include the probability that two levels are separated by an interval s containing n levels. We shall consider only the simplest case, $n = 0$.

Let $\omega(s)\,ds$ be the probability of finding a level at a distance between s and $s + ds$ from a given level. The probability we seek is given by $\omega(s)$ multiplied by the probability that there is no level in the interval s. This last factor can be calculated as follows. Divide the interval between 0 and s into elements of size Δs_n. The probability that there is no level in the interval Δs_n is given by $1 - \omega(s_n)\Delta s_n$. The the probability of finding no level in the interval 0 to s is given by

$$\prod_n [1 - \omega(s_n)\Delta s_n] = \exp \sum_n \log(1 - \omega(s_n)\Delta s_n) = \exp[-\sum \omega(s_n)\Delta s_n]$$

$$\to \exp\left[-\int_0^s \omega(s)\,ds\right]$$

‡Brody, Flores et al. (81); Porter (65); Bohigas and Weidenmüller (88), Bloch (68).

Finally, the probability $p(s)\,ds$ of finding a level between s and $s+ds$ from a given level with no level in between is

$$p(s) = C\omega(s)\exp\left[-\int_0^s \omega(s)\,ds\right] \tag{6.1}$$

where C is a normalizing constant. If $\omega(s)$ is a constant, one obtains the Poisson distribution

$$p(s) = \frac{1}{D}e^{-s/D}, \qquad \frac{\int_0^\infty p(s)s\,ds}{\int_0^\infty p(s)\,ds} = D \tag{6.2}$$

where D is the average spacing.

However, as we show shortly, levels with the *same quantum numbers* do not cross (for nonsingular perturbations); that is, as the residual interaction is changed, two levels may approach each other but will eventually repel each other. Under these circumstances one might use, as suggested by Wigner, $\omega(s) \sim s$, so that

$$p(s) = \frac{\pi}{2}\frac{s}{D^2}e^{-(\pi/4)(s/D)^2} \tag{6.3}$$

the Wigner distribution law for spacings. Note that the probability for small spacings is substantially smaller for this distribution compared with the Poisson.

The agreement of the Wigner distribution with experiment as shown in Fig. 6.1 is remarkable in view of the simplicity of the argument. The reduction for small s is clearly seen.[‡] Interestingly the Wigner distribution also gives a good fit to the spacing between the two lowest levels in nuclear having the same J and π as shown in Fig. 6.2.

To obtain additional insight into the spacing distribution has required the introduction of a model. We shall briefly[§] mention two statistical models, the Gaussian orthogonal ensemble (GOE) and the two body random Hamiltonian ensemble (TBRE), described at the end of Section 5. The former, although it is not realistic, as it assumes many-body forces equal in rank to the number of particles making up the system, has the advantage of being analytically tractable. For the most part, the properties of the TBRE require numerical determination. This model is also not completely realistic because it restricts the interaction to two-body forces, an assumption that is not correct because of its use of a finite-dimensional shell model space.

[‡]One should note that the Wigner distribution is found to be valid for atomic spectra [Porter and Rosenzweig (60)] as well as for the spacing of the first two levels with the same J and Π in each nucleus.

[§]The reader should be aware of the "unitary ensemble" introduced by Dyson (62).

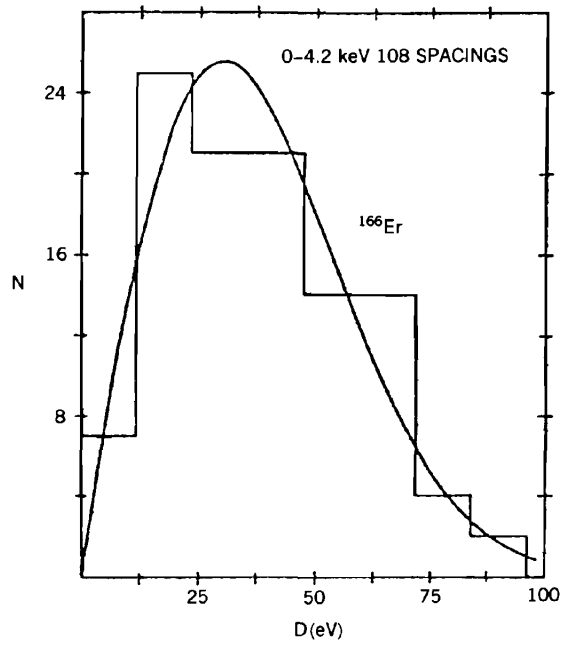

FIG. 6.1. Histogram for nearest-neighbor spacings for ^{166}Er, compared with Wigner's surmise [Liou, Camarda, et al. (72).] [From Mello (78).]

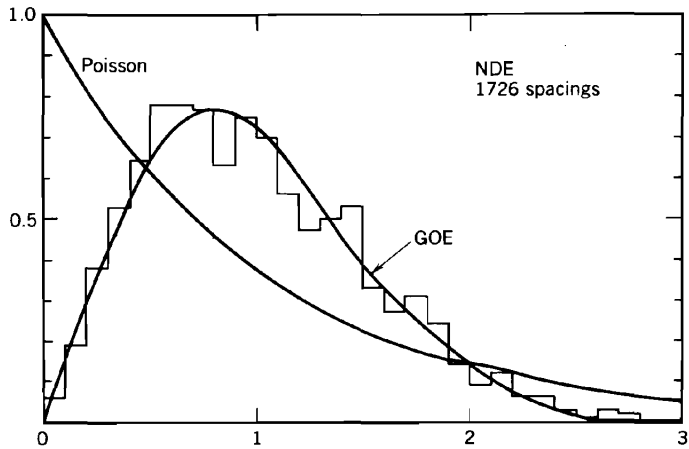

FIG. 6.2. Histogram for the nearest neighbor spacing distribution for the nuclear data ensemble plotted versus the level spacing in units of its mean volume [Bohigas, Hag and Pandey (83)]. [From Bohigas and Weidenmüller (88).]

The GOE assumes that the distributions of the individual matrix elements of the Hamiltonian are independent. This is unphysical because for residual two-body (or at most, few-body) forces usually envisaged the matrix elements are strongly correlated. The second assumption is that the joint distribution of all the matrix elements are invariant under a change of representation. This assumption is nut justifiable even if the representations involved are complete. There may be, indeed are expected to be, representations which because of dynamical reasons are more appropriate for the application of the statistical hypothesis; that is, the representations conform more closely to the physics of the system under study.

With this "caveat emptor" in mind, consider a two-dimensional infinitesimal rotation which transforms only the eigenfunctions Φ_1 and Φ_2, that is,

$$\Phi'_1 = \Phi_1 + \varepsilon\Phi_2$$
$$\Phi'_2 = \Phi_2 - \varepsilon\Phi_1$$

assuming that H is Hermitian and that Φ_1 and Φ_2 are real, the matrix elements of H transform as follows:

$$H'_{11} = \langle\Phi'_1|H\Phi'_1\rangle = H_{11} + 2\varepsilon H_{12}$$
$$H'_{22} = \langle\Phi'_2|H\Phi'_2\rangle = H_{22} - 2\varepsilon H_{12}$$
$$H'_{12} = H_{12} + \varepsilon(H_{22} - H_{11})$$
$$\left.\begin{aligned} H'_{1\mu} &= H_{1\mu} + \varepsilon H_{2\mu} \\ H'_{2\mu} &= H_{2\mu} - \varepsilon H_{1\mu} \end{aligned}\right\} \quad \mu > 2$$

The distribution function $P(H_{11}, H_{12}, H_{22}, H_{1\mu}, H_{2\mu}, \ldots)$ transforms as follows:

$$\frac{\partial P}{\partial \varepsilon} = 2H_{12}\frac{\partial P}{\partial H_{11}} + (H_{22} - H_{11})\frac{\partial P}{\partial H_{12}} - 2H_{12}\frac{\partial P}{\partial H_{22}} + \sum_{\mu>2}\left(H_{2\mu}\frac{\partial P}{\partial H_{1\mu}} - H_{1\mu}\frac{\partial P}{\partial H_{2\mu}}\right)$$

The invariance condition requires that $\partial P/\partial\varepsilon = 0$, which will be the case if

$$\frac{\partial P}{\partial H_{11}} = -\alpha H_{11}P \qquad \frac{\partial P}{\partial H_{12}} = -2\alpha H_{12}P \qquad \frac{\partial P}{\partial H_{22}} = -\alpha H_{22}P \tag{6.4}$$

$$\frac{\partial P}{\partial H_{1\mu}} = -2\alpha H_{1\mu}P \qquad \frac{\partial P}{\partial H_{2\mu}} = -2\alpha H_{2\mu}P \tag{6.5}$$

It is left as an exercise for the reader to prove by extensions of the argument

leading to (6.4) that the constant α in (6.5) is identical with the α in (6.4). Integrating (6.4) yields

$$P = Ce^{-\alpha\sum_{i,j}H^2{}_{ij}} = Ce^{-\alpha \mathrm{tr} H^2} \tag{6.6}$$

where C is a normalization constant. The invariance condition is thus extremely restrictive. Note that the distribution function for the diagonal elements, $\exp(-\alpha H_{ii}^2)$, has a wider spread than that for the nondiagonal elements, $\exp(-2\alpha H_{ij}^2)$. The fact that P can be expressed as a trace demonstrates explicitly the independence of P with regard to representation.

As an example of the application of this result for P, we use it to calculate the spacing distribution for the case of a two-dimensional space involving therefore only H_{11}, H_{12}, and H_{22}. For this case the energy eigenvalues, E_+ and E_-, are given by

$$E_\pm = \tfrac{1}{2}[H_{11} + H_{22} \pm \sqrt{(H_{11} - H_{22})^2 + 4H_{12}^2}] \tag{6.7}$$

The spacing

$$s = \sqrt{(H_{11} - H_{22})^2 + 4H_{12}^2} \tag{6.8}$$

is a positive-definite quantity, a result from which the absence of level crossing, alluded to earlier in this section, can be deduced. It is a result that is not restricted to the two-dimensional case.

From (6.6) and (6.8), the probability distribution for the spacing is given by

$$P(s) = C\int dH_{11}\int dH_{12}\int dH_{22}e^{-\alpha(H_{11}^2 + 2H_{12}^2 + H_{22}^2)}\delta(s - \sqrt{(H_{11} - H_{22})^2 + 4H_{12}^2}) \tag{6.9}$$

The integration is straightforward so we leave it to the reader to carry it out. The result is the Wigner distribution (6.3). However, this coincidence occurs only for the two-dimensional case. Agreement with the Wigner distribution is achieved again when the dimensionality becomes very large. The comparison with an exact calculation of Gaudin (61) is shown in Table 6.1.

Remarkably, it is actually possible to obtain the probability distribution for the eigenvalues of the GOE in closed form. Toward this end, note that the Hamiltonian matrix of dimensionality N has $N(N+1)/2$ independent matrix elements. Upon diagonalization the new variables are the N energy eigenvalues E_a and $N(N-1)/2$ parameters α_i describing the transformation to the diagonal basis. These parameters do not appear explicitly in (6.6) for P since

$$\mathrm{tr}\, H^2 = \sum E_a^2$$

Finally, it is necessary to transform from the volume element $dH_{11}dH_{12}dH_{22}$

TABLE 6.1 Comparison between the Wigner Two Level Distribution (p_w) and the Exact Calculation (p) of Gaudin

S/D	p	p_w
0	0	0
0.064	0.104	0.0996
0.127	0..207	0.1974
0.191	0.303	0.2915
0.255	0.395	0.3801
0.318	0.477	0.4617
0.382	0.549	0.5350
0.446	0.6117	0.5989
0.509	0.6630	0.6525
0.573	0.7032	0.6954
0.637	0.7308	0.7273
0.764	0.7547	0.7587
0.891	0.7396	0.7502
1.018	0.6933	0.7083
1.146	0.6255	0.6417
1.273	0.5445	0.5598
1.400	0.4587	0.4713
1.528	0.3750	0.3836
1.655	0.2978	0.3023
1.782	0.2301	0.2308
1.910	0.1730	0.1709
2.037	0.1267	0.1229
2.164	0.0906	0.0837
2.292	0.0631	0.0581
2.419	0.0429	0.0383
2.546	0.0286	0.0245
2.674	0.0185	0.0153
2.801	0.0117	0.0092
2.928	0.0062	0.0054
3.055	0.0030	0.0031
3.183	0.002	0.0017

Source: Gaudin (61).

$dH_{13}dH_{23}dH_{33}\cdots$ to $dE_1dE_2\cdots dE_N d\alpha_1\cdots d\alpha_{(N)(N-1)/2}$; that is, we need to compute the Jacobian of the transformation. Toward this end, note that the matrix element is linear in the energy eigenvalues E_α:

$$H_{ij} = \langle \Phi_i | H \Phi_j \rangle = \langle \sum_a \alpha_{ia}\chi_a | H \sum_b \alpha_{jb}\chi_b \rangle = \sum_a \alpha_{ia}^* E_a \alpha_{ja}$$

where the parameters α_i are selected from the set α_{ia} and $\chi_{a,b}$ are eigenfunctions of H. Therefore, the element in the Jacobian, $\partial H_{ij}/\partial E_a$, is independent of E,

while the remaining $(N)(N-1)/2$ elements $\partial H_{ij}/\partial\alpha_{ja}$ will be linear in E_a. Hence the Jacobian is a multinomial of degree $N(N-1)/2$ in the eigenvalues E_a. Finally, note that if any pair of eigenvalues are equal (i.e., if there is a degeneracy), the transformation from $\{E_a, \alpha_a\}$ space to H_{ij} space is singular. Hence the Jacobian must go to zero whenever two eigenvalues E_a and E_b are equal. Thus as far as the dependence upon E_a and E_b is concerned, the Jacobian is proportional to

$$\prod_{a<b=1}^{N} |E_a - E_b|$$

and P becomes[‡]

$$P(E_1,\ldots,E_N) \sim \prod_{a>b=1}^{N} |E_a - E_b| e^{-\alpha\sum_a E_a^2} \tag{6.10}$$

where we have integrated over the dependence on the parameters α_i. This result is referred to as the *Wishart distribution.* Evaluating the constant of proportionality in (6.10) and determining the distribution for the spacing and other measures of distribution requires elegant and ingenious mathematical arguments which we shall not describe here. It is from these results that one deduces that for large dimensionality, N, the Wigner result is recovered. Indeed, it seems that the Wigner result is approximately correct for large N even for the two-body (TBRE) case. This is illustrated by Fig. 6.3. These exact calculations also exhibit a long-range anticorrelation, which is presumably a consequence of the repulsion of energy levels.[§] It has been observed experimentally.

We turn finally to the distribution function for one of the amplitudes of the eigenvectors of the random Hamiltonian. If these are denoted by a_1, $a_2 \cdots a_N$, the joint distribution function is

$$P(a_1, a_2, \ldots, a_N) = \frac{2}{\Omega_N}\delta\left(1 - \sum_1^N a_i^2\right) \tag{6.11}$$

since the amplitudes must remain normalized under an orthogonal transformation. The quantity Ω_N is the total solid angle subtended by an

[‡]It has been pointed out by Dyson that this expression can be thought of as the configurational part of the partition function for a two-dimensional Coulomb gas with each particle held in a one-particle oscillator potential.

[§]The correlation function is evaluated by Dyson and Mehta (63). However, they did not deal with the GOE but rather with the "orthogonal ensemble" of unitary matrices, whose eigenvalues are of the form $e^{i\theta_i}$. Porter therefore refers to the ensemble as the COE, the circular orthogonal ensemble. One can consider the Dyson ensemble to be a theory of random S matrices, while Wigner, Porter, and Rosenzweig consider random Hamiltonian matrices with real matrix elements, assuming time-reversal invariance. The violation of time reversal led [Dyson [62)] to the consideration of "unitary ensembles." It leads to substantial differences for the spacing distribution from that which follows from the circular orthogonal ensemble.

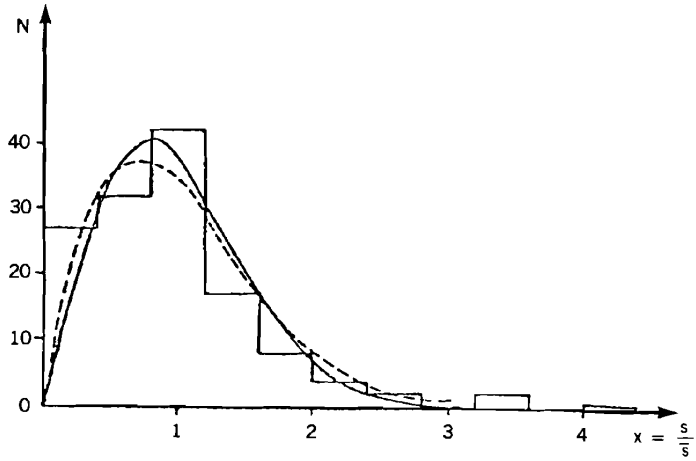

FIG. 6.3. Histogram obtained collecting the lowest energy difference between states with the same J and Π in the nuclear table. The solid line represents Wigner's distribution $p_w(x)$ and the dashed line shows the prediction of the TBRE in the ground-state region taken from Cota, Flores, Mello, and Yipez (74). The number of spacings is 135 and the probability of χ^2 is 3% when the histogram is compared with $p_w(x)$ and 13% when compared with the $\rho(0;x)$ of the TBRE. [From Mello (78).]

N-dimensional sphere. To show this, introduce N-dimensional spherical coordinates:

$$\begin{aligned} A^2 &= \sum a_i^2 \\ a_1 &= A\cos\vartheta_1 \\ a_2 &= A\sin\vartheta_1\cos\vartheta_2 \\ &\vdots \\ a_N &= A\sin\vartheta_1\sin\vartheta_2\cdots\sin\vartheta_{N-1} \end{aligned} \tag{6.12}$$

The volume element is given by

$$A^{N-1}dA\,d\Omega_N$$

so that

$$\begin{aligned} \int P(a_1,a_2,\ldots,a_N)\,da_1\cdots da_N &= \frac{2}{\Omega_N}\int \delta(1-A^2)A^{N-1}\,dA\,d\Omega_N \\ &= 2\int \delta(1-A^2)A^{N-1}\,dA = 1 \end{aligned}$$

as desired.

The distribution for a_1 is given by

$$P(\mathrm{a}) = \int P(a_1, \ldots, a_N)\delta(a_1 - a)\, da_1 \cdots da_N$$

$$= \int P(a_1 \cdots a_N)\delta(a_1 - a) A^{N-1}\, dA \sin^{N-2}\vartheta_1\, d\vartheta_1\, d\Omega_{N-1} \tag{6.13}$$

where we have used

$$d\Omega_N = \sin^{N-2}\vartheta_1 \sin^{N-3}\vartheta_2 \cdots \sin\vartheta_{N-3}\, d\vartheta_1 \cdots d\vartheta_{N-1}$$

$$= \sin^{N-2}\vartheta_1\, d\Omega_{N-1} \tag{6.14}$$

Note that $0 < \vartheta_\alpha < \pi$, $\alpha \neq N-1$, while $-\pi < \vartheta_{N-1} < \pi$. Hence

$$P(a) = \frac{\Omega_{N-1}}{\Omega_N} \int \delta(a - \cos\vartheta_1) \sin^{N-2}\vartheta_1\, d\vartheta_1$$

$$= \frac{\Omega_{N-1}}{\Omega_N} (1 - a^2)^{(N-3)/2} \tag{6.15}$$

One can readily show by integrating the first line of (6.14) that

$$\Omega_N = \frac{2\pi^{N/2}}{\Gamma(N/2)}$$

Assuming that $a^2 \ll 1$ and $N \gg 1$, (6.15) becomes

$$P(a)\, da = \left(\frac{N}{2\pi}\right)^{1/2} e^{-Na^2/2}\, da \tag{6.16}$$

Since the single particle width, Γ, is proportional to a^2, its distribution can be obtained directly from (6.16). Let

$$\frac{\Gamma}{\langle\Gamma\rangle} = Na^2$$

we then obtain the Porter–Thomas (56) distribution for the widths:

$$P(\Gamma)\, d\Gamma = \frac{1}{\sqrt{2\pi}} \left(\frac{\langle\Gamma\rangle}{\Gamma}\right)^{1/2} e^{-(1/2)(\Gamma/\langle\Gamma\rangle)} \frac{d\Gamma}{\langle\Gamma\rangle} \tag{6.17}$$

where $\langle\Gamma\rangle$ is the average of Γ.

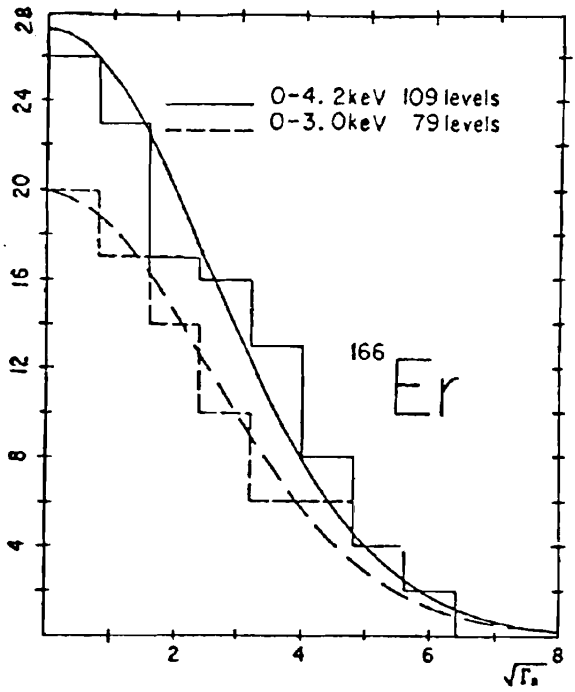

FIG. 6.4. Plot of the distribution of amplitudes for ^{166}Er from 0 to 3 and from 0 to 4.2 keV. The porter–Thomas curves are shown for comparison. [From Mello (78).]

The Porter–Thomas distribution has been amply verified experimentally as illustrated by Fig. 6.4. If ν channels contribute to the width, one can calculate the result by folding the Porter–Thomas distribution for single channels:

$$P_\nu(\Gamma) = \int P(\Gamma_1)P(\Gamma_2)\cdots P(\Gamma_\nu)\delta\left(\Gamma - \sum_1^\nu \Gamma_i\right) d\Gamma_1 \cdots d\Gamma_\nu \tag{6.18}$$

This calculation can be carried easily by using the representation of the δ function

$$\delta(\Gamma - \sum\Gamma_i) = \frac{1}{2\pi}\int \exp[ik(\Gamma - \sum\Gamma_i)]\, dk$$

Inserting this result into (6.18) yields

$$P_\nu(\Gamma) = \frac{1}{2\pi}\int dk\, e^{ik\Gamma}\left[\prod_1^\nu \int P(\Gamma_i)e^{-ik\Gamma_i} d\Gamma_i\right]$$

This integral can be carried out to obtain a single closed form when the average

widths for each channel are equal:

$$\langle \Gamma_i \rangle = \frac{\langle \Gamma \rangle}{\nu}$$

The one obtains the "χ^2 distribution for ν degrees of freedom":

$$P_\nu(\Gamma)\,d\Gamma = \left(\frac{\nu\Gamma}{2\langle\Gamma\rangle}\right)^{\nu/2} \frac{1}{\Gamma(\nu/2)} \exp\left(\frac{-\nu\Gamma}{2\langle\Gamma\rangle}\right)\frac{d\Gamma}{\Gamma} \tag{6.19}$$

One can readily show that

$$\langle \Gamma^2 \rangle - \langle \Gamma \rangle^2 = \frac{2}{\nu}\langle \Gamma \rangle^2 \tag{6.20}$$

showing that as the number of channels increase the variance decreases. For a large number of contributing channels it is good approximation to neglect fluctuations, so that

$$\langle f(\Gamma) \rangle \rightarrow f(\langle \Gamma \rangle) \qquad \nu \text{ large} \tag{6.21}$$

7. STATISTICAL THEORY OF NUCLEAR REACTIONS[‡]

As can be seen from Fig. 5.6, the level densities in the heavy nuclei quickly approach astronomical values with increasing excitation energy. For the lighter nuclei, the level density does not reach as large values for the same excitation energy, but the numbers are still substantial as illustrated by Figs 7.1 and 7.2. To obtain either theoretically or experimentally the cross section for the excitation of each of these levels is generally not possible or worthwhile. There are exceptions. At very low excitation energies, the level density is sufficiently small, so that the individual compound nuclear resonances can be observed. At higher excitation energies special structures such as the doorway state resonances (isobar analog resonances, the giant multipole resonances, etc.), which in fact involve averages over many levels, are of great importance. In the discussion that follows we assume that such unusual structures are not present in the energy domain being considered. Excluding these exceptions, the large level density precludes the study of the individual levels. Under these circumstances a statistical approach becomes unavoidable.

The justification of a statistical theory of nuclear reactions is similar in content to that used to justify statistical mechanics. Indeed, the statistical theory of nuclear reactions may be considered to be an example of nonequilibrium

[‡]Blatt and Weisskopf (52); Hauser and Feshbach (52).

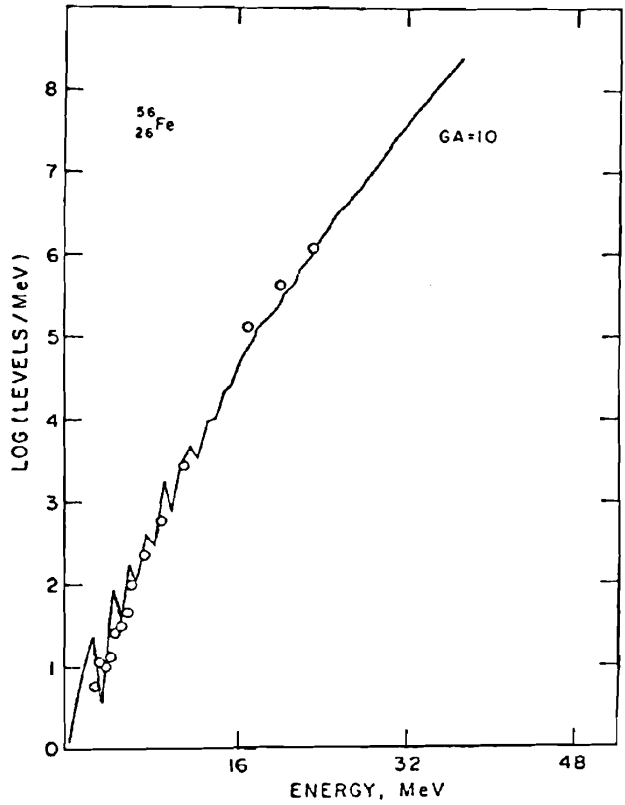

FIG. 7.1. Comparison of Hillman–Grover level density with experimental values for ^{56}Fe. Circles are experimental points. [From Lefort (76).]

statistical mechanics. At a sufficiently high excitation energy when the level density is large, it is reasonable to assume that the states are complicated linear combinations of simple states. As an example, consider a nucleon incident upon a nucleus for which a shell model description is adequate. The nucleon will excite the target by exciting one of the nucleons so that the system may be considered to be in a 2p–1h state. A second encounter with a target nucleon may lead to a 3p–2h state. Successive interaction will eventually generate 4p–3h components, 5p–4h components, and so on (see Fig. 7.3). The wave functions of the compound nuclear system will consist of a linear combination of the incident state and states belonging to these various excitation categories: 2p–1h, and so on. In terms of this shell model representation, the number of terms in the linear combination forming the wave function will be very large, on the order of the number of levels in an interval of a few MeV. Under these circumstances, it is not surprising that the transition amplitudes $\mathcal{T}_{cc'}$, which depend on the overlap between the initial wave function and the complex nuclear wave function, will be a complex random variable. That is, the value of $\mathcal{T}_{cc'}$,

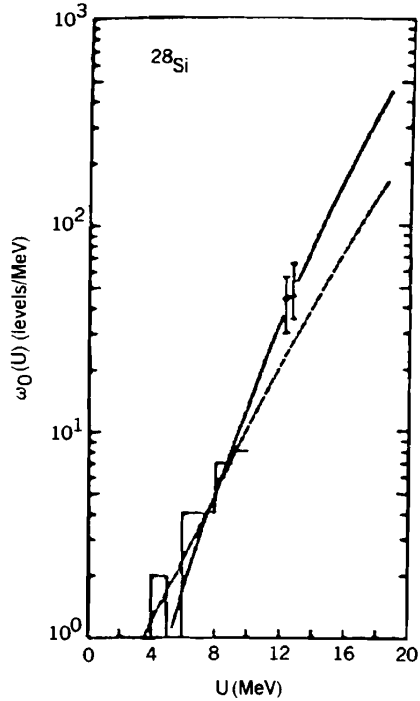

FIG. 7.2. Level density. [From Huizenga (72).]

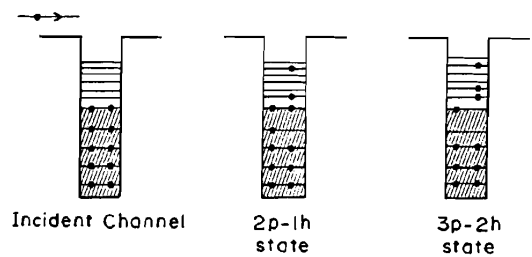

FIG. 7.3. Multistep nuclear excitation.

because of the complexity of the nuclear wave function, will depend on relatively accidental features of the latter. The value of $\mathscr{T}_{cc'}$ will fluctuate rapidly as the energy changes, giving rise to the Ericson-fluctuations discussed earlier in this chapter. The values of $\mathscr{T}_{cc'}$ obtained from a sufficiently large energy range form an ensemble with respect to which average properties of the system can be calculated. It is assumed, and this is a form of an ergodic theorem, that the ensemble average and the average with respect to an energy interval are equal.

Perhaps the most essential hypothesis made in the development of the statistical theory is the *random-phase* hypothesis. This hypothesis is the most direct application of the insight that the complexity of the nuclear wave function

will lead to effective randomness. We first provide a general statement of the random-phase hypothesis, as there will be many applications in differing contexts. Suppose that an amplitude u can be written as a sum as follows:

$$u = \sum_n u_n$$

We shall, moreover, assume that the average values of u and u_n, the nature of the average depending on the problem under consideration, are zero:

$$\langle u \rangle = 0 \qquad \langle u_n \rangle = 0 \tag{7.1}$$

The question is asked as to the average value of $|u|^2$, which generally will differ from zero:

$$\langle |u|^2 \rangle = \sum_{n,m} \langle u_n^* u_m \rangle \tag{7.2}$$

The random-phase assumption states that the phases of u_n are random, from which (7.1) follows immediately. To see this, let

$$u_n = e^{i\phi_n} |u_n|$$

The various possible values of ϕ_n ranging from 0 to 2π are assumed to be equally probable, so that the average is given by

$$\langle u_n \rangle = \frac{1}{2\pi} \int_0^{2\pi} u_n \, d\phi_n = 0$$

The same analysis applied to (7.2) yields

$$\langle u_n^* u_m \rangle = \delta_{nm} |u_n|^2 \tag{7.3}$$

so that

$$\langle |u|^2 \rangle = \sum_n |u_n|^2 \tag{7.4}$$

The dependence of this result on the representation used to obtain the expansion of u should be noted. The physics of the system under consideration dictates the selection of the representation to be used. It is through this choice that a physics content is given to the random phase hypothesis. We shall see many examples.

As a first application of the random phase assumption, we make use of the result of Kawai, Kerman, and McVoy (73) to be described later in this chapter. It states that it is possible to break up the transition matrix $\mathcal{T}$ into two parts:

a prompt (or direct) term, $\mathscr{T}^{(P)}$, the channel indices are suppressed for the time being, and a fluctuation (or resonance) term, $\mathscr{T}^{(FL)}$

$$\mathscr{T} = \mathscr{T}^{(P)} + \mathscr{T}^{(FL)} \tag{7.5}$$

so that upon taking averages

$$\begin{aligned} \langle \mathscr{T} \rangle &= \langle \mathscr{T}^{(P)} \rangle \\ \langle \mathscr{T}^{(FL)} \rangle &= 0 \end{aligned} \tag{7.6}$$

The cross section is proportional to $|\mathscr{T}|^2$. Taking the average assuming that a random relative phase exists between $\mathscr{T}^{(P)}$ and $\mathscr{T}^{(FL)}$ one obtains

$$\langle |\mathscr{T}|^2 \rangle = \langle |\mathscr{T}^{(P)}|^2 \rangle + \langle |\mathscr{T}^{(FL)}|^2 \rangle \tag{7.7}$$

or in terms of the cross section, the cross section can be given a corresponding decomposition

$$\langle \sigma \rangle = \sigma^{(P)} + \sigma^{(FL)} \tag{7.8}$$

The above results apply to the entire cross section. But they apply as well as the partial wave cross sections so that

$$\langle |\mathscr{T}(J\Pi)|^2 \rangle = \langle |\mathscr{T}^{(P)}(J\Pi)|^2 \rangle + \langle |\mathscr{T}^{(FL)}(J\Pi)|^2 \rangle \tag{7.9}$$

As a second example consider the application of the random phase hypothesis to the angular distribution (1.5). We then need to average $\mathscr{T}^{(FL)}_{c_1' c_1} \mathscr{T}^{(FL)*}_{c_2' c_2}$, where c stands for the quantum numbers α, l, s; $J\Pi$ so that

$$\mathscr{T}^{(FL)}_{c_1', c_1} \equiv \mathscr{T}^{(FL)}_{\alpha', \alpha}(l_1' s_1'; ls; J, \Pi)$$

Using the random-phase hypothesis,

$$\langle \mathscr{T}^{(FL)}_{c_1', c_1} \mathscr{T}^{(FL)*}_{c_2' c_2} \rangle = \delta_{c_1', c_2'} \delta_{c_1, c_2} |\mathscr{T}^{(FL)}_{c_1', c_1}|^2 \tag{7.10}$$

We then obtain for the angular distribution

$$\begin{aligned} \left\langle \frac{d\sigma^{(FL)}(\alpha', \alpha)}{d\Omega} \right\rangle = \frac{1}{k^2} \sum \frac{1}{(2I+1)(2i+1)} &(lsJ \| \sqrt{4\pi} Y_L \| lsJ)(l's'J \| \sqrt{4\pi} Y_L \| l's'J) \\ &\times \langle |\pi^2 \mathscr{T}^{(FL)}_{\alpha' \alpha}(l's'; ls; J\Pi)|^2 \rangle P_L(\cos \vartheta) \end{aligned} \tag{7.11}$$

Since [see (1.9)]

$$(lsJ \| \sqrt{4\pi} Y_L \| lsJ) \sim \begin{pmatrix} l & L & l \\ 0 & 0 & 0 \end{pmatrix}$$

only even values of L will occur in the sum in (7.11), with the consequence that the angular distribution is symmetric about 90°. This result follows directly from the fact that according to (7.10), the random-phase hypothesis permits interference only between states of the same parity. We shall leave it as an exercise for the reader to show that, in view of the fact that the polarization is an interference phenomenon, it will vanish under the random-phase hypothesis. Of course, this result applies only to the fluctuation term. Other polarization parameters such as D, the "depolarization," do not vanish.

The limiting form of isotropy follows from the general expression (7.11) only if additional assumptions are made. The assumption is made that the transition matrix $\mathscr{T}_{c',c}$ does not depend on the channel spin s'. Second, it is assumed that the density of states with a given spin s' is $(2s'+1)$. This differs from (5.54) in that the cutoff is not included. As a consequence, the implicit assumption is made that the principal contributions come from sufficiently low s'. Turning to (1.9), the s' dependent factors in the sum over s' of (7.11) are

$$\sum_{s'}(-)^{s'+L+J}(2s'+1)\begin{Bmatrix} l' & J & s' \\ J & l' & L \end{Bmatrix} = \sum_{s'}(-)^{s'+L+J}(2s'+1)\begin{Bmatrix} J & J & L \\ l' & l' & s' \end{Bmatrix}$$

$$= (-)^{L+l'+2J}\sqrt{(2J+1)(2l'+1)}\,\delta_{L0}$$

Since only the $L=0$ term survives, the angular distribution in this limit is isotropic. Isotropy is a consequence of the evaporation models of Weisskopf (31) and Frenkel (36).

The symmetry about 90° has been verified experimentally, and indeed deviations from it are taken to indicate the presence of prompt processes. An example of a symmetric angular distribution as it occurs in the reaction $^{58}\mathrm{Ni}(\alpha,p)^{61}\mathrm{Cu}$ is given in Fig. 7.4. An example from heavy-ion physics is shown in Fig. 7.5, where the colliding nuclei are $^{40}\mathrm{Ar}$ and $^{77}\mathrm{Sc}$.

We turn next to the evaluation of $\langle|\mathscr{T}_{cc'}^{(\mathrm{FL})}|^2\rangle$. Our goal will be to replace this term by an expression that can be evaluated through the use of the semiempirical optical model. The expression for $\mathscr{T}_{cc'}^{(\mathrm{FL})}$ is given by (4.4):

$$2\pi\mathscr{T}_{c'c}^{(\mathrm{FL})} = e^{i(\delta_f+\delta_i)}\sum_{\lambda} e^{i\phi_\lambda(c',c)}\frac{g_\lambda(c')g_\lambda(c)}{E-E_\lambda+(i/2)(\Gamma_\lambda+\Gamma'_\lambda)} \tag{7.12}$$

where $g_\lambda(c)$, a real quantity, is the magnitude of the matrix element $\langle\Phi_\lambda|H_{QP}|\psi_c^{(+)}\rangle$ connecting a channel c with wave function $\psi_c^{(+)}$ with the state for the compound system Φ_λ. The partial width $\Gamma_{\lambda c}$ is given by

$$\Gamma_{\lambda c} = g_\lambda^2(c) \tag{7.13}$$

and Γ_λ by

$$\Gamma_\lambda = \sum_c \Gamma_{\lambda c} \tag{7.14}$$

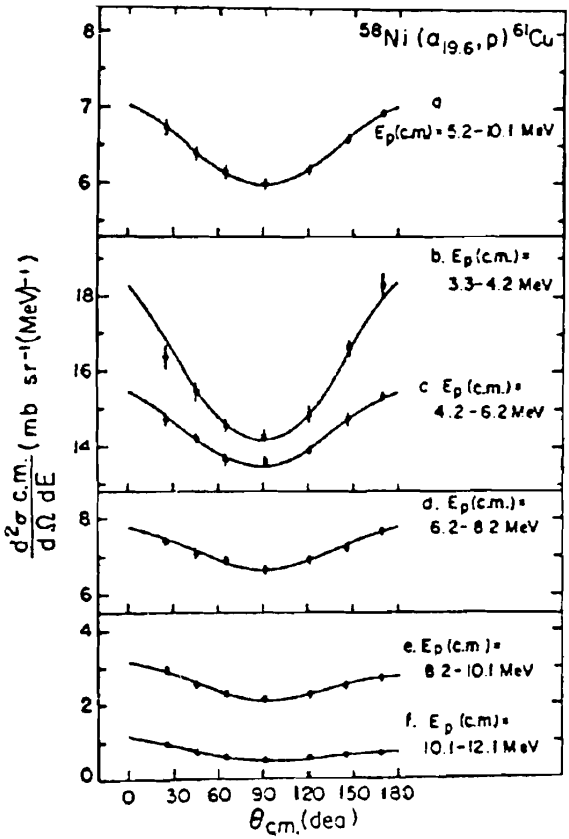

FIG. 7.4. Angular distribution for protons emitted by ^{62}Zn compound nuclei for several kinetic energy ranges in ^{58}Ni$(\alpha, p)^{61}$Cu-induced reactions at 19.67 MeV [Barker and Sarantites (74).] [From Lefort (76).]

The quantity Γ'_λ differs from zero when the levels overlap. However, it has the property [see (4.5)] that

$$\sum_\lambda \Gamma'_\lambda = 0 \tag{7.15}$$

so that Γ'_λ is not a positive-definite quantity such as Γ_λ.

In the preceding section it was shown that the distribution of the widths for the single-channel case is given by the Porter–Thomas distribution, (6.17), when the Hamiltonian is random. Equivalently, this means that the distribution of the amplitudes g is Gaussian.

$$P(g)\,dg = \frac{1}{\sqrt{2\pi\langle g^2\rangle}} \exp\left(\frac{-\frac{1}{2}g^2}{\langle g^2\rangle}\right) \tag{7.16}$$

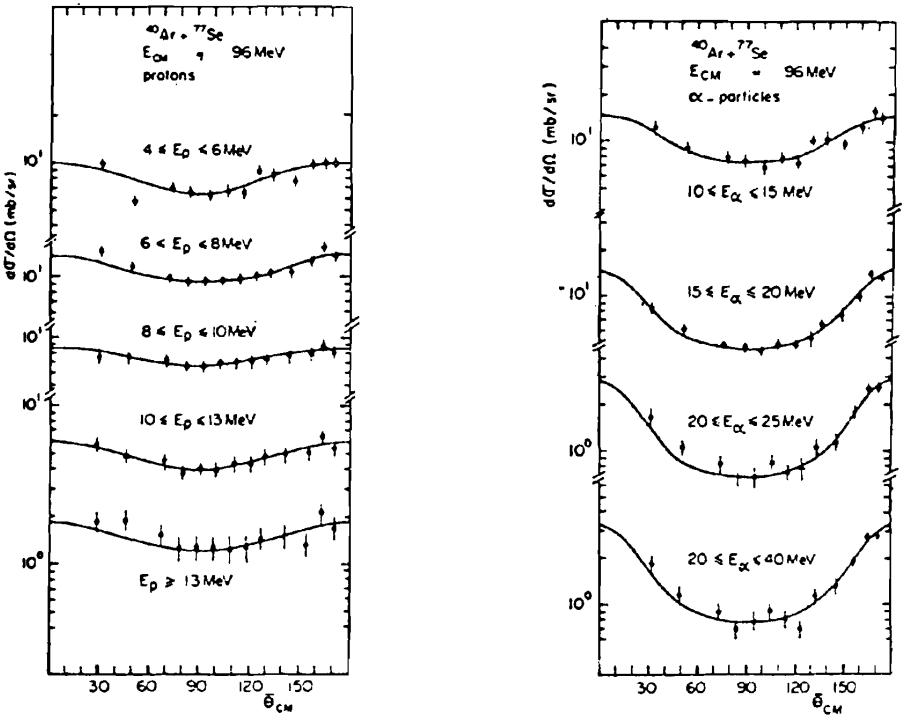

FIG. 7.5. Angular distributions for protons and α-particles emitted from ^{117}Te compound nuclei in several kinetic energy ranges [Galin, Gatty, et al. (74).] [From Lefort (76).]

where $\langle g^2 \rangle$ is the average value of g^2 taken with respect to this distribution:

$$\langle g^2 \rangle = \int_{-\infty}^{\infty} P(g) g^2 \, dg \tag{7.17}$$

The important point here is not the existence of a "derivation" but rather that it has been verified experimentally (see Fig. 6.4.). Since the distribution given by (7.16) is, according to the central limit theorem (see p. 251), that of a quantity composed of a sum of random quantities, g itself can be considered as random with

$$\langle g \rangle = 0 \tag{7.18}$$

Assuming the phase ϕ_λ to be random as well, (7.6), $\langle \mathscr{T}_{cc'}^{(\mathrm{FL})} \rangle = 0$, can be verified directly.

Of course, $\langle |\mathscr{T}^{(\mathrm{FL})}|^2 \rangle$ and therefore the partial cross section $\langle \sigma^{(\mathrm{FL})}(J\Pi) \rangle$ are

not zero. We proceed now to evaluate $\langle \sigma^{(\mathrm{FL})} \rangle$ where

$$\sigma^{(\mathrm{FL})}(J\Pi) = 4\pi^3 \lambda^2 |\mathscr{T}^{(\mathrm{FL})}(J\Pi)|^2$$

$$= \pi \lambda^2 \sum_{\lambda\mu} e^{i(\phi_i - \phi_\mu)} \frac{g_{\lambda f} g_{\mu f} g_{\lambda i} g_{\mu i}}{[E - E_\lambda + (i/2)(\Gamma_\lambda + \Gamma'_\lambda)][E - E_\mu - (i/2)(\Gamma_\mu + \Gamma'_\mu)]} \tag{7.19}$$

Note that E_λ, Γ_λ, and Γ'_λ are independent of the specific nature of the incident or final channel. The random-phase hypothesis yields

$$\langle \sigma^{(\mathrm{FL})}(J\Pi) \rangle = \pi \lambda^2 \sum_\lambda \left\langle \frac{\Gamma_{\lambda f} \Gamma_{\lambda i}}{(E - E_\lambda)^2 + \frac{1}{4}(\Gamma_\lambda + \Gamma'_\lambda)^2} \right\rangle \tag{7.20}$$

We evaluate the right-hand side in several limits:

1. There are a large number of exit channels. Under these circumstances the variance in $\Gamma_\lambda + \Gamma'_\lambda$ is reduced substantially [see (6.20)]. It is therefore a good approximation to rewrite

$$\left\langle \sum_\lambda \frac{\Gamma_{\lambda f} \Gamma_{\lambda i}}{(E - E_\lambda)^2 + \frac{1}{4}(\Gamma_\lambda + \Gamma'_\lambda)^2} \right\rangle \to \sum_\lambda \frac{\langle \Gamma_{\lambda f} \Gamma_{\lambda i} \rangle}{(E - E_\lambda)^2 + \frac{1}{4}(\Gamma_\lambda + \Gamma'_\lambda)^2}$$

A second assumption asserts that $\Gamma_{\lambda f}$ and $\Gamma_{\lambda i}$ are, for $i \neq f$, uncorrelated. Hence

$$\langle \Gamma_{\lambda f} \Gamma_{\lambda i} \rangle = \langle \Gamma_{\lambda f} \rangle \langle \Gamma_{\lambda i} \rangle \tag{7.21}$$

Since the ensemble over which the averages are made consist for each case of the widths $\Gamma_{\lambda f}$ and $\Gamma_{\lambda i}$ themselves, both $\langle \Gamma_{\lambda f} \rangle$ and $\langle \Gamma_{\lambda i} \rangle$ will be independent of λ. They will be designated by $\langle \Gamma_f \rangle$ and $\langle \Gamma_i \rangle$, respectively, where Γ_i is the average width for forming the compound nucleus in the energy region covered by the sum and Γ_f is the average width for decay into the final state.

We may therefore replace (7.20) by

$$\langle \sigma_{fi}^{(\mathrm{FL})}(J\Pi) = \pi \lambda^2 \langle \Gamma_f \rangle \langle \Gamma_i \rangle \sum \tag{7.22}$$

where

$$\sum = \sum_\lambda \frac{1}{(E - E_\lambda)^2 + \frac{1}{4}(\Gamma_\lambda + \Gamma'_\lambda)^2} \tag{7.23}$$

The factorization explicitly shown in (7.22) can be used to obtain an interesting result. If $\langle \sigma_{fi}^{(\mathrm{FL})} \rangle$ is sumed over all possible final states, one obtains the

cross section for the forming of the compound nucleus‡

$$\sum_f \sigma_{fi}^{(\mathrm{FL})} = \sigma_i^{(c)} = \pi \lambda^2 \langle \Gamma \rangle \langle \Gamma_i \rangle \sum \tag{7.24}$$

We can now eliminate the $\sum$ factor between (7.22) and (7.24), obtaining

$$\sigma_{fi}^{(\mathrm{FL})} = \sigma_i^{(c)} \frac{\langle \Gamma_f \rangle}{\langle \Gamma \rangle} \tag{7.25}$$

and

$$\frac{\sigma_{fi}^{(\mathrm{FL})}}{\sigma_{gi}^{(\mathrm{FL})}} = \frac{\langle \Gamma_f \rangle}{\langle \Gamma_g \rangle} \tag{7.26}$$

Thus the probability of decay of the compound system in a final channel is given by the branching ratio $\langle \Gamma_f \rangle / \langle \Gamma \rangle$, which is independent of the incident channel i and therefore of the manner in which the compound system was formed. This is referred to as the *Bohr independence hypothesis.*

Verification of the Bohr independence hypothesis in either form (7.25) and (7.26) is difficult since it holds individually for each partial wave with given values of J and Π but not for the sum of such terms; that is, although each term in the sum factors, the sum itself will generally not. However, if a compound system can be formed by two different methods (i.e., by using differing projectiles and targets), if the energy domain of the compound system is the same for the two, if the distribution of the J's and parities are the same, and so on, the ratio of the cross sections for identical products should be constant over their energy spectrum. Meeting all these conditions is not simple unless the reaction picks out a unique final J and Π. Examples of a comparison between two such reactions is given in Figs 7.6 and 7.7 [see the discussion by J.M. Miller (72)].

To make further progress, the relationship to the optical model of the quantities we have been using will be exploited. This procedure is advantageous since the parameters of the optical model potential can be determined empirically by fitting the elastic scattering (and polarization if available) and the total cross section.

The optical model has been derived in Chapter III and will be discussed in greater detail in Chapter V. We briefly review some salient features here. It states that the energy average of the wave function $\langle \psi \rangle$ is the solution of a Schrödinger equation with a complex potential. In the many-channel case, the Schrödinger equation reduces to a set of coupled equations for the open-channel wave functions. In the present context the relevant quantities is the transmission

‡This is not exact since (7.21) and therefore (7.22) are not correct for the elastic term $i = f$. In writing (7.24) we are assuming that the elastic scattering width is small, as should be the case when many channels are open.

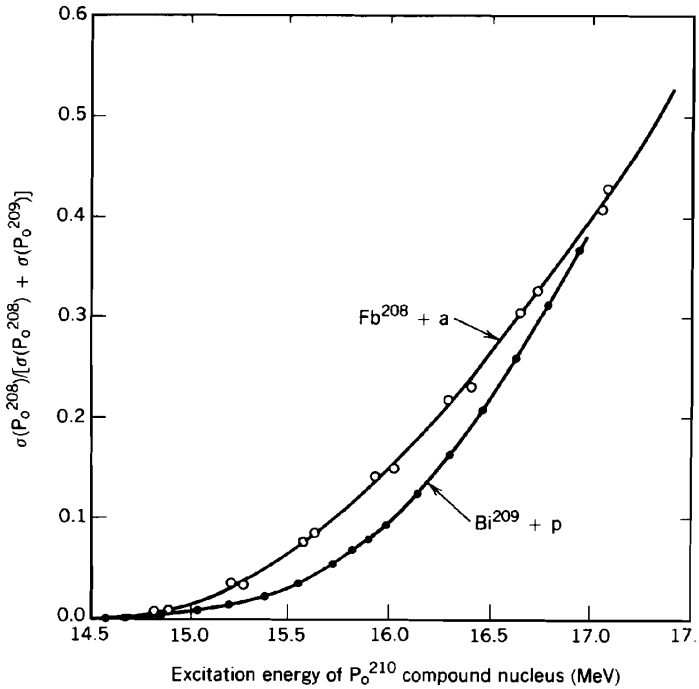

FIG. 7.6. Experimentally measured values of $\sigma(Po^{208})/[\sigma(Po^{208}) + \sigma(Po^{209})]$ as a function of the excitation energy of the Po^{210} compound nucleus prepared in two ways: $p + Bi^{209}$ and $\alpha + Pb^{206}$ [Grover and Nagle (64)]. [From Miller (72).]

coefficient T_c. We employ the generalization $T_{cc'}$ (where the subscript denotes the open channels) defined by Satchler (63) as follows:

$$T_{cc'}^{(\mathrm{opt})} = \delta_{cc'} - \sum_{c''} S_{cc''}^{(\mathrm{opt})} S_{c'c''}^{(\mathrm{opt})*} \tag{7.27}$$

where $S^{(\mathrm{opt})}$ is the energy-averaged S matrix, which can be obtained from the energy-averaged wave function $\langle \psi \rangle$ of the optical model. If the optical model conserved flux (which it does not because of the process of energy averaging), $S^{(\mathrm{opt})}$ would be unitary and $T^{(\mathrm{opt})}$ would be zero. The transmission coefficient T_c is the diagonal element of the matrix $T^{(\mathrm{opt})}$:

$$T_c \equiv T_{cc}^{(\mathrm{opt})} = 1 - \sum_{c''} |S_{cc''}^{(\mathrm{opt})}|^2 \tag{7.28}$$

If we write the total S matrix as

$$S = S^{(\mathrm{opt})} + S^{(\mathrm{FL})} \tag{7.29}$$

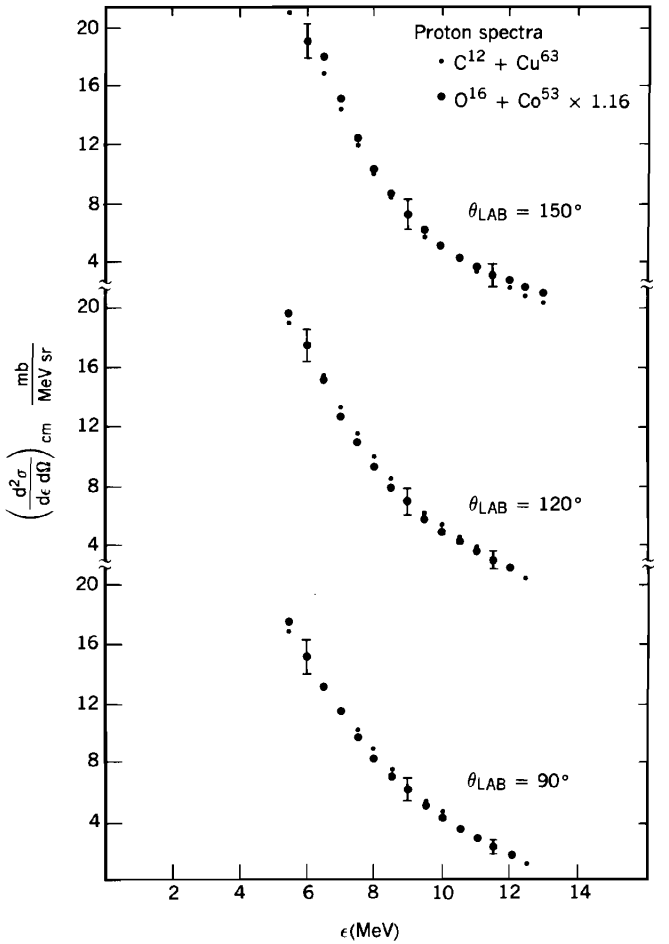

FIG. 7.7. Energy spectra of emitted protons. Cross sections from $O^{16} + Co^{59}$ multiplied by 1.16 [D'Auria, Fluss, et al. (68]. [From Miller (72).]

where

$$\langle S^{(FL)} \rangle = 0 \tag{7.30}$$

we see that

$$T_c = \left\langle \sum_{c''} |S^{(FL)}_{cc''}|^2 \right\rangle \tag{7.31}$$

Note. To prove this, use the unitarity condition $SS^\dagger = 1$, replace S by (7.29).

Then average using (7.30). One then finds that

$$T_{cc'} = \left\langle \sum_{c''} S^{(\mathrm{FL})}_{cc''} S^{(\mathrm{FL})*}_{c'c''} \right\rangle \tag{7.32}$$

Using $S^{(\mathrm{FL})} = -2\pi i \mathscr{T}^{(\mathrm{FL})}$ and expression (7.12), we have

$$S^{(\mathrm{FL})}_{cc'} = -ie^{i(\delta_c + \delta_{c'})} \sum_{\lambda} \frac{e^{i\phi_\lambda} g_{\lambda c} g_{\lambda c'}}{(E - E_\lambda) + (i/2)(\Gamma_\lambda + \Gamma'_\lambda)} \tag{7.33}$$

Substituting in (7.31) and using the random-phase approximation,

$$T_c = \left\langle \sum_{\lambda, c''} \frac{|g_{\lambda c}|^2 |g_{\lambda c''}|^2}{(E - E_\lambda)^2 + \frac{1}{4}(\Gamma_\lambda + \Gamma'_\lambda)^2} \right\rangle \tag{7.34}$$

In the limit of a large number of channels, so that $(\Gamma_\lambda + \Gamma_{\lambda'})$ is a constant equal to $\langle \Gamma \rangle$, and assuming independence of $\Gamma_{\lambda c} = |g_{\lambda c}|^2$ and $\Gamma_{\lambda c''}$, (7.34) becomes

$$T_c = \langle \Gamma_c \rangle \langle \Gamma \rangle \sum \tag{7.35}$$

where $\sum$ is given by (7.23). Substituting this relationship into (7.22) yields the familiar result

$$\sigma^{(\mathrm{FL})}_{fi}(J\Pi) = \pi \lambda_i^2 \frac{T_i T_f}{\sum_a T_a} \tag{7.36}$$

Note that in the derivation it was not necessary to evaluate $\sum$, so that the question of the distribution of E_λ, the end point effects, the size of $\langle \Gamma \rangle$ relative to D, the method of averaging did not arise. Moreover, it has *not* been necessary to assume that $T_c \ll 1$, which is a required and heavily criticized feature of many of the derivations of (7.36).

The angular distribution, (7.11), is given by

$$\left\langle \frac{d\sigma^{(\mathrm{FL})}_{fi}}{d\Omega} \right\rangle = \sum \frac{1}{(2I+1)(2i+1)} (lsJ \parallel Y_L \parallel lsJ)(l's'J \parallel Y_L \parallel l's'J) \sigma^{(\mathrm{FL})}_{fi}(l's'; ls; J\Pi) P_L(\cos \vartheta) \tag{7.37}$$

where we have used (7.19). Similarly, the total fluctuation cross section according to (1.6) is given by

$$\langle \sigma^{(\mathrm{FL})}_{fi} \rangle = \sum \frac{2J+1}{(2I+1)(2i+1)} \sigma^{(\mathrm{FL})}_{fi}(l's'; ls; J\Pi) \tag{7.38}$$

where one uses (7.36) for $\sigma^{(\mathrm{FL})}_{fi}$.

The cross sections given by (7.36) and (7.38) describe the excitation of a particular final state in the residual nucleus. However, for all except the rather low-lying states, it is more appropriate to regard the spectrum of the residual nucleus forming a continuum with a level density given by $\omega_f(U,J)$. Then the angle integrated spectrum (for example) is given by

$$\left\langle \frac{d\sigma_{fi}^{(\mathrm{FL})}}{dU} \right\rangle = \pi\lambda^2 \sum \omega_f(U,J) \frac{2J+1}{2I+1} \frac{T_f(J\Pi)T_i(J\Pi)}{\sum_c [T_c + \int T_c(J\Pi)\omega_c(U_c,J)]} \tag{7.39}$$

where both a sum and an integral are included in the denominator in order to take account of both the discrete and continuum level spectrum.

Equations (7.36)–(7.39) (to be suitably modified by the width fluctuation factor whose importance has been emphasized by Moldauer) referred to as the Hauser–Feshbach (52) theory are the fundamental results of the statistical theory of nuclear reactions. Their application is discussed in Section 9. For the present, note that one only needs the optical model transmission coefficients. In applying (7.36) one would need to know as well the energies, spins, and so on, of the levels to be excited as well as of those which are competitive (i.e., contribute to the denominator). To apply (7.39), one needs to know, in addition to the transmission coefficients, the density of levels of the residual nucleus.

It will be useful (but not essential) to evaluate the sum, $\sum$, of (7.23). A few comments are in order. Qualitatively, the sum over λ will contain those levels with energies E_λ that fall within the averaging interval in energy, ΔE. The energy E is at the midpoint of the interval ΔE so as to avoid end effects. Thus as E moves, ΔE moves with it. When the width (in a single channel) is very large, it is not always possible to avoid end effects since in that case the requirements of unitarity would require a very tight correlation among the levels [Mello and Feshbach (72)]. One of the consequences would be an instability of the averages to the interval size ΔE. Experimentally, this would manifest itself as an instability with respect to the energy resolution and could be so identified. The analysis that follows assumes the absence of end effects.

In calculating $\sum$ we shall also assume that new channels do not become open in the interval ΔE; that is, there are no thresholds in the interval. This is generally not the case, particularly as the excitation energy increases. As Kerman and Sevgen (76) point out, one consequence of this assumption is that unitarity need no longer be satisfied exactly.

Finally, some attention should be paid to the size of ΔE. For the present discussion it is to be of such a size that fine structure (Ericson–Brink fluctuations) and doorway state resonances but not the single-particle structure are averaged. Therefore, ΔE satisfies the inequalities

$$\Gamma_{SP} \gg \Delta E \gg \Gamma_d, \Gamma_\lambda, D \tag{7.40}$$

where Γ_{SP} is the single-particle width, Γ_d, the doorway state width, Γ_λ the width of the fine-structure resonances, and D is the distance in energy between them (D^{-1} = density of levels).

With these various caveats in mind, we proceed to evaluate $\sum$, replacing the sum by an integral

$$\sum = \frac{1}{D} \int_{E-(1/2)\Delta E}^{E+(1/2)\Delta E} \frac{dE_\lambda}{(E-E_\lambda)^2 + \frac{1}{4}(\Gamma_\lambda + \Gamma'_\lambda)^2} \tag{7.41}$$

Replacing Γ_λ and Γ'_λ by their average values over the interval, $\langle \Gamma \rangle$ and $\langle \Gamma' \rangle = 0$, respectively, $\sum$ becomes

$$\sum = \frac{2}{D\langle \Gamma + \Gamma' \rangle} \int_{x_-}^{x_+} \frac{dx}{1+x^2}$$

where $x_\pm = (2/\langle \Gamma + \Gamma' \rangle)(E \pm \frac{1}{2}\Delta E)$. If $\Delta E \gg \langle (\Gamma + \Gamma') \rangle$ as assumed and in the absence of important end effects, as assumed, the limits of the integral can be taken to be $\pm \infty$, so that

$$\sum = \frac{2\pi}{D\langle \Gamma \rangle} \tag{7.42}$$

Equation (7.22) now reads

$$\sigma_{fi}^{(\mathrm{FL})} = \pi \lambda\!\!\!^{-2} \frac{2\pi \langle \Gamma_i \rangle \langle \Gamma_f \rangle}{D\langle \Gamma \rangle} \tag{7.43}$$

Moreover, the value of T_c given in (7.35) becomes

$$T_c = \frac{2\pi}{D} \langle \Gamma_c \rangle \tag{7.44}$$

a result to which we have referred in Section 2 of this chapter. Finally, from (7.24) one obtains

$$\sigma_i^{(c)} = \pi \lambda\!\!\!^{-2}_i T_i \tag{7.45}$$

We remind the reader that the value of $\sum$, (7.42), is not needed to obtain the fundamental equations (7.36)–(7.39).

2. We consider next the case when the exit channels are so few in number that fluctuations in the total widths Γ_λ must be considered. We return to (7.20):

$$\langle \sigma^{(\mathrm{FL})}(J\Pi) \rangle = \pi \lambda\!\!\!^{-2} \sum_\lambda \left\langle \frac{\Gamma_{\lambda f} \Gamma_{\lambda i}}{(E-E_\lambda)^2 + \frac{1}{4}(\Gamma_\lambda + \Gamma'_\lambda)^2} \right\rangle \tag{7.20}$$

It is more convenient in this situation to evaluate the energy average directly:

$$\langle \sigma^{(\mathrm{FL})}(J\Pi) \rangle = \pi\lambda\!\!\!^{-2} \frac{1}{\Delta E} \int_{E_0-(1/2)\Delta E}^{E_0+(1/2)\Delta E} dE \sum_{\lambda} \frac{\Gamma_{\lambda f}\Gamma_{\lambda i}}{(E-E_\lambda)^2 + \frac{1}{4}(\Gamma_\lambda + \Gamma'_\lambda)^2} \tag{7.46}$$

It is possible to choose ΔE to be large compared to $\Gamma_\lambda + \Gamma'_\lambda$, yet small enough so that their energy variation as well as that of E_λ is negligible. This possibility exists because the scale over which these quantities change is on the order of the single-particle width, Γ_{SP}, that is, of the order of several MeV, whereas Γ_λ, the width of the fine structure, must of course be much smaller than Γ_{SP}. Neglecting end effects (we remind the reader that the observer will always choose ΔE so as to minimize these effects), the integral can readily be evaluated:

$$\langle \sigma_{fi}^{(\mathrm{FL})} \rangle = \frac{\pi\lambda\!\!\!^{-2}}{\Delta E} \sum_{\lambda} \frac{2\pi\Gamma_{\lambda f}\Gamma_{\lambda i}}{\Gamma_\lambda + \Gamma'_\lambda}$$

or

$$\langle \sigma_{fi}^{(\mathrm{FL})} \rangle = \pi\lambda\!\!\!^{-2} \frac{2\pi}{D} \left\langle \frac{\Gamma(f)\Gamma(i)}{\Gamma + \Gamma'} \right\rangle \tag{7.47}$$

If we assume that Γ and Γ' do not fluctuate, (7.47) reduces to (7.43). It is convenient to introduce a correction factor expressing the difference:

$$W \equiv \left\langle \frac{[\Gamma(f)/\langle\Gamma(f)\rangle][\Gamma(i)/\langle\Gamma(i)\rangle]}{(\Gamma + \Gamma')/\langle\Gamma\rangle} \right\rangle \tag{7.48}$$

W is referred to as the *width fluctuation* correction factor [Dresner (57); Moldauer (64)]. This correction factor should be most important when the number of exit channels are few, as would be the case near the threshold for the excitation of the first inelastic level. In any event, one would expect that under these circumstances the levels E_λ are well separated, so that Γ' vanishes approximately. Assuming that each Γ satisfies the Porter–Thomas distribution, it is relatively easy to evaluate W. To illustrate, suppose that there are only two channels, Γ_1 and Γ_2, so that

$$W_2 = \frac{\langle\Gamma_1\rangle + \langle\Gamma_2\rangle}{\langle\Gamma_1\rangle\langle\Gamma_2\rangle} \left\langle \frac{\Gamma_1\Gamma_2}{\Gamma_1 + \Gamma_2} \right\rangle$$

$$= [\langle\Gamma_1\rangle + \langle\Gamma_2\rangle] \frac{1}{2\pi} \int_0^\infty dx_1 \int_0^\infty dx_2 \frac{e^{-(1/2)x_1}}{\sqrt{x_1}} \frac{e^{-(1/2)x_2}}{\sqrt{x_2}} \frac{x_1 x_2}{x_1\langle\Gamma_1\rangle + x_2\langle\Gamma_2\rangle}$$

where $x_a = \Gamma_a/\langle\Gamma_a\rangle$. The integration can be performed after an integral

representation of the denominator is introduced:

$$W_2 = [\langle\Gamma_1\rangle + \langle\Gamma_2\rangle]\frac{1}{2\pi}\int_0^\infty d\alpha \int_0^\infty dx_1\sqrt{x_1}e^{-[(1/2)+\alpha\langle\Gamma_1\rangle]x_1} \times \int_0^\infty dx_2\sqrt{x_2}e^{-[(1/2)+\alpha\langle\Gamma_2\rangle]x_2}$$

or

$$W_2 = [\langle\Gamma_1\rangle + \langle\Gamma_2\rangle]\int_0^\infty \frac{d\alpha}{(1+2\alpha\langle\Gamma_1\rangle)^{3/2}(1+2\alpha\langle\Gamma_2\rangle)^{3/2}} \tag{7.49}$$

This integral can be performed exactly with the result for W that follows:

$$W_2 = \frac{\langle\Gamma_1\rangle + \langle\Gamma_2\rangle}{(\sqrt{\langle\Gamma_1\rangle} + \sqrt{\langle\Gamma_2\rangle})^2} \tag{7.50}$$

A plot of W_2 as a funtion of $\langle\Gamma_2\rangle/\langle\Gamma_1\rangle$ is shown in Fig. 7.8. Since it is a symmetric function of $\langle\Gamma_1\rangle$ and $\langle\Gamma_2\rangle$, only the values of W_2 from $\langle\Gamma_2\rangle/\langle\Gamma_1\rangle$ equal to zero to 1 are shown. We see that W_2 is generally considerably less than 1 approaching $\frac{1}{2}$ for $\langle\Gamma_2\rangle/\langle\Gamma_1\rangle = 1$. The effect of this correction is therefore to reduce the cross section from the value given by (7.36).

It is easy to generalize this result to the case in which there are more than two open channels. A review has been presented by Gruppelaar and Ruffo (77). An interesting case occurs when there are many such channels, for then one

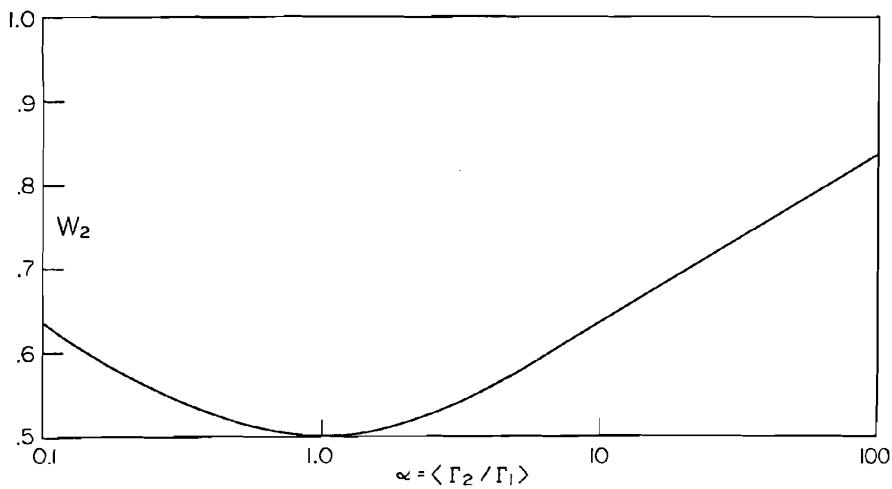

FIG. 7.8. Width fluctuation factor [see (7.50)].

can establish a connection with the discussion in Section 6. Consider

$$W_N = \frac{\langle \Gamma \rangle}{\langle \Gamma_1 \rangle + \langle \Gamma_2 \rangle} \left\langle \frac{\Gamma_1 \Gamma_2}{\sum \Gamma_i} \right\rangle, \qquad \langle \sum \Gamma_i \rangle = \langle \Gamma \rangle$$

Then it can readily be shown in the limit of a large number, N, of open channels that

$$W_N \simeq \left[1 + 3 \frac{\langle \Gamma_1 \rangle + \langle \Gamma_2 \rangle}{\langle \Gamma \rangle} \right]^{-1} \tag{7.51}$$

showing that neglecting the fluctuations in the total width, Γ is a good approximation only if that width is large compared to Γ_1 and Γ_2, even if the number of channels is large.

This treatment fails in the difficult intermediate regime when the levels overlap, at which point it is necessary to take account of the fluctuations in Γ'. Very little information is available regarding these fluctuations. One possibility is to assume that they are independent of the other parameters of the problem and that their distribution is given by a Gaussian:

$$P(\Gamma')\, d\Gamma' = \frac{1}{\sqrt{2\pi \langle \Gamma'^2 \rangle}} \exp\left(- \frac{\frac{1}{2}\Gamma'^2}{\langle \Gamma'^2 \rangle} \right) d\Gamma'$$

With this assumption (7.50) for W_2 would be replaced by

$$W_2 = \frac{\langle \Gamma_1 \rangle + \langle \Gamma_2 \rangle}{\sqrt{2\pi \langle \Gamma'^2 \rangle}} \int_0^\infty d\alpha \frac{\exp[-\alpha\Gamma' - \frac{1}{2}\Gamma'^2 / \langle \Gamma'^2 \rangle}{(1 + 2\alpha \langle \Gamma_1 \rangle)^{3/2} (1 + 2\alpha \langle \Gamma_2 \rangle)^{3/2}} \tag{7.52}$$

so that in principle by studying the width fluctuation correction factor, one would be able to determine $\langle \Gamma'^2 \rangle$. However, there are many other corrections (discussed in Section 8), which makes this possibility illusory.

Fluctuation scattering can also contribute to elastic scattering. This process is referred to as *compound elastic scattering*. In that case $\Gamma_{\lambda f}$ and $\Gamma_{\lambda i}$ are no longer independent and (7.22) is not valid. We must instead calculate $\langle \Gamma_1^2 \rangle$. Using the Porter–Thomas distribution, one finds that

$$\langle \Gamma_1^2 \rangle = 3 \langle \Gamma_1 \rangle^2 \tag{7.53}$$

so that the width fluctuation correction for compound elastic scattering has the value of 3 in this limit. Introducing the fluctuations in Γ due to Γ_1 will reduce this value; the leading term is $1/[(1 + 5\langle \Gamma_1 \rangle / \langle \Gamma \rangle]$. In the limit of a single channel W reduces to unity, so that for compound elastic scattering W can have a rather broad range of values.

8. EFFECT OF THE DIRECT REACTIONS ON THE STATISTICAL THEORY

The discussion of Section 7 is based on the assumption that the partial widths $\Gamma_{\lambda c}$ are uncorrelated, and not correlated to the energies E_λ. It is assumed that an energy average can be replaced by an ensemble average in which the $\Gamma_{\lambda c}$ are random following a Porter–Thomas distribution. For large values of Γ involving many contributions for which the width fluctuation correction, W, is unimportant, one obtains the Bohr independence hypothesis, that is, factorization of the partial cross sections. The relation of these factors to the transmission factor, T_c, (7.35), is established using the same assumptions. This derivation of (7.36) does not require the evaluation of $\sum$, about which there has been some debate; it makes no assumption regarding the size of T_c, nor is it necessary to introduce $\sigma_c^{(c)}$, the cross section for the formation of the compound nucleus or to make use of (7.44) connecting T_c with Γ_c/D.

The statistical assumptions with regard to $\Gamma_{\lambda c}$ and E_λ have been the subject of a spirited debate extending for nearly two decades. Correlations do exist because of the existence of direct (prompt) reactions which can contribute to the cross section and importantly, modify the wave functions which are to be inserted into the defining matrix elements.

Moldauer (75a, 75b) particularly, and more recently Weidenmüller and his collaborators [Engelbrecht and Weidenmüller (73); Tepel, Hofman, and Weidenmüller (74); Tepel (75); Hofman, Richert, Tepel, and Weidenmüller (75); and Hofman, Richert, and Tepel (75)], have emphasized the importance of the correlations imposed by unitarity. Unitarity requires that

$$SS^\dagger = 1$$

or

$$\sum_b S_{ab} S_{cb}^* = \delta_{ac} \tag{8.1}$$

We see that the elements of S (or $\mathscr{T}$, which is linearly related to S) must satisfy a number of nonlinear relations, which in turn impose relations between the sets of quantities $\phi_\lambda, g_{\lambda a}$, and E_λ [see (III.2.37), the discussion of the reactance matrix K, and (III.6.11) and the ensuring discussion]. The result, $\sum \Gamma'_\lambda = 0$, which we have used repeatedly, can be considered to be a consequence of unitarity. The unitarity condition can be very restrictive when the average of the partial widths $\langle \Gamma_{c\lambda} \rangle$ are large compared to the spacing in energy $\langle D_\lambda \rangle$. In that case [see Mello and Feshbach (72)] the individual values of $\Gamma_{c\lambda}$ are very large, so that very strong correlations must then exist between the various $\Gamma_{\lambda c}$ in order to satisfy unitarity. Under these circumstances, the results obtained both theoretically and experimentally become very sensitive to the manner in which averages are carried out and to the size of the averaging interval ΔE. It is noteworthy that such sensitivities have not been observed, indicating that their

occurrence is either rare or more likely that the analysis of the experimental data naturally selects out such large widths and regards them as nonstatistical.

Before attempting to perform the difficult task of taking the effects of unitarity into account, one should first understand if it is essential to do so in order to provide a statistical interpretation of nuclear reactions. We need to be particularly concerned with real situations and the manner in which data are analyzed.

Kerman and Sevgen (76) point out that unitarity need not be satisfied exactly since, in the energy domain under discussion, $\Gamma \gg D$, there is a high probability for new channels to become open in the averaging energy interval ΔE. Unless the effect of these is included in the statistical treatment, and that is generally not done in the many open-channel situations we are considering, there will be a loss of flux to the new channels, with a consequent failure of unitarity. Taking this effect into account quantitatively requires the introduction of new parameters, as discussed by Kerman and Sevgen.

A second point is that unitarity is not the only condition to be placed upon the transition amplitudes since they all are deduced from a common Schrödinger equation using the nuclear Hamiltonian, which is of course not random. These correlations cannot be stated as explicitly as the unitarity conditions, but they are certainly as real. One must ask which of these many restrictions are to be applied and which are to be neglected.

The point is that the statistical theory is an approximation; it cannot be exact. Statistics enters when the matrix elements of the Hamiltonian involve such complicated wave functions that the value of these matrix elements can be considered to be random, following Gaussian probability distributions. It should be noted that the distribution does not tell us when the particular value of the matrix element occurs. It can only provide the frequency with which it does. Thus statistical description can and does fail if inappropriately applied. It will fail, for example, if the wave functions are not sufficiently complicated. As we shall discuss in Chapter VI, only after the system has gone through a number of interactions will the necessary complication be developed. If the reaction product is produced at an early stage, the statistical theory will of course fail. The nature of the physical phenomena is the important issue.

Moreover, it may be argued that it is not useful to regard a pole term in the S matrix with a large partial width as a statistical fluctuation. As pointed out earlier, a consequence of a large average width is a close correlation among the properties of all the levels in the averaging interval as well as a marked sensitivity to the size of the averaging interval. This situation can hardly be described as statistical. And indeed, in an analysis of such data one would label such structures as nonstatistical and would consider them worthy of further study.

The reader is referred to the review by Mahaux and Weidenmüller (79) for a detailed discussion of the impact of unitarity and a summary of the present understanding.‡ The present understanding depends very heavily on numerical

‡References to the pioneering work of Moldauer and other will be found there.

studies. Weidenmüller and his associates have employed the representation of the $\mathscr{T}$ matrix in terms of the reactance matrix, $\mathscr{K}$ [see (III.2.44) and the material following], using a pole expansion of $\mathscr{K}$ [see (III.6.7)], which can be obtained from (III.2.43). Unitarity is thereby guaranteed. The pole parameters are assumed to be random. Moldauer (75a) has also performed a number of calculations with similar results. We mention two of these. First, one obtains a verification of the random-phase hypothesis for the S matrix in the case where the number of terms Λ in the pole expansion of K is large, and Λ is large compared to the number of open channels. The result is that $\langle S_{ab}^{(\mathrm{FL})} S_{cd}^{(\mathrm{FL})} \rangle$ vanishes unless two pairs of indices coincide. The second result, discovered by Moldauer (75a), is referred to as *M cancellation*. Briefly, he finds that the various correlation corrections cancel leading to (7.36), including the width fluctuation correction (7.48) multiplicatively. This result holds for nonelastic cross sections. The situation for elastic scattering will be discussed below following the methods of Kawai, Kerman, and McVoy (73). This paper addresses two questions of importance in the present context. The first to be discussed asks for a formulation of the problem of reactions that explicitly separate the $\mathscr{T}$ matrix into two components, the direct and fluctuation, that is, into $\mathscr{T}^{(\mathrm{DI})}$ and $\mathscr{T}^{(\mathrm{FL})}$, with the energy average of $\mathscr{T}^{(\mathrm{FL})}$ equal to zero. We have made repeated use of this separation in this chapter. The second deals with the width correlations, which are induced by the presence of the direct reactions.

The essence of the solution of the first question lies in the fact that the optical model does provide calculation of the energy averaged amplitude. It will be recalled [(Eq. (III.3.16)] that the averaged many-channel amplitude satisfies the equation

$$(E - H^{(\mathrm{opt})}) \langle P\Psi \rangle = 0 \tag{8.2}$$

with

$$H^{(\mathrm{opt})} = H_{PP} + H_{PQ} \frac{1}{E - H_{QQ} + iI} H_{QP} \tag{8.3}$$

This is to be compared with the exact equation satisfied by $P\Psi$ [Eq. (III.2.7)]:

$$\left(E - H_{PP} - H_{PQ} \frac{1}{E - H_{QQ}} H_{QP} \right) (P\Psi) = 0 \tag{8.4}$$

Equation (8.3) is obtained using the Lorentzian averaging function, with I the energy averaging interval. The comparison suggests rewriting (8.4) as follows:

$$\left[E - H^{(\mathrm{opt})} - H_{PQ} \left(\frac{1}{E - H_{QQ}} - \frac{1}{E - H_{QQ} + iI} \right) H_{QP} \right] (P\Psi) = 0$$

This equation can be restored to the canonical form (8.4):

$$\left[E - H^{(\mathrm{opt})} - V_{PQ}\frac{1}{E - H_{QQ}}V_{QP}\right](P\Psi) = 0 \tag{8.5}$$

where

$$V_{PQ} = H_{PQ}\sqrt{\frac{iI}{E - H_{QQ} + iI}} \tag{8.6}$$

Equation (8.5) is equivalent to the coupled equations:

$$\begin{aligned}(E - H^{(\mathrm{opt})})(P\Psi) &= V_{PQ}(Q\Psi)\\ (E - H_{QQ})(Q\Psi) &= V_{QP}(P\Psi)\end{aligned} \tag{8.7}$$

The $\mathscr{T}$ matrix for this system is [Eq. (III.2.30′)]

$$\mathscr{T}_{fi} = \mathscr{T}_{fi}^{(\mathrm{opt})} + \left\langle \psi_f^{(-)} \middle| V_{PQ}\frac{1}{E - H_{QQ} - W_{QQ}}V_{QP}\psi_i^{(+)} \right\rangle \tag{8.8}$$

where $\psi_{f,i}$ are the distorted wave solutions of

$$(E - H^{(\mathrm{opt})})\psi_{f,i} = 0$$

with appropriate boundary conditions, while

$$W_{QQ} \equiv V_{QP}\frac{1}{E^{(+)} - H^{(\mathrm{opt})}}V_{PQ} \tag{8.9}$$

Since by definition

$$\langle \mathscr{T} \rangle = \mathscr{T}^{(\mathrm{opt})}$$

it follows that the second term of (8.8) is $\mathscr{T}^{(\mathrm{FL})}$, so that

$$\begin{aligned}\mathscr{T}_{fi}^{(\mathrm{FL})} &= \left\langle \psi_f^{(-)} \middle| V_{PQ}\frac{1}{E - H_{QQ} - W_{QQ}}V_{QP}\psi_i^{(+)} \right\rangle\\ \langle \mathscr{T}_{fi}^{(\mathrm{FL})} \rangle &= 0\end{aligned} \tag{8.10}$$

thus achieving the desired decomposition.

As a beneficial dividend, the coupling potential V acquires a desirable dependence on H_{QQ}. As one can see from (8.6), the contributions to V from the eigenfunctions of H_{QQ} whose energy differs substantially from E is correspon-

dingly reduced so that the problems of convergence raised, for example, by Simonius (74) are resolved. This has a sound physical basis since the contributions of these distant "resonances" should be included in the optical model. It is achieved at the cost of an energy dependence which is, however, relatively weak, such as that of the optical potential itself. Note that the formalism of Chapter III can be used without any formal change in view of (8.7).

Because of (8.10), the cross section can be written

$$\sigma_{fi}(J\Pi) = \sigma_{fi}^{(\mathrm{opt})} + \sigma_{fi}^{(\mathrm{FL})}$$

where [see (7.12)]

$$\langle \sigma_{fi}^{(\mathrm{FL})} \rangle = 4\pi^3 \lambda_i^2 \langle |\mathscr{T}_{fi}^{(\mathrm{FL})}|^2 \rangle = \pi \lambda_i^2 \left\langle \left| \sum_\lambda \frac{e^{i\phi_\lambda(f,i)} g_\lambda(f) g_\lambda(i)}{E - E_\lambda + (i/2)(\Gamma_\lambda + \Gamma'_\lambda)} \right|^2 \right\rangle$$

Using the random-phase approximation this reduces to

$$\begin{aligned} \langle \sigma_{fi}^{(\mathrm{FL})} \rangle &= \pi \lambda_i^2 \left\langle \sum_\lambda \frac{g_\lambda^2(f) g_\lambda^2(i)}{(E - E_\lambda)^2 + \frac{1}{4}(\Gamma_\lambda + \Gamma'_\lambda)^2} \right\rangle \\ &\simeq \pi \lambda_i^2 \langle g_\lambda^2(f) g_\lambda^2(i) \rangle \sum \end{aligned} \tag{8.11}$$

where in (8.11) we have retained the assumption that one can neglect the correlations between the numerator and denominator of the pole expansion because of the assumed large number of participating open channels. If now one neglects the correlations among the g's, the results of Section 13.7 follow.‡

We now include the correlations but make the approximation (or assumption) that only pairwise correlations are important:

$$\langle g_\lambda^2(f) g_\lambda^2(i) \rangle = \langle g_\lambda^2(f) \rangle \langle g_\lambda^2(i) \rangle + \langle g_\lambda(f) g_\lambda(i) \rangle \langle g_\lambda(i) g_\lambda(f) \rangle \tag{8.11'}$$

Defining the matrix

$$\langle g_\lambda(f) g_\lambda(i) \rangle = X_{fi}$$

the cross section equation (8.11) becomes

$$\sigma_{fi}^{(\mathrm{FL})} \simeq \pi \lambda_i^2 \sum [X_{ff} X_{ii} + X_{fi} X_{if}] \tag{8.12}$$

The second term in brackets represents a significant change from the discussion of Section 7. The Bohr independence hypothesis, for example, is not valid if this term is significant.

‡This derivation differs from that given by Kawai, Kerman, and McVoy (73) in that the sum, $\sum$, is not evaluated explicitly.

We now must relate the optical model transmission factor $T_{fi}^{(\mathrm{opt})}$ and the matrix X. From (7.27), (7.30), and the unitarity condition one can immediately show that [see (7.32)]

$$T_{fi} = \left\langle \sum_c S_{fc}^{(\mathrm{FL})} S_{ic}^{(\mathrm{FL})*} \right\rangle \tag{8.13}$$

Inserting (7.36′) and using the random-phase approximation,

$$T_{fi} = (\sum) \sum_c \langle g_\lambda(f) g_\lambda(c) g_\lambda(i) g_\lambda(c) \rangle$$

Again making the pair correlation assumption, one finds that

$$T_{fi} = (\sum) \sum_c [\langle g_\lambda(f) g_\lambda(i) \rangle \langle g_\lambda(c) g_\lambda(c) \rangle + \langle g_\lambda(f) g_\lambda(c) \rangle \langle g_\lambda(c) g_\lambda(i) \rangle]$$

In terms of X,

$$T_{fi} = \sum [X_{fi} \operatorname{tr} X + (X^2)_{fi}] \tag{8.14}$$

or equivalently

$$T = \sum (X \operatorname{tr} X + X^2) \tag{8.15}$$

The problem of expressing $\sigma_{fi}^{(\mathrm{FL})}$ in terms of T_{fi} is reduced to solving this equation for X. The principal limitation on this development arises from the pair correlation assumption, which will fail if Γ is too large, for then many level correlations will become important. Equation (8.14) is in agreement with a conjecture of Vager (71).

The simple result (7.36) follows if the second term in (8.15) is neglected. Then

$$T = \sum X \operatorname{tr} X \tag{8.16′}$$

Taking the trace of both sides one can solve for $\operatorname{tr} X$ and finally for X:

$$X \simeq \frac{T}{(\sum \operatorname{tr} T)^{1/2}} \tag{8.16}$$

We recover (7.36) if this result is substituted for the first term of (8.12). Note again that $\sum$ drops out and needs not to be evaluated. If both terms in (8.12) are included,

$$\sigma_{fi}^{(\mathrm{FL})} \simeq \frac{\pi \lambda_i^2 (T_{ff} T_{ii} + T_{fi}^2)}{\sum_c T_{cc}} \tag{8.17}$$

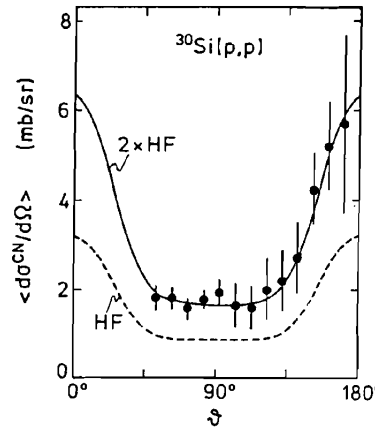

FIG. 8.1. Angular distribution of the average CN cross section for the elastic scattering ^{30}Gi (p, p) for 8.5 MeV $< E_p <$ 10.7 MeV. The filled circles are the measured values; the direct elastic contribution has been determined from the analyzing power and has been subtracted. The dashed curve is calculated from the Hauser–Feshbach formula; the full curve is twice this value [Kretschmer and Wangler (78)]. [From Mahaux and Weidenmüller (79).]

Factorization and the Bohr hypothesis are no longer exactly valid. In the case of the compound elastic scattering ($f = i$),

$$\sigma_{\text{el}}^{(\text{FL})} = \frac{2\pi\lambda\!\!\!^{-2}_i T_{ii}}{\Sigma T_{aa}} \tag{8.18}$$

We see in this case the appearance of a factor of 2, compared to simpler results that would be obtained if (7.39) were used for this case. Experimental varification of the factor of 2 is shown in Fig. 8.1.‡

To go beyond (8.16), we solve (8.15) for X in terms of T and

$$X = \tfrac{1}{2}\left(-\operatorname{tr} X + \sqrt{(\operatorname{tr} X)^2 + \frac{4T}{\Sigma}} \right) \tag{8.19}$$

In principle one can take the trace of both sides and so obtain an equation for

‡It will be recalled that the width fluctuation correction calculated in Section (7) is 3 rather than 2. The reason for the difference can be seen from (8.11′), which states that for $f = i$,

$$\langle g_\lambda^2(i) g_\lambda^2(i) \rangle = 2\langle g_\lambda^2 \rangle^2$$

But the left-hand side equals $\langle g_\lambda^4(i) \rangle$. If the Gaussian distribution is used for g_λ [or the Porter–Thomas for $\Gamma_\lambda(i)$], one obtains

$$\langle g_\lambda^4(i) \rangle = 3\langle g_\lambda^2 \rangle^2 \qquad \text{(Porter–Thomas)}$$

We see that the pair correlation assumption is not consistent with the Porter–Thomas distribution. The factor of 2 corresponds to an exponential distribution for Γ_λ. This is in agreement with the numerical calculations of Moldauer (75a) in the limit of large tr T.

tr X:

$$(N+\tfrac{1}{2})\,\mathrm{tr}\,X=\tfrac{1}{2}\sum_c\sqrt{(\mathrm{tr}\,X)^2+\frac{4T_{cc}}{\sum}} \tag{8.20}$$

This equation for tr X is not solvable analytically and one must resort to numerical methods. Tepel, Hoffman, and Weidenmüller (74) provide a simple approximate solution. Here we shall be content with obtaining the first-order correction to (8.16′) and solving for tr X. This is accomplished by expanding the square root in (8.19) to second-order. We find that

$$\mathrm{tr}\,X=\frac{1}{(\sum \mathrm{tr}\,T)^{1/2}}[(\mathrm{tr}\,T)^2-(\mathrm{tr}\,T^2)]^{1/2} \tag{8.21}$$

Equation (8.16) is obtained if $\mathrm{tr}(T^2)$ is dropped compared to $(\mathrm{tr}\,T)^2$. Since the former is proportional to N and the latter to N^2, this appears to be a good approximation. If we now examine the result for X,

$$X=\left[\frac{\mathrm{tr}\,T}{\sum[(\mathrm{tr}\,T)^2-\mathrm{tr}\,T^2]}\right]^{1/2}\left(T-\frac{T^2}{\mathrm{tr}\,T}\right)\sim\frac{1}{[\mathrm{tr}\,T\sum]^{1/2}}\left(T-\frac{T^2}{\mathrm{tr}\,T}\right) \tag{8.22}$$

(8.16) will be recovered in the limit where tr T is large. To summarize, the conditions for the validity of (8.16),

$$(\mathrm{tr}\,T)^2\gg\mathrm{tr}\,T^2 \tag{8.23a}$$

and

$$T_{fi}\,\mathrm{tr}\,T\gg(T^2)_{fi} \tag{8.23b}$$

Inequality (8.23a) is a necessary condition. It should be borne in mind that the values of the matrix elements of T can be obtained from the multichannel optical model so that inequalities (8.23) can be verified, the matrix elements of X can be obtained approximately from (8.22) or numerically from (8.20) and (8.19), and finally, $\sigma_{fi}^{(\mathrm{FL})}$ from (8.12).

Further discussion will be found in the review by Mahaux and Weidenmüller (79). We have not included the connection of the results above with the understanding of the "precompound" reactions. These are discussed in Chapter VI.

9. APPLICATIONS OF THE STATISTICAL THEORY

The statistical theory of nuclear reactions is applicable when the level density of the residual nucleus is large, that is, when its excitation is sufficiently high, corresponding to the low-energy portion of the spectrum of the emitted particle.

It applies as well at sufficiently low projectile (generally, neutron) energies for which the direct reactions do not make a significant contribution. For high-energy projectiles, the direct reactions dominate. However, the residual nucleus may be left in a highly excited state. Its subsequent decay may be calculated using statistical theory.

A. Angular Distributions

As a consequence of the random-phase hypothesis, the angular distributions are symmetric about 90°. When the residual nucleus is excited to an energy for which all possible orientations of its spin over the surface of a sphere occur with equal probability, the angular distribution is isotropic. An example of isotropy is furnished by an early experiment by Rosen and Stewart (55) from the low-energy portion of the neutron spectrum produced by the inelastic scattering of 14.1-MeV neutrons by Bi (Fig. 9.1). Inelastic scattering to particular levels in ^{209}Bi by 2.5-MeV neutrons [Cranberg, Oliphant, Levin, and Zafaratos (67)] demonstrate the symmetry about 90° (Fig. 9.2). Similar results are shown for ^{206}Pb, with the addition of a small contribution from the direct reaction process. Examples for heavy ions (^{40}Ar + ^{77}Sc → α + X) and for ^{58}Ni(α, p) were given earlier in Figs. 7.5 and 7.4. The collision of light ions also furnish examples as illustrated in Fig. 9.3.

The success of this prediction, symmetry about 90°, has led to its use to identify reactions that are dominated by statistical processes. As we shall see in Chapter VI, this is not entirely correct, as symmetry about 90° is also a

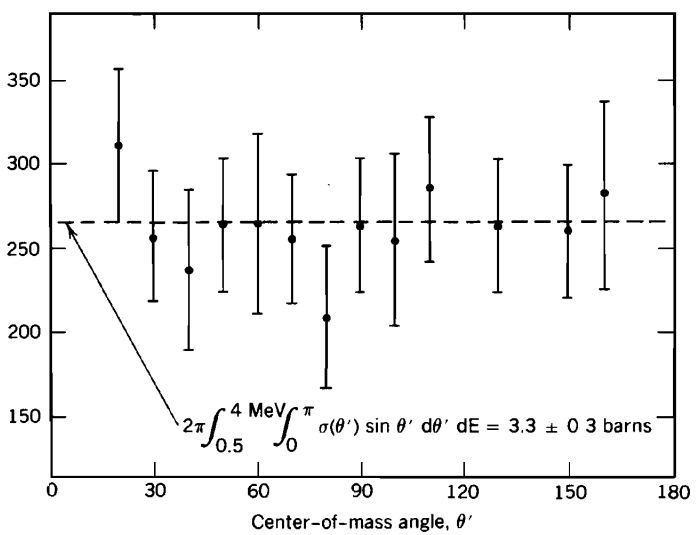

FIG. 9.1. Angular distribution of inelastically scattered 14.1-MeV neutrons from bismuth [Rosen and Stewart (55)]. [From Ribe (63).]

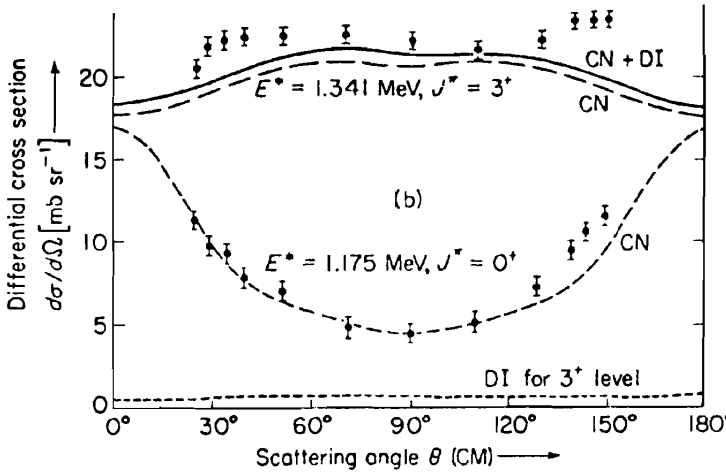

FIG. 9.2. Fits to the measured angular distributions of 2.5-MeV neutrons inelastically scattered to two levels in ^{206}Pb. In the calculation of the compound nucleus cross section (CN) the width fluctuation factor was taken into account. The direct interaction contribution is labeled DI [Cranberg, Oliphant, Levin, and Zafaratos (67)]. [From Marmier and Sheldon (70).]

feature of the statistical multistep compound process of which the statistical theory described in this chapter is a limiting case.

B. Energy Spectrum

We next consider the energy spectrum of the emitted particle, considering the case in which the excitation energy of the residual nucleus is sufficiently high that the residual nucleus levels effectively form a continuum with level density $\omega_f(U)$. The angle integrated cross section in the statistical theory is given by (7.39) multiplied by the width fluctuation correction if needed:

$$\left\langle \frac{d\sigma_{fi}^{(\mathrm{FL})}}{dU} \right\rangle = \pi \lambda_i^2 \sum_f \omega_f(U,J) \frac{2J+1}{(2I+1)(2i+1)} \frac{T_f(J\Pi) T_i(J\Pi)}{\sum_c [T_c + \int dU_c T_c \omega_c(U,J)]} \tag{9.1}$$

where the complete parametric dependence of T_f is $T_f(l's'; J\Pi)$, where we recall that l' is the orbital angular moment of the emitted particle, and s' is the channel spin. These combine vectorially to form J:

$$\mathbf{l}' + \mathbf{s}' = \mathbf{J}$$

T_i depends similarly on the entrance channel l and s. The level density $\omega_{s'}(U)$ takes into account the spin of the emitted particle i' as well as the spin of the residual nucleus, I'. The denominator sums over all ways in which the compound

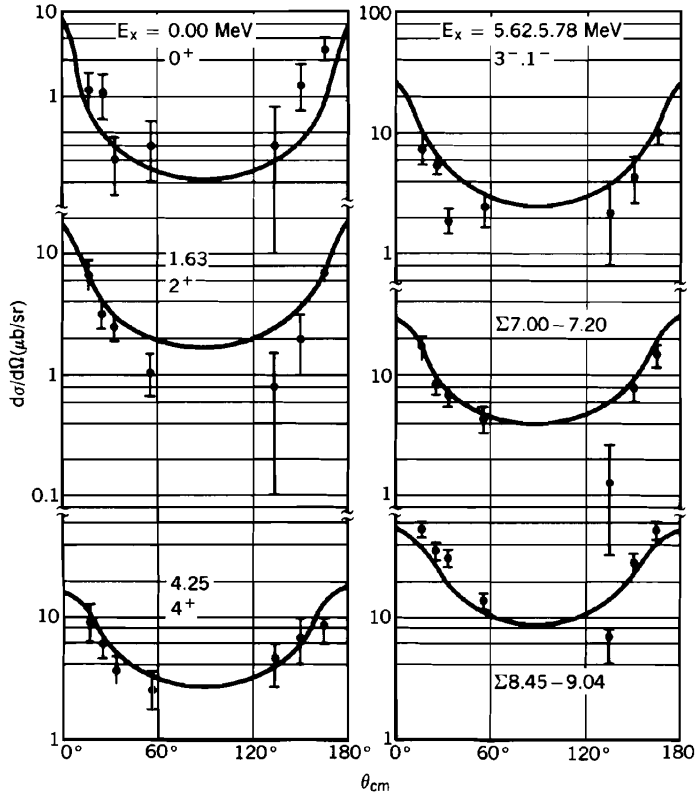

FIG. 9.3. Angular distribution for the reaction $^{12}C(^{14}N, {}^{6}Li)^{20}Ne$, $E_{cm} = 36$ MeV compared with the predictions of the statistical model (HF) [Belote, Anyas-Weiss, et al. (73)]. [From Stokstad (85).]

system can decay, including different modes of decay symbolized by the subscript c. The decay can occur to discrete levels as well as to the continuum part of the spectrum of the residual nuclei. To obtain the Weisskopf formula, (I.4.5), a number of approximations to (9.1) need to be made. It is assumed that T_f and T_i depend only on the orbital angular momenta l' and l, respectively. Second, we assume, as was done in the derivation of the isotropic angular distribution (see p. 301), that

$$\omega_f(U, J) \simeq (2s' + 1)(2l' + 1)\omega_0(U) \tag{9.2}$$

Finally, the discrete sum in (9.1) is dropped and in fact it is assumed that the residual nucleus for all the exit channels is the same. Inclusion of the effect of other types of exit channels is straightforward and left for the reader to derive.

With these approximations (9.1) becomes

$$\left\langle \frac{d\sigma_{fi}^{(\mathrm{FL})}}{dU} \right\rangle = \pi \lambda\!\!\!^{-2}_i \omega_0(U) \frac{\sum_{l'}(2l'+1)T_f(l')\sum_l(2l+1)T_i(l)}{\sum_{c,l_c}\int dU_c T_c(l_c)(2l_c+1)\omega_0(U_c)} \tag{9.3}$$

Defining

$$\sigma_a^{(c)} \equiv \pi \lambda\!\!\!^{-2}_a \sum_l (2l+1)T_a(l) \tag{9.4}$$

[that this agrees exactly with (7.4)], we obtain the Weisskopf result:

$$\left\langle \frac{d\sigma_{fi}^{(\mathrm{FL})}}{dU_f} \right\rangle = \sigma_i^{(c)}(E) \frac{\mu_F E' \sigma_f^{(c)}(E')\omega_0(U_F)}{\sum_a \int dU_a E'' \sigma_a^{(c)}(E'')\omega_0(U_a)\mu_a} \tag{9.5}$$

where μ_a is the reduced mass of the particle emitted in channel a.

Note that in this derivation no use was made of the law of detailed balance, as is the case for the traditional derivation given in Chapter I. Detailed balance cannot, in fact, be used without further justification since the cross section in (9.5) is energy and state averaged, and detailed balance holds between particular states with well-defined energies. Recall that for a given initial state

$$U_a = E - E' + Q_a$$

where E is the initial kinetic energy in the center-of-mass coordinate system, E' is the final kinetic energy of the emitted particle, and Q_a is the "Q" for the reaction. Casting ω_0 into an exponential form,

$$\omega_0 = \exp[S(U)]$$

and expanding $S(E+Q-E')$ about $E+Q$,

$$S(U) = S(E+Q-E') = S(E+Q) - E'\left(\frac{\partial S}{\partial U}\right)_{E+Q=U}$$

one obtains

$$\omega_0 = e^{S(E+Q)} e^{-E'/T} \tag{9.6}$$

where

$$\frac{1}{T} \equiv \left(\frac{\partial S}{\partial U}\right)_{E+Q=U} \tag{9.7}$$

T is referred to as the nuclear temperature. Substituting (9.6) into (9.4) yields

the Weisskopf–Frenkel evaporation formula. When S equals $2\sqrt{a(U-\Delta)}$ (see p. 278),

$$T=\left[\frac{1}{a}(E+Q-\Delta)\right]^{1/2} \tag{9.8}$$

Inserting (9.6) into (9.4), we observe that

$$\frac{1}{E'\sigma_f^{(c)}(E')}\left\langle\frac{d\sigma_{fi}^{(FL)}}{dU}\right\rangle \sim e^{-E'/T} \tag{9.9}$$

where we have omitted multiplicative factors that do not depend on E'. Thus the logarithm of the left-hand side of (9.9) should be a straight-line function of E' with a negative slope equal to $(1/T)$.

Another and somewhat more general result states that for a given E, the left-hand side of (9.9) depends only upon U_f, and in principle one should therefore be able to determine ω_0. The branching ratio, that is, the ratio of the differential cross sections for two differing reactions initiated by the same

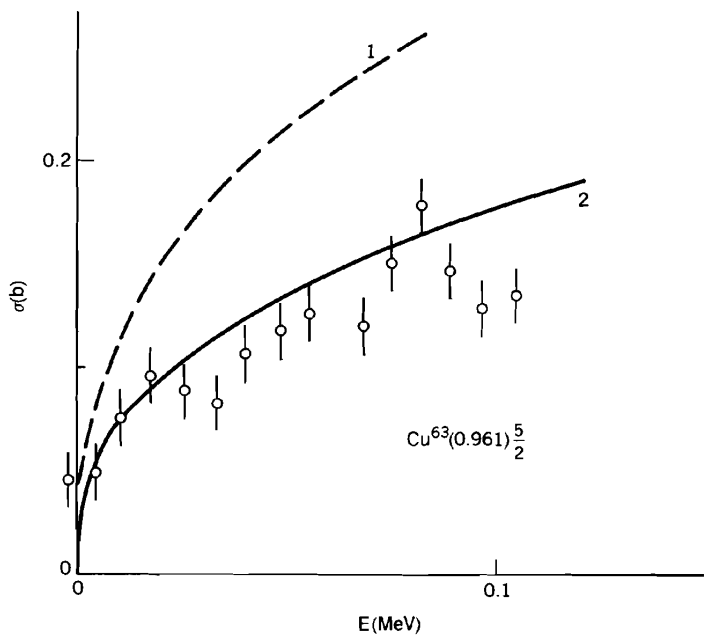

FIG. 9.4. Inelastic neutron scattering exciting the 0.961-MeV level in ^{63}Cu. The curve labeled (1) does not include the width fluctuation factor; curve (2) does. [From Tucker, Wells, and Meyerhoff (65).]

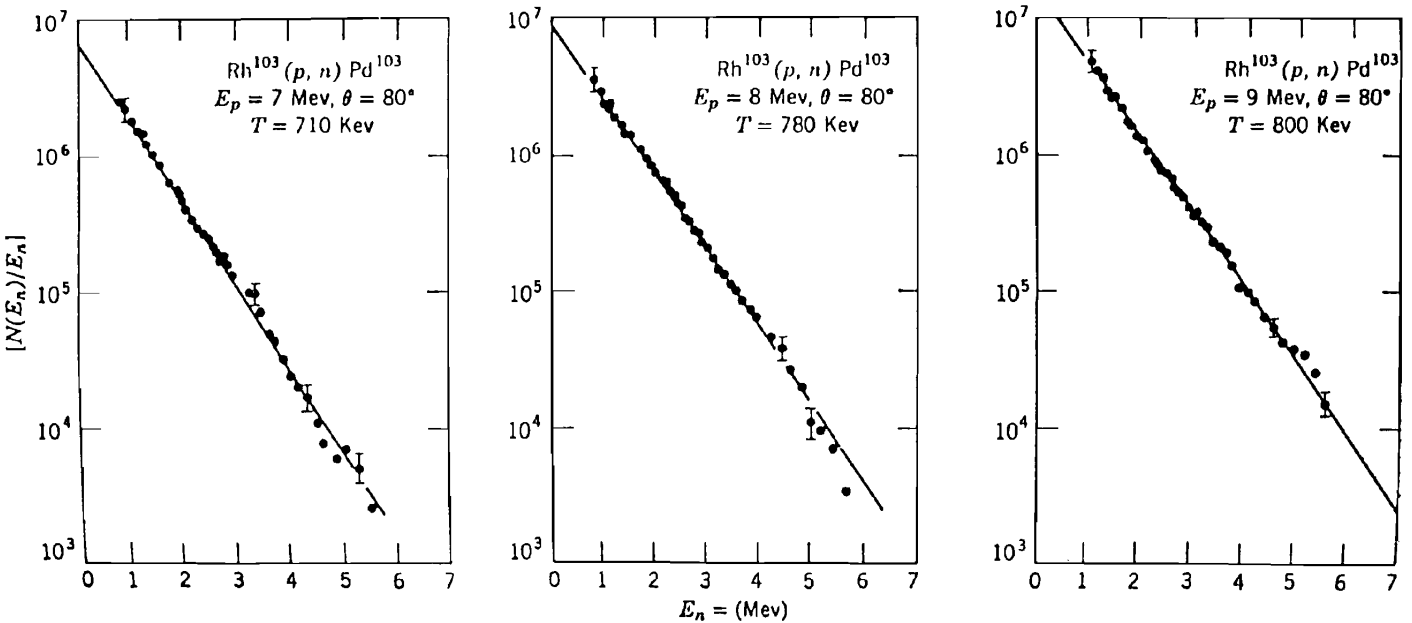

FIG. 9.5. Spectrum of neutrons from the Rh(p, n) reaction at a neutron emission angle of 80°. [From Holbrow and Barschall (63).]

projectile, is

$$\frac{\langle d\sigma_{ai}^{(\mathrm{FL})}/dU_a \rangle}{\langle d\sigma_{bi}^{(\mathrm{FL})}/dU_b \rangle} = \frac{\mu_a E_a \sigma_a^{(c)}(E_a)\, \omega_0(U_a)}{\mu_b E_b \sigma_b^{(c)}(E_b)\, \omega_0(U_b)} \tag{9.10}$$

The dominant factors in the ratio (if one is well above the thresholds) is given by the ratio of the level densities at the appropriate excitation energies.

We conclude this section with some experimental results that provide examples of the application of these results. We begin with the simplest case, that in which the spin and energies of the levels of the residual nuclei are known up to a sufficiently high energy. Then the cross section is given by (7.38) corrected

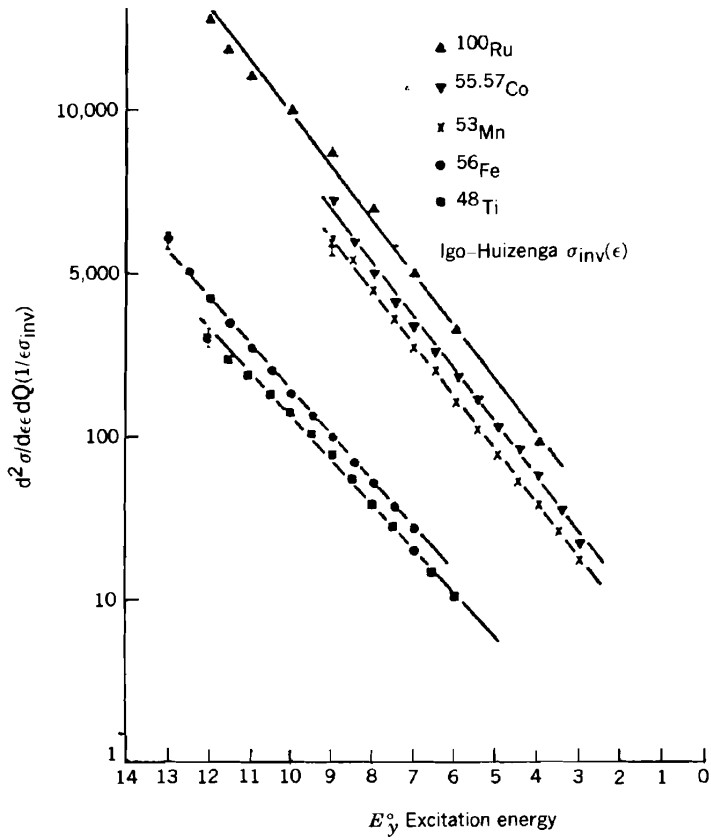

FIG. 9.6. Energy spectra of α-particles plotted as $d^2\sigma/d\varepsilon\, d\Omega(1/\varepsilon\sigma_{\mathrm{inv}})$ versus excitation energy. The inverse cross section σ_{inv} is calculated from an optical model by Igo and Huizenga [Sherr and Brady (61)]. [From Lefort (76).]

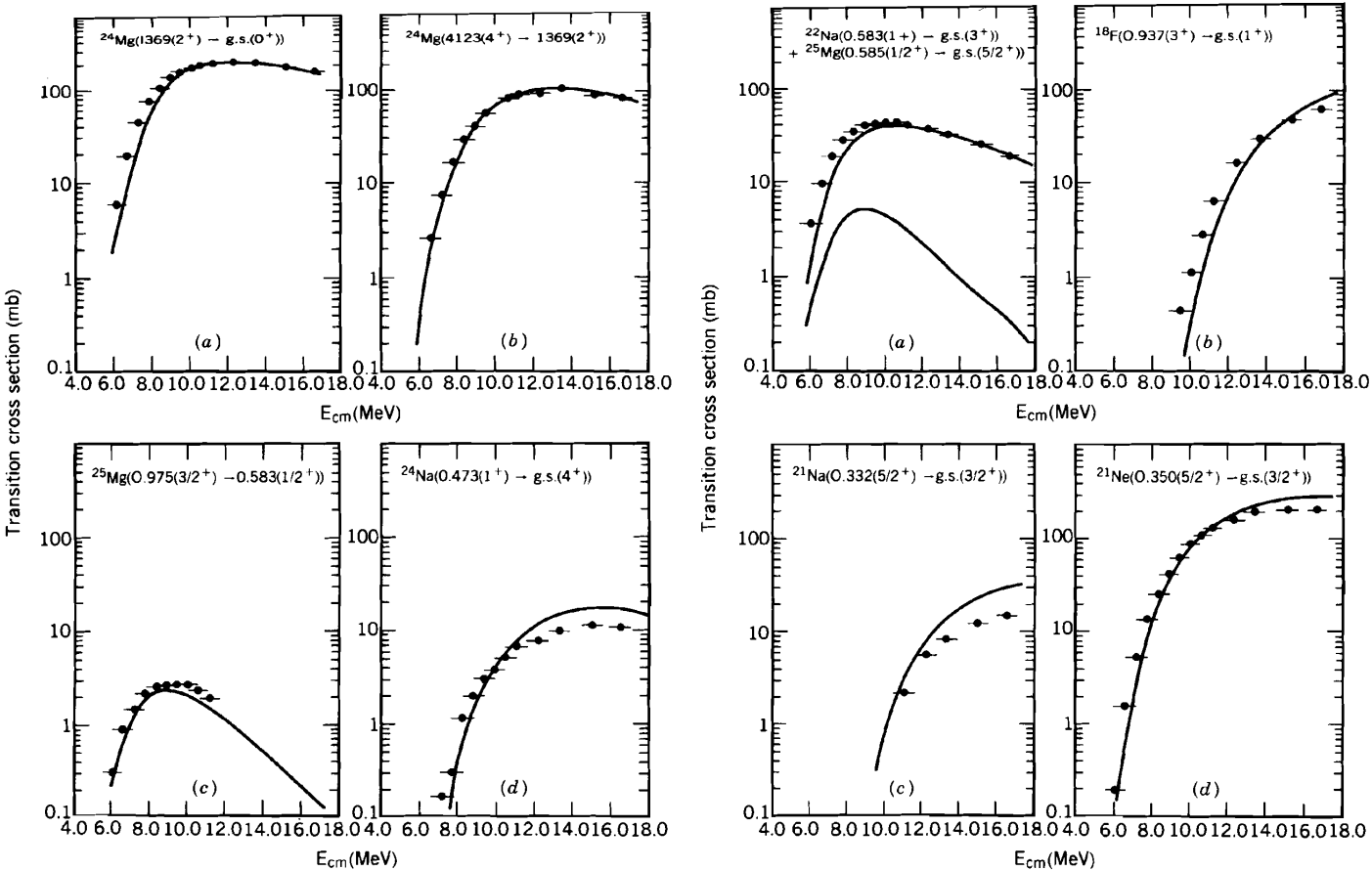

FIG. 9.7. Absolute γ-ray yields from $^{12}C + ^{14}N$-induced reactions. The full curves are absolute Hauser–Feshbach predictions [Erb, Olmer, et al. (73)]. [From Stokstad (85).]

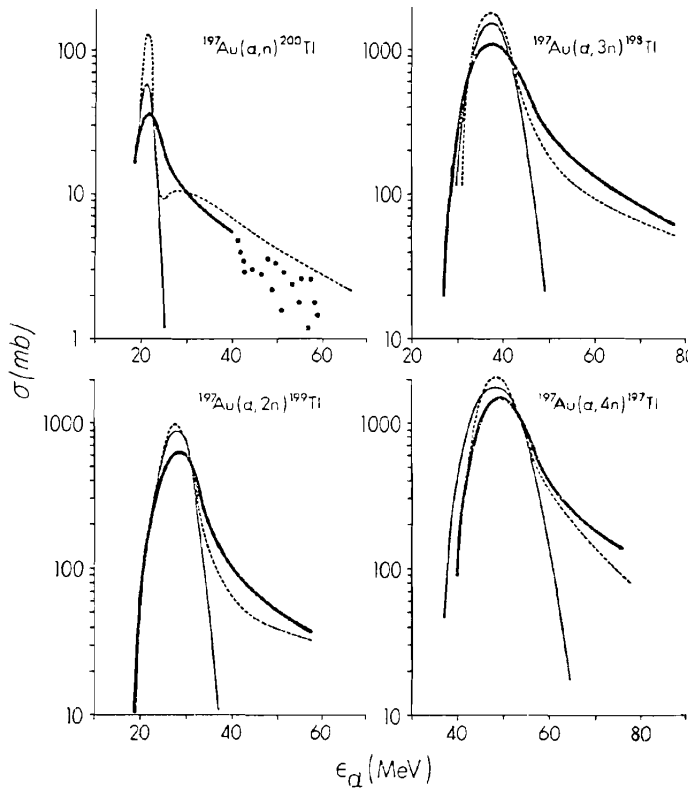

FIG. 9.8. Calculated and experimental excitation functions for the reactions ^{197}Au(α, xn). The heavy solid curves represent experimental yields. The thin solid curves represent equilibrium statistical model calculations. [From Blann (72).]

by the width fluctuation correction W_J:

$$\langle \sigma^{(\mathrm{FL})} \rangle = \sum \frac{2J+1}{(2I+1)(2i+1)} \frac{T_f(l', s'; J\Pi) T_i(l, s; J\Pi)}{\sum T_a(l_a, s_a; J\Pi)} W_J \tag{9.11}$$

An example of the application of this formula in which it is assumed that all values of J of the compound system which are allowed by angular momentum and parity conservation are included in the sum is shown in Fig. 9.4. We see the important effect of the width correction factor in some cases.

In Fig. 9.5 we present some of the results of Holbrow and Barschall (63), who considered the Rh(p, n) reaction. The straight line on the semilog plot is

FIG. 9.9. Comparison between the experimental spectrum for protons emitted in CsI(n, p) reaction (full line) at various energies and the calculated evaporate (—·—) and preequilibrium (---) contributions. [From Gadioli and Milazzo-Colli (73).]

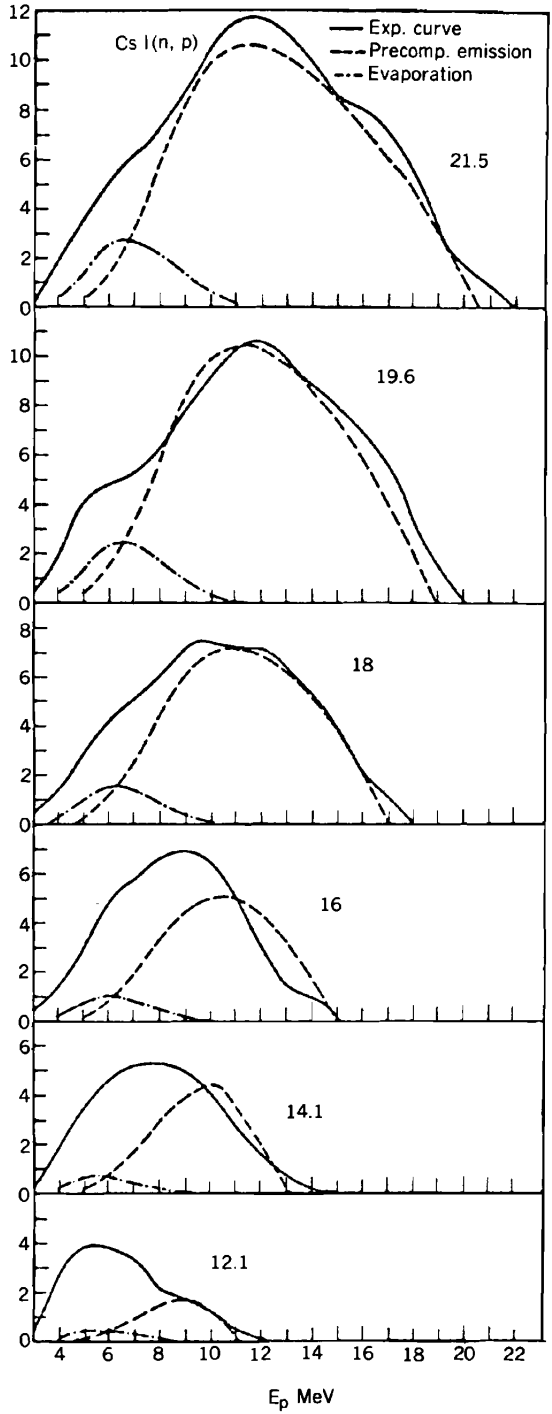
Cs I(n, p)
Exp. curve
Precomp. emission
Evaporation
21.5
19.6
18
16
14.1
12.1
E_p MeV

in agreement with (9.9) [assuming that $\sigma_f^{(c)}(E')$ is a constant equal to πR^2, where R is the nuclear radius]. The derivation from the straight line occurs at low neutron energy near the threshold for the $(p, 2n)$ reaction. Another example is given in Fig. 9.6, in which α-particle spectra produced in a (p, α) reaction involving a variety of target nuclei are given. As a final example, the prediction of γ-ray yields in light-ion reactions are shown in Fig. 9.7. Note that no adjustable parameters are used in this case.

The examples given in the section above show, in view of the crudeness of the statistical model, a surprisingly excellent agreement with experiment. This agreement indicates that once entrance and exit channel effects are included through the transmission coefficients, the remaining features of the reactions do not depend on the details of the nuclear Hamiltonian. From the theoretical development of the fundamental equations (7.39) and (9.11), a necessary condition for their validity appears to be that the wave functions involved be sufficiently complicated so that the matrix element of the residual potential with respect to these wave functions is a random number. However, the wave function does have simple components, and if the reaction is dominated by these, statistical considerations will fail. The condition for the validity of the statistical theory is not only that the wave function be complicated but also that the complicated components dominate. A rephrasing of these considerations using time-dependent language is instructive. In the early phase of the reaction, only simple states can be developed, the complicated states requiring a relatively long period of time involving the residual interaction acting many times. If the reaction terminates at an early stage, the statistical theory will fail. Indeed, a direct reaction may be involved, and then the angular distribution will be asymmetric, peaked toward the forward direction. The statistical theory will be valid only if the reaction terminates at a sufficiently late stage. In Chapter VI we discuss a formalism that includes both the early and late stages. That theory will provide criteria for which the statistical theory is a limiting result. For example, at sufficiently low energies, one requires that emission by the system is much less probable than proceeding to the next stage of complication, so that most of the reaction will involve emission from very complicated states.

For the present it will suffice to point to some examples of the failure of the statistical theory. In Fig. 9.8 we present a comparison between the cross section for the production of neutrons as indicated by the collision of α-particles striking ^{197}Au. The failure of the statistical model as the α-particle energy increases is evident. Another example is shown in Fig. 9.9, where the proton spectrum when neutrons of the indicated energies are incident on *CsI*. Neither the shape nor the magnitude of the evaporation contributions resemble the experimental results. Will the discrepancy be made up by the single step direct process? We shall provide some examples in Chapter VI to show that generally it will not suffice.